UNIVERSIDADE
BEIRA INTERIOR

Protein A chromatography designed for improved antibody capture

(Versão final após defesa)

Rodrigo Anselmo Rouqueiro

Dissertação para obtenção do Grau de Mestre em

Biotecnologia

(2º ciclo de estudos)

Orientador: Prof. Doutora Ana Cristina Mendes Dias Cabral

Coorientador: Prof. Doutora Carla Cruz

Covilhã, março de 2021

Aos meus pais,

por todos os valores transmitidos e amizade.

Acknowledgements

Inicialmente gostaria de agradecer à professora Ana Cristina Mendes Dias Cabral pela oportunidade de integrar o seu grupo de investigação, pelo seu suporte e pela orientação neste trabalho.

Não menos importante, foi a incansável ajuda da professora Carla Cruz, que me ajudou a superar dificuldades encontradas ao longo deste percurso.

Quero também agradecer a todos os meus colegas do CICS-UBI, em especial às amizades aqui criadas ou fortalecidas, por todos os bons momentos proporcionados, por toda a ajuda e troca de ideias.

Aos meus pais, que fizeram de mim aquilo que sou hoje, a quem devo tudo, que acreditam sempre no meu percurso e que nunca me deixam esquecer do que sou e das minhas capacidades.

Um agradecimento muito especial à minha Ana, por toda a partilha, por toda a amizade, por todas as conversas, por todos os bons momentos, por todo o apoio nos momentos mais difíceis e acima de tudo, por todo o amor.

"O futuro está cheio de momentos impossíveis à espera de acontecerem." José Luís Peixoto

Eternamente grato!

Resumo Alargado

Com um peso molecular de aproximadamente 54 kDa a proteína A de origem estafilocócica, tal como o nome indica, é um domínio proteico exposto na superfície da bactéria Gram-positiva S*taphylococcus aureus*. Esta proteína contém cinco domínios homólogos com capacidade de ligação a IgG, designados E, D, A, B e C, respetivamente, começando no grupo terminal amina. Para além desta região constituída por cinco domínios, fazem parte da sua estrutura outras duas regiões: a que liga à parede celular (XM) e a sequência sinal que é acionada na secreção (S). É frequentemente usada como ligando na cromatografia de afinidade, o tipo de cromatografia mais seletivo usado na Biotecnologia, que adicionalmente é a primeira escolha na maioria dos processos industriais. Este tipo de separação é baseado na interação reversível entre a proteína A, covalentemente ligada à matriz, e a biomolécula a ser capturada, no presente estudo um anticorpo policlonal (IgG).

Nas primeiras abordagens em que se aplicaram este tipo de resinas, foram utilizadas formas nativas de Proteína A. Como forma de contornar algumas nuances relacionadas com o uso destas formas nativas, foram introduzidas algumas melhorias, nomeadamente: a possibilidade de trabalhar num largo intervalo de pH (2-11), o aumento da estabilidade conformacional do ligando, a compatibilidade com agentes redutores de limpeza e capacidade de conseguir altas taxas de recuperação (>95%) com alto nível de pureza 99%. Sendo a última vantagem um ponto fulcral, uma vez que os produtos purificados devem apresentar os níveis de purificação estabelecidos por entidades reguladoras, como a Agência europeia do medicamento (EMA) e a Organização mundial da saúde (OMS). Assim, dependendo do principal propósito ao qual o produto será aplicado, diferentes níveis de pureza são exigidos, tendo os produtos usados em extratos de crude o menor valor de pureza, e os biofármacos o maior, onde a pureza seguida da homogeneidade são parâmetros críticos para a segurança do paciente ao qual serão administrados. No presente trabalho, o produto alvo foi o anticorpo, acima mencionado.

Anticorpos, são glicoproteínas com aproximadamente 150 kDa de tamanho. Estas moléculas pertencem à superfamília das imunoglobulinas (Ig), a sua principal função é a identificação e neutralização de organismos externos ou antigénios e são secretados pelas células B, que por sua vez são células sanguíneas brancas denominadas linfócitos B. A maior parte dos anticorpos encontrados no soro, pertencem à classe das IgG e a maioria da informação existente é também relativa a esta classe. A estrutura dos anticorpos consiste em

três grandes fragmentos; dois deles são fragmentos que se ligam a antigénios (FAb) e cada um tem apenas um único local de ligação para o alvo específico; o terceiro e último fragmento, não liga a antigénios, porém parte dele é uma região cristalizável bastante importante (Fc). Adicionalmente, cada anticorpo é formado por 4 polipéptidos, dois deles de cadeia leve (com cerca de 25 kDa cada) e os outros dois de cadeia pesada (com 50 kDa cada). Estas cadeias são por sua vez ligadas entre elas, por pontes dissulfeto e juntas conferem a famosa forma de "Y" em que os braços são os FAb e o tronco o domínio Fc.

Foi já demonstrado que os anticorpos são uma solução chave e a abordagem terapêutica para um largo espectro de doenças e condições médicas. Anticorpos e seus derivados têm vindo a ganhar cada vez mais atenção no campo biofarmacêutico e presentemente existem diversos novos produtos terapêuticos baseados em anticorpos monoclonais humanos à espera de serem aprovados. É importante realçar que o geral envelhecimento da população e a melhoria de vida nos mercados emergentes, também ajudaram na expansão farmacêutica global aumentando as vendas de anticorpos monoclonais. Assim, uma maior necessidade de produto levou consequentemente a uma necessidade de técnicas de produção e purificação mais eficientes.

No entanto, o aumento da produção de biomoléculas terapêuticas não tem vindo a ser acompanhada pelo desenvolvimento dos processos de "*downstream"*, que são a parte mais dispendiosa do sistema de produção. A redução de custos implica aumentar o rácio final do produto por unidade de tempo (ou seja, o rendimento global), sendo a forma mais comum de conseguir este aumento de escala de operação, a utilização de colunas cromatográficas maiores ou aumentar a capacidade de purificação da fase estacionária, pela otimização das suas propriedades físico químicas.

Posto isto, e dado que a formação do complexo IgG – proteína A tem um impacto importante no processamento das etapas de "*downstream", nomeadamente* na captura e purificação de anticorpos, devido à alta seletividade da ligação, o que pode levar à eliminação de impurezas com rendimentos superiores a 95% em apenas um passo, a intenção final deste trabalho é desenvolver uma coluna monolítica de proteína A integrando um novo ligando em que se pretende ter uma melhor performance na captura de anticorpos do sobrenadante celular. Reduzindo deste modo os custos de *"downstream"* e melhorarando o processo.

No presente estudo o nosso esforço focou-se em dois objetivos principais: a avaliação termodinâmica das propriedades da matriz, mais especificamente de um monólito 2,5% QA,

analisando a resposta deste à adsorção de uma proteína modelo (Albumina de soro bovino - BSA); e avaliação da capacidade de um novo ligando projetado para a captura de anticorpos.

O primeiro objetivo foi alcançado usando um Microcalorímetro de Fluxo (FMC), múltiplas injeções com diferentes volumes e com a mesma concentração de BSA foram efetuadas. Isto levou a que dependendo do "loop", a coluna fosse submetida a diferentes concentrações de proteína à superfície, resultando em diferentes respostas. Foram ainda realizadas injeções consecutivas de maneira a se perceber o que aconteceria em condições de sobrecarga e a avaliar em que ponto o monólito atingiria a saturação. Como já referido foi utilizada na análise calorimetria de fluxo, uma vez que esta permite perceber melhor os mecanismos cinéticos e as forças motrizes envolvidas no processo de interação entre as biomoléculas e os suportes cromatográficos.

Por sua vez, o segundo objetivo, é subdividido em três objetivos distintos; o estudo da interação do novo ligando de proteína A, que contém oito domínios de ligação, com o anticorpo IgG; otimização de diferentes procedimentos para a imobilização do referido ligando; e comparação do novo ligando de proteína A com o já existente MabSelect SuRe comercializado pela Merck (quatro domínios de ligação) em termos de potencial de isolamento do anticorpo IgG. Foram utilizadas duas variantes do protótipo do novo ligando: um marcado com uma cauda de poli-histidina (B8 (RH4)) e o outro marcado com uma cauda de cisteína-lisina-cisteína-lisina (B8 cys-lys-cys-lys). Estes estudos, foram realizados num biossensor baseado em ressonância de plasmões de superfície (Biacore T200), que oferece diferentes tipos de chips permitindo a utilização de diferentes abordagens na captura dos ligandos.

Palavras-Chave

Anticorpos; Captura; Proteína A; Novos Ligandos; Microcalorimetria de fluxo; Monólito; Ressonância Plasmónica de superfície.

Abstract

Protein A affinity chromatography has been the most used purification method for therapeutic antibodies in industrial processes, once it selectively purifies exploring molecular recognition and is an easy methodology. However, this type of chromatography has some cost-associated drawbacks and upstream titer limitations. This, coupled to the demand for high purity and quality requirements from regulatory agencies and to the increasingly growth of monoclonal antibodies importance in therapeutic market, led to some work with the purpose of getting a better performance of engineered protein A ligands. Nowadays, derivate from the wild type Staphylococcal protein A (with five different antibody-binding domains, A, B, C, D, E), engineered variants are present in the market. All the domains consist in three α-helices, which bind to the CH_2 region in the Fc part of the antibody and one of the most popular engineered variants is the tetrameric Z form, a mutant from the B-domain.

The present work is part of a major aim where we intent to develop a Protein A monolithic column that shows better performance for the capture of antibodies from cell culture supernatant. Thus, two different main goals are studied: the thermodynamic evaluation of matrix properties (2,5% QA monolith) by analyzing its response to the adsorption of a model protein (Bovine serum albumin (BSA)); and the capacity assessment of an engineered ligand for antibody capture. The first goal was achieved using a Flow Microcalorimeter (FMC) and it is subdivided in two parts: first, multiple injections of different volumes with the same BSA concentration were performed submitting the column to different protein surface concentrations; and later, multiple consecutive injections were performed to understand what happens under overloading conditions and to observe the point at which the monolith stops to adsorb. The second aim is subdivided in three different objectives: interaction study of protein A novel ligand, presenting eight binding domains, with an IgG antibody; optimization of different ligand immobilization procedures; and comparison of the novel ligand with the commercial already existent engineered Z form (four domains, MabSelect SuRe), in terms of antibody isolation potential. Two prototypes variants of the novel ligand with 8 B binding domains were used. One of them is marked with a poly-histidine tag (B8(RH_4)) and the other is tagged with cysteine-lysine-cysteine-lysine tail (B8 cys-lys-cys-lys). These two are thought, as previously mentioned, to be used primarily in protein A chromatography, namely in the direct capture of monoclonal antibodies due to the high specificity of the antibody-protein A bind.

Keywords

Antibodies; Capture; Protein A; Novel ligands; Flow microcalorimetry; Monolith; Surface plasmon Resonance.

Table of contents

List of Figures

List of Tables

List of Acronyms

AC	Affinity chromatography
ADA	Anti-drug antibody
AEX	Anion exchange chromatography
AMI	Acute myocardial infarction
ATR	Attenuated total reflection
BSA	Bovine serum albumin
C	Free protein concentration
CBS	Consensus binding site
CEX	Cation exchange chromatography
CHO	Chinese Hamster Ovary
CIP	clean-in-place
DBC	Dynamic binding capacity
DEAE	Diethyl aminoethyl
DHFR	Dihydrofolate reductase
DNA	Deoxyribonucleic acid
EBC	Equilibrium binding capacity
EMA or EMEA	Evaluation of Medical Products
Fab	Fragment Antibody binding
Fc	Fragment crystallizable
FDA	Food and Drug Administration
FMC	Flow Microcalorimetry
HIC	Hydrophobic interaction chromatography
hmAb	Human monoclonal antibody
IEC	Ion exchange chromatography
Ig(G)	Immunoglobulin (G)
ITM	Isotheral Titration Calorimetry
LB	Langmuir-Blodgett
LBL	Layer-by-layer
LC	Liquid chromatography

LOD	Limit of detection
mAb	Monoclonal antibody
MTX	Methotrexate
pI	Isoelectric point
PSP	Propagating surface plasmons
PTM	Post-translational modifications
q	Adsorbed protein concentration, binding capacity
QA	Trimethylamino- hydroxypropyl
RIU	Refractive index unit
RNA	ribonucleic acid
RPC	Reversed phase chromatography
SEB	*Staphylococcal enterotoxin* B
SEC	Size exclusion chromatography
SPA	Staphylococcal Protein A
SPR	Surface Plasmon Resonance
SPRI	Surface plasmon resonance imaging
SPW	Surface plasmon wave
TRPA	Thermal Responsive Protein A
UV	Ultraviolet
WHO	World Health Organization

Chapter 1. - Introduction

1.1. Proteins

1.1.1. Importance of protein therapeutics

Proteins, complex molecules composed by amino acids, have a wide range of functions in our body. Supporting the transport of molecules from one organ to another or within cell, creating receptors and channels in cell membranes, helping intracellular and extracellular scaffolding or simply catalyzing biochemical reactions, proteins are the most dynamic biomolecules and responsible for different roles when compared to another macromolecules in our organism [1]. In the year of 1980, it was introduced the first recombinant protein for medical treatments, human insulin. This led to an increase of recombinant proteins use [2].

Since then, the significant growth in its application provided the reformulation of a wide range of industries including cosmetics, pharmaceuticals, diagnostics, research and development, food and transformation of bioprocesses. These products must present established purity levels according to the regulatory authorities, like the European Agency for the Evaluation of Medical Products (EMEA), the U.S. Food and Drug Administration (FDA) and the World Health Organization (WHO). Depending on the main purpose where they will be applied, the level of purity will be different. With the lowest value, almost without purification or lightly refined, the products can be used as crude extracts, and with the highest value, biopharmaceuticals, where the purity followed by homogeneity are critical parameters for the good application and to ensure the patient safety [3, 4].

Proteins can be produced by bacterial, yeast, plant, insect, or mammalian cells through recombinant DNA technology. Encoding DNA inside the host cell will lead to protein expression and then the product is purified from them. Examples of these proteins are monoclonal antibodies, human insulin and many other different biological medical products [3]. As mentioned before, these proteins are used in medical treatments, being preferentially chosen over small molecules due some great advantages which include the capacity of performing complex and high specific functions not mimicable by chemical compounds, more capacity of non-interference with natural biological processes and consequently reduction in elicit immune responses [1], and minor approval time when compared to chemical drugs [5]. There is also a continue increasing market trend, previous existing documents indicate the scale up of this market from US$85 billion in 2010 to $208 billion in the present year (2020), essentially

due to the market of monoclonal antibodies and human insulin [6, 7]. Forethought to be revised upwards due to the current pandemic of Covid-19.

1.1.2. Properties and structure

Composed by amino acids as building blocks, proteins are highly structured amphoteric biopolymers and usually they have compact structure. Also, they can change their conformation, depending on the binding substrates, interphase conditions and on the environment [8, 9]. In terms of complexity, the protein structure is divided in four distinct levels [9]:

Primary structure – it is essentially the order that amino acids present in the polypeptide chain.

Secondary structure – consists in the three-dimensional structures, named α – helices, β – sheets and loops, that are result of amino acid chain folding.

Tertiary Structure – based on the previous mentioned three-dimensional structures folding, with intramolecular interactions predominantly based on disulfide bridges and hydrophobic interactions, being these interactions responsible to form a tight core where the hydrophobic domains will be, being the charged polar residues expose on the surface.

Quaternary Structure –formed by aggregation of two or more polypeptide chains in a complex structure particularly geometrized and essential to the correct biological function. This final cluster leads to a globular or fibrous shape stabilized by disulfide and hydrogen bonds, hydrophobic interactions, and salt bridges.

In order to increase the structural and functional diversity, the majority of eukaryotic proteins are target to post-translational modifications (PTM). Which consist on the covalent bounding of new functional groups to the protein followed by folding processes that will lead to the correct mature protein functionality. These functional groups could be amino, carboxylate, phenolic, thiol and many others [3, 9, 10]. When the modifications are altered or incomplete, it can take to different biological activities, changes in stability and variation of properties like charge, hydrophobicity, size and solubility, resulting in different characteristics from the desired, which is a huge problem on the scale-up when biotechnology is used to produce proteins [11].

1.1.3. Protein A

Staphylococcal Protein A (SPA) is a protein domain exposed on the Gram-positive bacterium *Staphylococcus aureus*'s surface, with a molecular weight around 54 kDa, that contains five homologous IgG-biding domains designated respectively E, D, A, B and C, starting from the amino terminus [12]. All the domains show an anti-parallel three α-helical bundle (58 amino acids) with a three-dimensional structure stabilized by a hydrophobic core and have strong affinity and selectivity to every isotype of IgG, except the IgG3 [13]. SPA has also high affinity to IgG from several species like human, pig, rabbit, and guinea pig. On the other hand, it only shows weak interaction with mouse, ruminant and almost inexistent interaction with chicken species [14]. In addition to the region that has the five domains, there are two more regions in its structure: the signal sequence, processed on the secretion (S) and the region that binds the cell-wall (XM) [13].

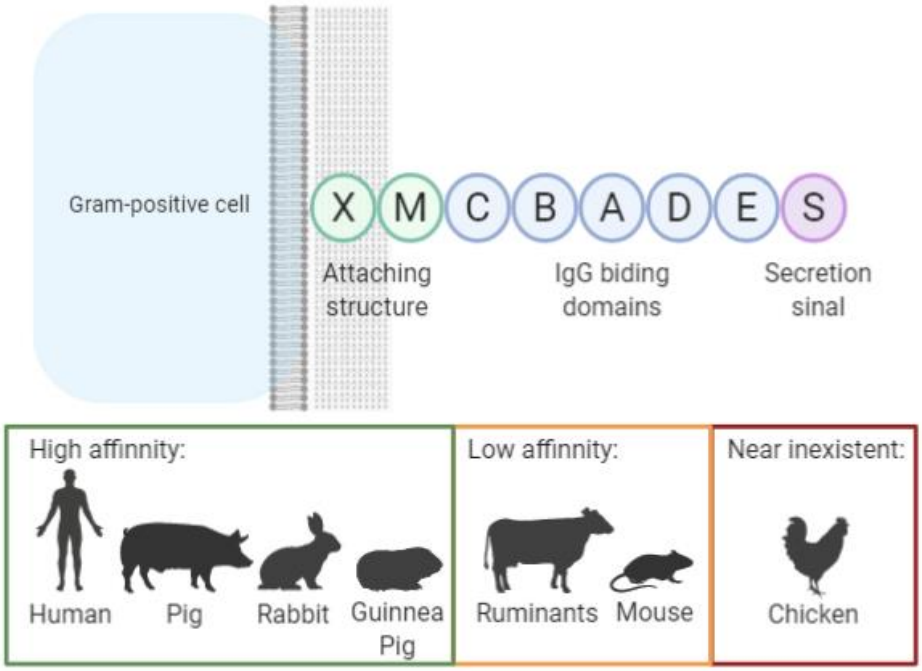

Figure 1: Protein A domains and its affinity to different types of species. Adapted from [13].

Protein A is highly used as ligand in affinity chromatography, the most selective type of chromatography used in biotechnology, more specifically Protein A chromatography, being the first choice in majority of the industrial processes. The affinity separation is based on a reversible interaction between protein A covalently coupled to the matrix and the biomolecule to be captured, in this case an antibody (IgG) [15]. In first trials using Protein A resins, native forms of SPA were used as described before. However these proteins secreted from E. coli

usually are manipulated to have the cell-wall region deleted, presenting instead a molecular weight around 42 kD [16, 17].

To overcome some of the drawbacks related with the Protein A native forms use, like the presence of residues vulnerable to proteolysis and alkaline hydrolysis, engineering improvements were made to reach operational advantages like: possibility to work on a wide pH range (2-11), ligand conformational stability, compatibility with cleaning reducing agents, and capacity of achieving high recovery (>95%) with purities around 99% [16].

A well-known example of Protein A resin stability improvement is the one where its B domain is mutated and renamed Z domain. Basically, it consists in two amino acids substitutions in the B domain: namely Ala (position 1) by Val to furnish a non-palindromic restriction site; and Gly (position 29) by Ala, to prevent the presence of Asn-Gly dipeptide, as it is one of the amino acid sequences most sensitive to alkaline conditions. Alterations that led to resin higher alkaline stability and its tolerance to harsh elution and clean-in-place (CIP) conditions [18, 19]. Another advancement in protein A resins was its response to temperature [20], mutations at the protein A core were made, to reach the called Thermal Responsive Protein A (TRPA).

Antibodies bind at low temperatures and elute at higher temperatures. Protein A has its native structure at 2-10^{o}C, unfolds at 40^{o}C and with temperature decreasing returns to its refolded form, being able to adsorb antibodies again. In this way, all the process happens at neutral pH avoiding protein A leakage, usual on commonly rummage-sale acidic conditions used at the elution step [20]. Also to reduce non-specific binds with culture components and improve the performance of the resin, PEGylation has been applied, basically it increases the selectivity for antibodies in more than 15% and reduce the contaminants at a factor of ≥2, slowing as well the association kinetics and decreasing pore diffusion [21].

Commercially there are available a wide range of Protein A resins, but the most used to antibody capture from the feedstock are: MabSelect SuRe (by GE Healthcare), where B domain is manipulated creating the Z domain and every ligand has 4 sequential units of Z domain; and TOYOPEARL AF-rProtein A HC, where the C domain is engineered to create the Y domain were ligands have 6 repetitive units of the Y domain. In addition to the previous examples, a lot of new studies and re-engineering have been done, majority if not all of them with the same purpose, get more knowledge about Protein A chromatography and reduce the costs on mAbs downstream processing once protein A capture step is the most expensive step on the process and presently not explored in its full potential [22].

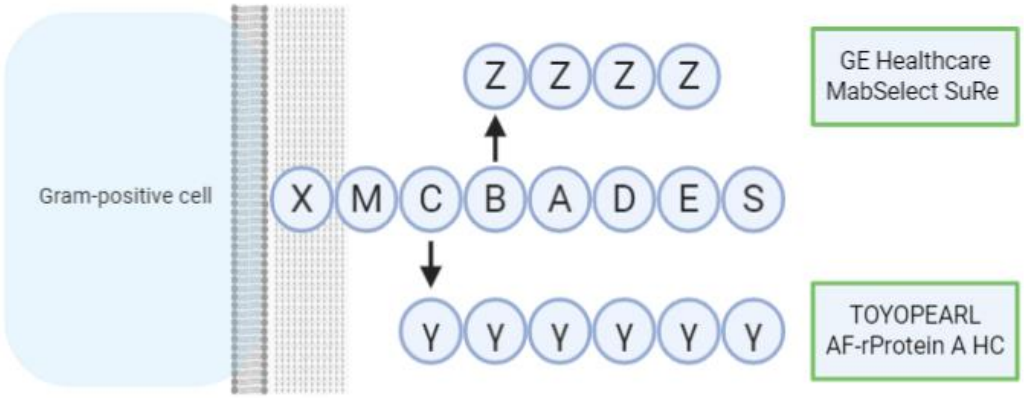

Figure 2: Commercial protein A resins and its structure domains. Adapted from [13].

1.1.4. Antibodies

Antibodies are glycoproteins with size around 150 kDa. These large molecules belong to the immunoglobulin (Ig) superfamily which main function is to identify and neutralize foreign organisms or antigens, being secreted by B cells (white blood cells called B-lymphocytes) [23].

Their structure consists in three fragments; two FAb fragments that binds antigens, as the name suggests (Fragment Antibody binding) and which only have a unique binding-site for a specific target; and the Fc fragment that doesn't bind antigens but part of it is an important region (c- crystallizable). Furthermore, antibodies are based on four polypeptides, two light chains (around 25 kDa each) and two heavy chains (around 50 kDa each). The chains are linked between them by disulfide bonds and together they confer the famous antibodies Y-shape, where the arms are the Fab's and the stem is the Fc [24]. Particularly, this bridge zone is the main difference between the IgG superfamily subclasses, the linkage zone length is related to the IgG functionality and with their flexibility. The Fc region is also connected to the two FAb domains by two disulfide bridges between their cysteines. This linkage region has folding characteristics and depending on its length it can confer flexibility to the antibody. [25]

The biggest part of antibodies found in serum belong to the IgG class and most of the information, like the previous one, is related to this class. There are four subclasses of IgG in humans, 1,2,3 and 4, being the first one (IgG1) the most abundant and impactive isotype. It is primarily induced by antigens, but it is also induced by proteins and polysaccharides as allergens leading to an antibody response [26, 27]. IgG1 represents around 68% of the mAbs on the market, as it links to all Fcγ receptor classes and has a high specificity [28].

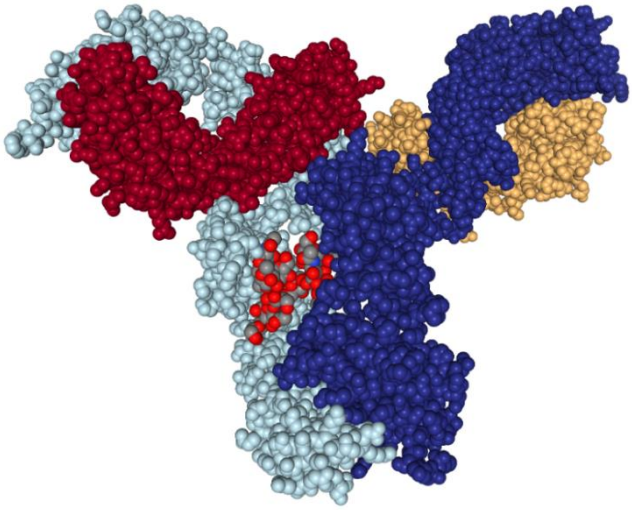

Figure 3: Crystallographic structure of an IgG1 (1HZH.pdb) where can be seen the three fragments, one Fc and two Fabs. It is also represented the two light chains (dark red and yellow) and the two heavy chains (dark and light blue). Additionally, linked to the N-terminal of both heavy chains is a group of carbohydrates which have a core common to all human IgG (red round structure) [29].

Antibodies have been shown to be a solution and a key therapeutic approach for a wide range of diseases and medical conditions, they and antibody derivates are getting great attention in the biopharmaceutical field, presently there are many new therapeutics products based on human monoclonal antibodies (hmAbs) waiting for approval [30]. Since the first licensed mAb product, namely Orthoclone OKT3 approved in 1986, to prevent the rejection on kidney transplant, that the number of these therapeutics in clinical trials or already approved has been increasing consistently over the past decades [31, 32]. The improvement of standard living in emerging markets and the general ageing of population, have also helped the global pharmaceutical market expansion by increasing the growth in monoclonal antibody product sales. The higher doses of mAb products and the advancements referred before conducted to a high product requirement and consequently in a necessity of an even more efficient production and purification techniques [6].

1.1.4.1. Monoclonal Antibodies

In nature the immune response to a strange antigen or organism is normally polyclonal [33]. Monoclonal antibodies only recognize one epitope on the surface of the antigens, contrary to the polyclonal antibodies that recognize different epitopes. The first described report of *in vitro* murine mAbs production by hybridomas was made by Kohler and Milstein in

1975 [34], being also the first important progress towards the development of human mAbs as therapeutic agents. Hybridoma development, at the beginning consisted on the mouse immunization with the target antigen, followed by spleen removal for isolation of B-cells antibody producers. Then B-cells are fused to myeloma cells forming the hybridoma cells, that link a faster immortal growth process with a specific production of mAbs. After that, positive clones capable of producing the target antibody are screened and selected for *ex vivo* expansion [35]. Nevertheless, around 1980, when murine mAbs arrived at the clinical development it was discovered that they had significant drawbacks. Because part of the cell line is of murine origin, murine mAbs are often associated with allergic reactions and induction of anti-drug antibodies (ADAs), which is translated in therapy limitations such as reduced serum half-life, weak immune response and human anti-mouse antibody reactions [33].

To overcome this problem, it was necessary to make the antibody more human. Two different methods helped to make it possible, hybridization and humanization. The first one replaces murine regions of the antibodies for human regions, except Fab regions, resulting an antibody with structure around 66% human and 33% mouse, denominated chimeric antibody. ReoPro® (Abciximab) was the first chimeric fractioned mAb to get to the market. The first complete chimeric mAb to reach the market was Rituxan® (Rituximab) [34]. On the other hand, humanization involves genetic engineering and basically replaces selectively murine regions of the antibody for human regions, achieving an antibody with composition around 90% human [36].

In the middle of the 1990s, by mice humanization, the production of murine mAbs presenting high affinity to human antigens became a routine process [37]. Taking account the good evolution that mAbs were having, in 2001 it was predicted that 100 approved mAbs would be on the market in 2010 [38]. But this didn't happen, being at 2008 only 20 mAbs (not all of them human) approved, and around 150 human mAbs were starting their clinical studies. More recently (specifically in 2017), there were already nearly 50 mAbs approved by the two major entities for therapeutics approval (EMA and FDA) [6, 39].

Nowadays, mAbs are used predominantly as therapeutics in autoimmune and inflammatory diseases, but they are also spreading to other different therapeutics areas where we are assisting to a growth in patient populations [39]. This, has led us to the necessity of higher monoclonal antibodies doses and to the requirement of an even more efficient production and purification of mAbs [40].

1.1.4.2. Advances on mAbs production and purification

As in any other protein manufacture procedure using biotechnology, mAbs processing can be divided in two steps; the upstream process including sub steps like host selection, cell fermentation and protein production; and the downstream process that goes from the harvest, passing through the lysis (if necessary), separation and the purification of the desired product.

Two of the main reasons that have led to an increase in biopharmaceuticals yield and productivity, were the research and development of the upstream processes and the high improvement of DNA recombinant technologies [41]. In the case of mAbs industry, a more effective mAbs production was developed by combining cell culture technology with genetic engineering using expression systems. One of those developed systems, still used today, is a mammalian expression system where Chinese Hamster Ovary (CHO) are used as host [41]. The reason why CHO cells are the most used to produce therapeutic proteins, is because their use presents several advantages as: their flexibility to grow and to adapt in high densities culture suspensions, being adjustable to genetic modifications, their capacity do scale-up to 10000 L bioreactors and reduced susceptibility to some viral infections [42]. In addition, with the development of cell culture technology (more properly feed development), it was reached with CHO systems a productivity over 10 g/L of antibody [41, 43].

For the production of mAbs, CHO cells are usually adapted in suspension cultures [41]. Their ability to grow in suspension allows to: decrease the waste due to the reduction of material used (culture flasks and roller bottles are not necessary); reduce the clarification responsibility, eliminating the use of structures to keep the adherent cultures in stirred-tank bioreactors, as microcarriers (commonly under fed-batch or perfusion modes of operation) [44]. Compared to perfusion mode, fed-batch continues to dominate the culture of CHO cells in the sector of biopharmaceutics due to some positive factors as: practical implementation, reduced probability of contamination, small footprint and good consistency of the loots. Nevertheless, there are some cases in mAbs production that still use perfusion or continuous systems, namely ReoPro® from abciximab and Remicade® from infliximab [45].

After transformation, it is necessary to select the transformed and highly productive CHO cells. This selection can be done by antibiotics or with a metabolic system [42]. The first type of selection was used for a consistent space time, but the costs associated to maintain the cells in antibiotics and the extra necessary steps to take out the antibiotics from the production media during downstream processing, led to the use by industries of systems

modified with the dihydrofolate reductase (DHFR) gene resistant to methotrexate (MTX) [46]. MTX is used as selective marker that realizes the enzymatic conversion of folate to tetrahydrofolate, necessary for syntheses of purines and pyrimidines [47]. In use of this system, CHO cells are transformed with recombinant DNA containing the interest gene side-by-side and linked with DHFR gene, so with gene amplification the levels of MTX increase (drug analogue to folate). Consequently, if cells are not highly producers, they will not produce enough DHFR and MTX will bind to all the DHFR, inhibiting the production of tetrahydrofolate. As result, in absence of an exogenous source of glycine and thymidine (like the medium) and with a low expression of DHFR, since as mentioned, tetrahydrofolate is necessary to produce pyrimidines and purines, the cell will die [48].

When finished the selection of the highly productive CHO cells and when they had also produced the wanted antibodies, it is necessary their separation from other undesired parts. Commonly, the harvest is first centrifuged to get clarified. After that, usually a filtration is made to separate the cells and some extracellular metabolites (heavy ones) from the antibodies. In addition, when the solution has a complex mix and in order to provide a further clarification, a depth filtration can be done to retain molecules at the filter and separate them from the antibodies [49]. This pre-purification process is usually done in order to allow the product capture on chromatographic columns directly from the clarified feedstock [50]. Otherwise, the direct antibody capture from the harvest could compromise the correct working of the chromatographic column and even its lifetime. Definitely, special attention must be given to the separation and purifications steps, since they are considered the most expensive in the entire mAbs downstream processing [51], being the capture chromatographic step identified as one of the main bottlenecks.

1.2. Liquid chromatography

According to its definition, liquid chromatography (LC) is a process where a mixture of molecules or components transported by a fluid phase (called mobile phase) are separated by interaction with the fixed bed material (denominated stationary phase). To separate the mixture, it is explored a range of interactions and mechanisms that promote partition between the phases to the separation of interest products. In short, different phase compositions lead to different interactions and molecules that interact stronger with stationary phase (high affinity to the resin) will run slower through the column than the ones with mobile phase

affinity (low affinity to the resin) [3]. It can also happen that the product with high affinity to the resin stays retained into the support while the rest of the mixture comes out, then with change of the protein/ligand biophysical properties or by competitive adsorption, the molecules are recovered [52].

1.2.1. Chromatography types and branches

The most common chromatography used after clarification to capture biopharmaceutical products of interest, is in the majority of times, liquid chromatography. This is due to its efficient capacity to adsorb and separate the desired biomolecules. Depending on the application, chromatography can be subdivided in two types: Preparative chromatography, where the objective is to isolate pure substance for posterior use [53]; and analytical chromatography, which the main purpose is the separation of molecules to make identification analysis, quantification, and to study protein's structure, post-translational modifications and function [54, 55]. Additionally, liquid chromatography can be divided into five main branches (Table 1, Fig. 4) defined by the type of stationary phase ligand nature [3].

Stationary phase ligand nature	Mobile phase	Elution	Acronym	LC branches
None	Aqueous	-	SEC	Size exclusion
Hydrophobic	Water-organic solvent mixture	Increasing organic solvent percentage	RPC	Reversed phase
Mildly hydrophobic	High anti-chaotropic salt concentration aqueous solution	Decreasing salt concentrations	HIC	Hydrophobic interaction
Charged	Aqueous solution low salt concentration	Increasing salt concentrations	IEC	Ion exchange
Biospecific	Aqueous	Dependent on the system	AC	Affinity

Table 1: LC branches based on stationary phase and mobile phase properties. Adapted from [3].

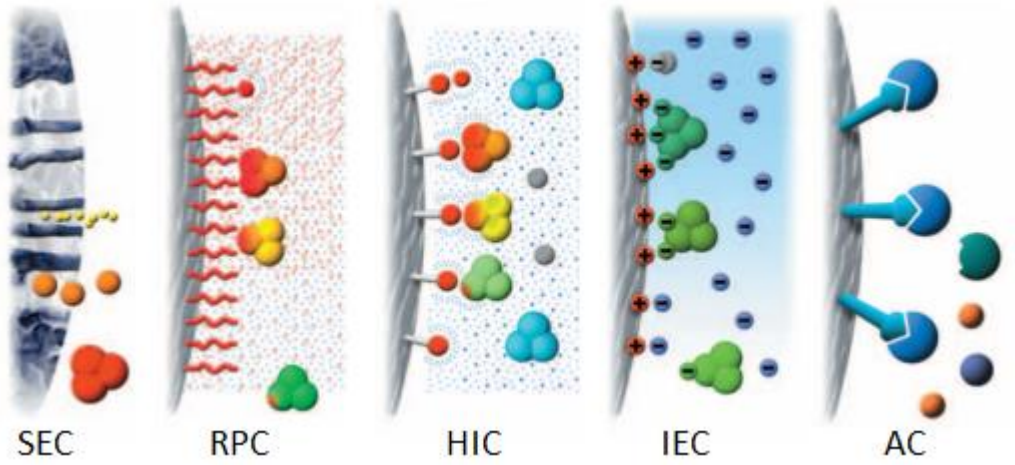

Figure 4: Illustration of liquid chromatography molecule-stationary phase base interaction. Respectively SEC, RPC, HIC, IEC and AC [56].

1.2.1.1. Size exclusion chromatography

One of them, is size exclusion chromatography (SEC), also known as gel-filtration chromatography. This branch of chromatography is commonly used in two different occasions; in the capture step where partially purify the interest product from a big part of impurities that came from the upstream; in the polishing step for desalting and to separate undesired forms like aggregates or protein isomers from the wanted molecules [52], and in analytics for the measurement of average molecular mass and for determination of hydrodynamic parameters [57].

SEC is composed by an aqueous mobile phase and the stationary phase does not have any ligands, as there is no ligand interaction between the stationary phase and the molecules. In this procedure the retention time only depends on the biomolecule molecular size or in a few cases molecular weight. Namely, big molecules will not fit in smaller pores, so they will pass around them and consequently pass quicker through the column. Oppositely, small molecules have great fit to get inside smaller pores, this means a longer path and, consequently, a longer retention time compared to bigger molecules [11].

SEC is also a process with controlled entropy, due the different hydrodynamic volumes between proteins and function of their molecular configuration, weight and molecular conformation (more specifically the shape) [11].

1.2.2.2. Reversed phase chromatography

In reversed phase chromatography (RPC), another branch of LC, the most common operation mode is the gradient elution with a specific ratio of water-miscible organic solvent. Basically, the backbone of this process is the separation of the molecules by their hydrophobicity level. First, the sample needs to present low concentration of organic solvent promoting the binding of the protein hydrophobic domains to the high hydrophobic ligand. So, greater the protein hydrophobicity, the stronger is the affinity for the stationary phase and longer the retention time. After adsorption of the interest protein to the column, an elution needs to be done. To promote elution organic modifiers like methanol, isopropanol, ethanol and acetonitrile are added. These will increase again the affinity of the mobile phase to the protein, consequently promoting its desorption [52].

When a non-polar molecule is transferred from a polar environment to a non-polar one, a decrease in free energy and heat capacity is detected, resulting on an increment of the entropy levels. This can be explained, as described by the preferential interaction theory, mainly by the reorganization of the water molecules related to the adsorption driving forces [57]. In terms of applicability, is a powerful technology to use in analytical chromatography, but it may have some drawbacks in preparative chromatography. The use of organic solvents is an obstacle for method approval by the regulatory agencies. Also the fact that not all proteins can be in contact with organic solvents, due to irreversible denaturation by exposing the hydrophobic domains that usually are inside the globular core [3] is a downside.

1.2.1.3. Hydrophobic interaction chromatography

As the last one, also the hydrophobic interaction chromatography (HIC), uses the hydrophobic interaction to separate molecules. It uses aqueous solution with high salt concentration and mildly hydrophobic stationary ligands. Comparatively with the last process, while in the RPC the interactions are controlled by the solvent mixture, since the mobile phase

is quite stronger in hydrophobicity, in HIC they are promoted by salt concentration in the mobile phase [3]. Basically, this method uses anti-chaotropic/kosmotropic salts to promote the protein hydrophobic character, avoiding the problems associated with the organic solvents [56]. These salts stabilize the water-water interaction, affecting the water molar concentration and the protein hydration shell. When the concentration of salt is added, a phenomenon called salting out happens, promoting the interaction between the protein and the ligand. After protein adsorption, the salt concentration is decreased which during the gradient will reduce the interactions between the support and the protein, proceeding the elution [3].

1.2.1.4. Ion exchange chromatography

Once ion exchange chromatography (IEC) presents high binding capacities, versatility, resolving power and the ability to preserve biomolecules biological activity, it is one of the most widely used chromatography branches applied for the separation of proteins [58]. Proteins can assume a superficial net charge, ordered by media pH and due to the amino acids charge, this could be very useful to reversibly interact with the oppositely charged ligands immobilized on the column. After the support equilibrium with the free counter-ions, the interest protein is passed through and its interaction with the column will disturb this equilibrium, promoting the exchange. Subsequently, elution is promoted by increasing salt ions concentration on the mobile phase, as high ionic strength levels generate a charge shield around the protein and the ligand surface reducing the electrostatic interaction [59].

Essentially, ion exchange interaction plays with the fact that each protein has its own surface charge dependent from the amino acids present on their surface. As each amino acid has different values of pKa, the surface charge will be very dependent on the solution pH (Table 2). When the pH is above pI, the protein charge will be negative, linking to positively charged supports and exchanging anions, called anion exchange chromatography (AEX). On the other hand, if the pH is under the pI, the charge will be positive, protein will link to a negatively charged support and exchange cations, called cation exchange chromatography (CEX) [60]. At a certain value of pH, the proteins do not present net charge, usually called isoelectric point (pI). But, even at protein´s isoelectric point adsorption can occur due to the asymmetrical surface charge distribution. Additionally, post translational modifications must be taken in consideration, since they cause micro-heterogeneity in protein surface and consequently play an important role in the net charge [3]. Table 3 shows a list of the most used ion exchange ligands on current systems and its structure [65].

Ligand name	pKa	Charge of the ligand (Z) dependent on the solution pH							
		<2	2-2,5	2,5-3	3-5	5-7	7-10	10-11	>11
Trimethyl aminomethyl	12,2	Z=+1							Not stable
Trimethyl aminoethyl	>13								
Diethyl-(2-hydroxypropyl aminoethyl)	12,2								
Trimethylamino - hydroxypropyl	12,2								
Dimethyl aminoethyl	≈10	Z=+1					0<Z<1		Z=0
Diethyl aminoethyl	6-9	Z=+1				0<Z<1		Z=0	
Carboxymethyl	3,5-4,5	Z≈0			-1<Z<0	Z=-1			
Sulfopropyl	2-2,5	Z≈o		Z=-1					
Sulfoethyl	2	Z≈0	Z=-1						
Sulfomethyl	2	Z≈0	Z=-1						

Table 2: Ligands charge at different pH solution values. Adapted from [61].

The first step in a chromatographic procedure is equilibrate the stationary phase with buffer on adequate pH value and ionic strength to bind negatively and positively charged proteins respectively to anion exchange and cation exchange supports. This will lead to a concentration of the bound biomolecules in the column while the biomolecules with the same charge as the medium will flow through and elute, during or after the sample application. Next to the loading of the sample and elution of the non-binding biomolecules the conditions are changed by changing the buffer, more commonly by increasing the salt concentration of the mobile phase (ionic strength). As the ionic strength increases the bound biomolecules starts to

elute once the salt ions start to compete for the medium biding sites. The first biomolecules to be eluted at the selected pH are the lowest net charged ones, the ones with higher net charge will be most strongly retained and be eluted later. So, controlling the changes in ionic strength, different biomolecules can be eluted differentially in a purified and concentrated form. At last, the final step is the regeneration of the column, usually this is reached using very high ionic strength buffers, removing all the strongest bounded biomolecules. Before a reutilization, the column must be re-equilibrated using the same conditions of the first step. For several applications the previous identified steps are repeated cyclically (Fig. 5) [62].

Table 3: List of most used ion exchange ligands on current systems and its structure. Adapted from [61].

Ligand name	Acronym	Strength	Type of IEC	Structure
Trimethyl aminomethyl	Q	Strong	Anion exchange	$-O-CH_2N^+(CH_3)_3$
Trimethyl aminoethyl	TMAE			$-O-CH_2CH_2N^+(CH_3)_3$
Diethyl-(2-hydroxypropyl aminoethyl)	QAE			$-O-CH_2CH_2N^+(CH_2CH_3)_2(CH_2CHOHCH_3)$
Trimethylamino - hydroxypropyl	QA			$-O-CH_2CHOHCH_2N^+(CH_3)_2$
Dimethyl aminoethyl	DMAE	Weak	Anion exchange	$-O-CH_2CH_2NH^+(CH_3)_2$
Diethyl aminoethyl	DEAE			$-O-CH_2CH_2NH^+(CH_2CH_3)_2$
Carboxymethyl	CM	Weak	Cation exchange	$-O-CH_2COO^-$
Sulfopropyl	SP	Strong	Cation exchange	$-O-CH_2CH_2CH_2SO^{3-}$
Sulfoethyl	SE			$-O-CH_2CH_2SO^{3-}$
Sulfomethyl	S			$-O-CH_2SO^{3-}$

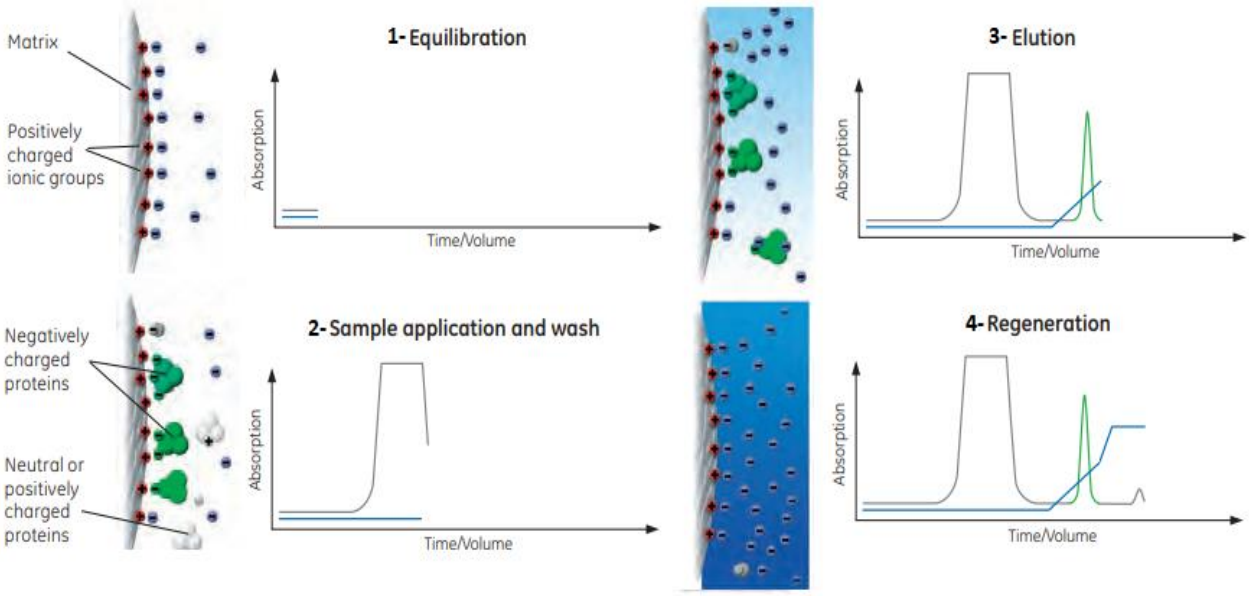

Figure 5: Anion-exchange separation steps and its graphical representation. Adapted from [63].

1.2.1.5. Affinity chromatography

In affinity chromatography (or biospecific interaction chromatography (AC)), ligands (natural or synthetic) that are very similar or equal to the ones present in biological organisms are commonly used. AC is based on the natural biospecific interaction that molecules have between them, it separates the interest molecule from the mixture by a reversible interaction between the product and the ligand on the stationary phase. As interactions are tremendously specific, sometimes pH extreme conditions are required for the elution, since the desorption of the interest protein is too difficult to achieve [64]. Nevertheless, because of its specificity, throughput and easy use, it is generally chosen for the separation of biomolecules [65].

One of the most used examples is the protein A chromatography, usually applied in purification of mAbs. Due to its high dynamic binding capacity, capacity to use at high flow rates, selectivity towards IgG antibody types, great yield and achieved purities (> 99%) when starting from cell culture supernatant, protein A became one of the most important unit operations for antibody capture. However, like any other technique, it has some disadvantages as the high process cost and the necessity of subsequent polishing chromatographic steps [13].

IgG-protein A interaction

The formation of the IgG-protein A complex has important impacts in antibodies downstream processing, due to the high selectivity of affinity binding between the antibody Fc region and the Protein A ligand, that can guide to the elimination of impurities with values higher than 95% just in a single step [66]. The formation of this complex happens between the CH2 and CH3 domains of the Fc region from the antibody, also known as consensus binding site (CBS). This phenomenon occurs through van der Waals and electrostatic interactions in the CH2 and only through electrostatic interactions in the CH3 [67, 68]. The Fc, as said before is one of the three fragments from the antibody structure, known as the crystallizable region and the one that does not bind the antigen.

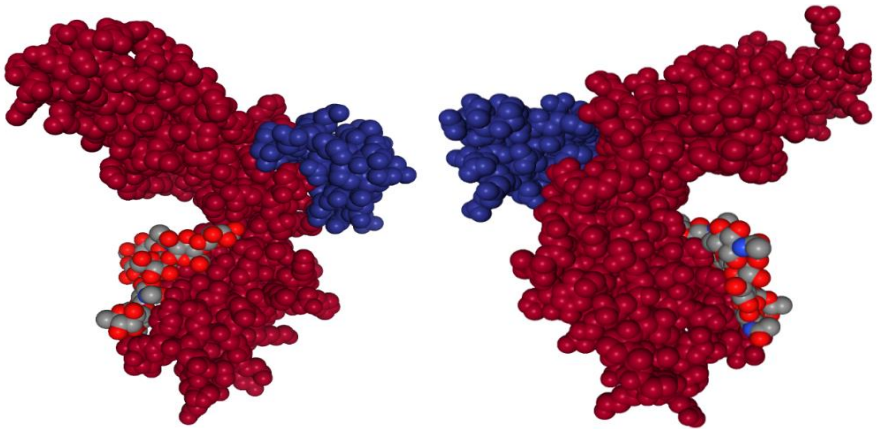

Figure 6: Crystallographic structure (left and right view) of the protein A antibody-binding B-domain (blue structure) to the Fc region (dark red structure). It can also be seen, the group of carbohydrates which has a core common to all human IgG (red structure) (1FC2.pdb) [69].

1.2.2 Different stationary phases

As mentioned before, the requirement of high production quantities brought by the biomolecules with therapeutic purpose is not being accompanied by the downstream process' improvements, which is the most expensive part of the production system [70]. The only way to reduce the costs is increase the final ratio product per time unit, in another words, the overall throughput. The most common path to get this is the scale-up of operation, by using more or bigger chromatography columns, using continuous methods or increasing the stationary phase capacity of purification, essentially by an optimization of its physical and chemical properties [3, 58].

The support matrix of a stationary phase must present some desirable features, some of them are high mechanical strength, high surface functionality for immobilization of ligands, low non-specific adsorption, absence of toxic leachable and stability in cleaning in place (CIP) and sanitation solutions. A variety of materials that satisfy these requirements are available and they can be classified in three main groups, accordingly to their general properties.

The first class are the natural polymers, this group is defined by low solid densities (high water percentage 90-96%), limited mechanical strength, smaller pores (gels), easy functionalization, resistance to CIP and low non-specific binding. As example of matrix materials in this group we can mention agarose, cellulose, dextran, and chitosan.

Other class, are the synthetic polymers, defined by higher solid densities (50-80% water), possibility of larger pore sizes, greater mechanical strength, resistance to CIP, moderate or high non-specific binding and relatively difficult to functionalize. This group has matrix material elements like, acrylic polymers, poly(methacrylate), poly(styrene-divinyl benzene), acrylamido and vynil co-polymers.

Finally, the inorganic materials group (third one) is defined by the highest solid densities (30-60% water), possibility of larger pore sizes, rigidity, may not be resistant to CIP, moderate or high non-specific binding and relatively difficult to functionalize. Examples of matrix materials are hydroxyapatite, silica, controlled pore glass, zirconia and TiO_2 [3].

Most of supports used to date are based on particles (beads) that are packed into a column forming a homogeneous bed [71, 72]. From the up mentioned groups, the materials that satisfy the requirements for stationary phases are: gels, using materials as agarose or cellulose per example; rigid porous media, with silica, alumina and others as base; and composite media, with silica/dextran or agarose/dextran mixes. More recently continuous stationary phases, known as monoliths, have appeared. These can be produced from organic or inorganic materials or from a mix of both, we will come later to this topic.

A high binding capacity is a crucial parameter when the high productivity is desired. As almost all the separation techniques are dependent on the interaction between the ligand and the molecules, if the surface of interaction increases, the number of available sites for molecule interaction can also increase leading to a higher capacity (beads and monoliths support matrices are usually porous) [58]. However, porosity is a form to enhance the surface area as long the pore size is enough to the molecule pass through the porous network [3]. Another important aspect, when constructing stationary phases, is the form of how the surface modification is taken to introduce the ligands. The global architecture of the ligand will affect

the binding capacities and sometimes the non-specific interactions, these ones could unpredictably influence the adsorption process for an individual molecule, so it is necessary to modify chemically the support matrix in order to functionalize it [58]. There are some general possibilities to connect ligands to the pore wall of a resin (Fig. 7): without spacer, when ligands are connected directly on the surface wall, which could limit the interaction since many of them are accessible; with spacers, this ones developed to attend the accessibility problem, but according to some controversial discussions in the literature is believed they can induce non-specific interaction; and polymeric modification, based on grafted ligands, showing a more promising different path to solve the accessibility issue and with a high binding capacity [58].

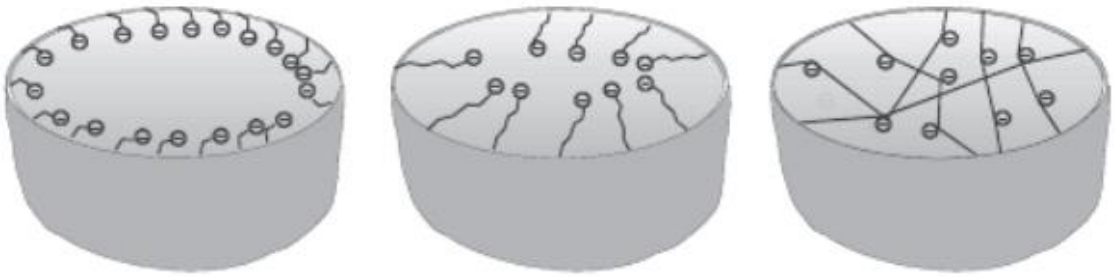

Figure 7: Three different ligand architecture in the stationary phase pore wall, from the left to the right, without spacer, with spacers and polymeric modification [58].

1.2.2.1. Monoliths

Monoliths are the fourth-generation chromatography material, coming after the beads, the porous particle-based columns and the membrane adsorbers [73]. They are considered a special type of chromatographic column, due the fact they have a single unit of a homogenous stationary phase with various interconnected channels [74]. Also, they have become popular as an efficient tool for the purification of large molecules, since they have high mass transfer properties and short purification times. Once the stationary phase of these structures could be of many different chemistries, it allows the purification of different types of biomolecules with different characteristics [73].

Even with some limitations like cannot be used for size exclusion chromatography (SEC), occurrence of fouling/clogging leading to an increase of pressure and decrease of DBC without the possibility of back-flush (in the case of tubular monolithic columns) and problems with lipids because they bind irreversibly in the column, this type of columns have several advantages as:

- The biomolecule separation occurs predominantly by convective flow through the monolith channels, which have a 1,000 nm diameter, allowing high flow velocity and consequently, high throughput purifications [75].
- High porosity due to their large interconnected channels, consequently, the pressure drop in this type of columns is much lower than in particle-based resins [76, 77].
- Low absolute surface area, although due to their porous structure they have high adsorption area leading to high DBC [73].
- Lower overall process time than particle-based resins due to the high flow velocity and low pressure drop [78].
- The stationary phases allow a high degree of freedom, because they can be made with a range of raw materials, different morphologies and channel diameters [79]. Additionally, they can be divided in three main groups: organic, polymer-based, which media as a good pH stability and customizability, but the columns are not very stable mechanically reducing their lifetime; inorganic, silica based, with excellent stability and separation efficiency, however with an high time consuming and sophisticated manufacturing ; and hybrids combining the advantages of the last two [80].
- High customizability, since they can be modified to the needs. As mentioned before, there are various chemistries, also, there are different actives binding sites, shapes and sizes (disks and tubes) available. Related with the disk shape (0.34 mL), there is a minor advantage that enable the black-flush in order to resolve clogging problems, since they do not have a specific flow direction.
- Scalability, since they are easy to scale up without modify the column. Disks can be stacked up until four in the same housing, increasing the efficiency and capacity without decreasing the resolution [73].

Monolithic supports have been extensively used for the purification of different biomolecules, which can be divided in three main classes: virus, the major class, applied in gene therapy and in the production of recombinant proteins [81]; nucleic acids, since the plasmid-based DNA introduction (1990s), extensively used in medical diagnosis [81]; and proteins, as different materials and chemistries can be used for monoliths, the principles used in conventional particle-based chromatography can be applied. For example, ion-exchange monoliths have been used for the purification recombinant proteins [82], bovine serum albumin was purified by HIC monoliths [83] and affinity chromatography was used for the purification of immunoglobulin G [84].

Figure 8: DEAE Weak anion exchanger monolith with the respective housing.

1.3. Biomolecules adsorption

Adsorption is defined as the concentration of species at the solid stationary phase surface. More specifically, it is usually described as the relation between free protein concentration (C) and the adsorbed protein concentration (q) in the solid phase at equilibrium [3]. In liquid-solid systems this relation is temperature dependent, so it is generally determined at a constant temperature and because of that it is named adsorption isotherm. Their data is very important in order to reach great process analysis, design and optimization in adsorption chromatography [3].

The interaction with the surface can result from different types of forces, like for example dispersion-repulsion forces (van der Waals) and electrostatic forces that depend on the net charge of the molecule. The concentration of molecules near the surface depends on the distance from it, since the short-ranged repulsive forces are dominant very close to the surface, but as the distance of it increase, they decrease very quickly. On the other hand, electrostatic forces are from long-range nature [3]. Looking for what have been said the process seems quite simple, but adsorption of macromolecules is generally more complicated than that and not agreeable to a precise theoretical treatment. Because of some complicating factors and due to the complexity of the method, an empirical or semi-empirical approach is needed to describe the adsorption equilibrium. So, following empirical determinations of adsorption equilibria, the data is usually correlated using suitable adsorption isotherms, as mentioned before [3].

1.3.1. Langmuir model

Among many, Langmuir model is the most widely used to explain adsorptive phenomena in chromatography. Originally developed for gases adsorption on metal surfaces, Langmuir isotherm is a model commonly used to describe the protein adsorption equilibrium. As mentioned before, these isotherms are obtained while maintaining constant the temperature, but also, the pH and the mobile phase composition [3, 58]. This model define that molecules are adsorbed on a limited number of sites, where each site can afford only one molecule and are organized as monolayers. At the low concentration range, it is expected a linear relationship between the bound molecules and the free molecules at equilibrium. But at higher concentrations, the adsorption sites become saturated and the relation becomes non-linear reaching a maximum capacity, and leading to a curvature in the isotherm, turning it into an asymptote. So, the maximum capacity is generally limited by the accessible area or by the number of binding sites, while the linear limit is dependent on the concentration of accessible binding sites [3].

Accordingly, the binding capacity (q) has to be defined for a specific process, resin and for each type of molecule [58] being represented as:

$$q = \frac{\text{Bound molecules}}{\text{Volume of packed resin}} \quad (1)$$

Langmuir model also states that every adsorption site is energetically equivalent and there is no interaction between adsorbed molecules [85]. Thus, by assuming equilibrium the next equation will be reached for describing this type of isotherm:

$$q = \frac{q_m K_a C}{1 + K_a C} \quad (2)$$

Where q is the adsorbed concentration, q_m the maximum adsorption capacity, C the concentration in solution at equilibrium and Ka the association constant (equilibrium constant). At low protein concentration, if one has $K_aC \ll 1$, it can be reduced to the linear isotherm expression:

$$q = q_m K_a C = mC \qquad (3)$$

Where m is a constant, which is called the Henry constant. Oppositely, if K_aC»1 the isotherm approaches the maximum capacity $q=q_m$.

In figure 9 it's possible to see a Langmuir isotherm and how K_a and q_m can be obtained [1].

Nevertheless, is important to say that the original model may not be able to explain all biomolecules adsorption, because it does not take in count the solute-solute interactions and the steric rearrangements on the support ligands [86].

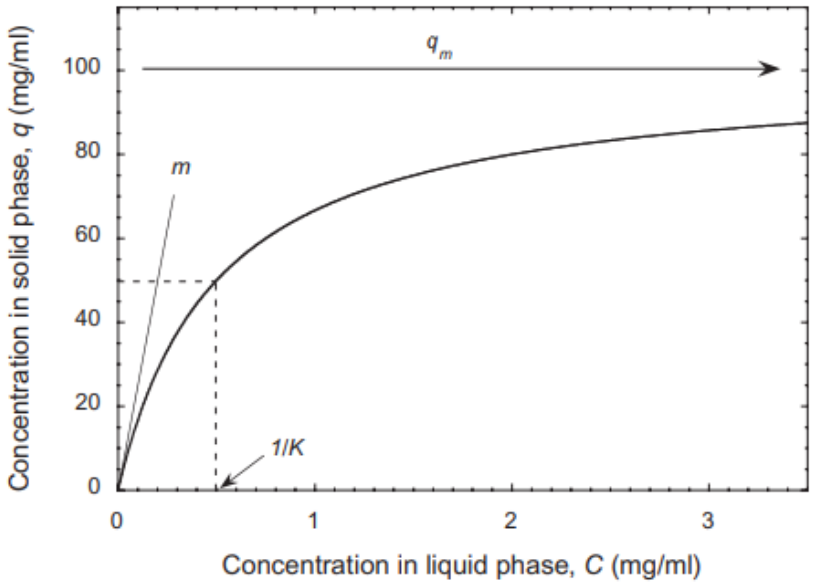

Figure 9: Langmuir adsorption isotherm with the limiting behavior for low and high C values. m is the initial slope and 1/K is the liquid phase concentration at equilibrium with one-half of q_m [3].

As mentioned before, the capacity of chromatographic column to capture molecules is frequently characterized by the dynamic binding capacity (DBC), an important topic to characterize the support [3]. DBC can be related to the equilibrium binding capacity (EBC), known as static capacity q_m. EBC is applicable only in conditions where the column has infinite efficiency when it is not influenced by dispersive factors. Under these circumstances it depends only on thermodynamics and molecule feed concentration, being expected to be independent of flow and column length. However, the relation between EBC and DBC is more

complicated being dependent on the exact nature of the dispersive mechanism. Even, in cases with very favorable binding, DBC can reach 75% of the maximum static capacity (q_m) [3].

1.3.2 Thermodynamic study of adsorption

As seen, traditional methods, like Langmuir isotherms, cannot totally characterize complex adsorption mechanisms in liquid chromatography. Still, they are a good initiation to explain the adsorption for example in IEC and HIC supports. The main problem with these methods is that they are limited, since they do not consider non-ideal effects associated with the adsorption of biomolecules like large proteins [87]. So, in order to solve this problem, these complex mechanisms usually are studied by thermodynamic analysis.

The thermodynamic parameters of adsorption and desorption can be accessed by batch equilibrium experiments, analyzing van't Hoff plots or from microcalorimetric measures. In the past few decades, Isotheral Titration Calorimetry (ITM) and Flow Microcalorimetry (FMC) showed a great capacity to help understand and underlying adsorption mechanism of a wide range of biomolecules at different chromatographic supports [86, 88, 89].

At the liquid-solid interface, different types of interactions occur between the biomolecules, sorbent, solvents, and other solutes, contributing all as a net to the biomolecule behavior. The viability of a protein to be adsorbed is determined by the change in the standard Gibbs free energy (ΔG), in the case of a reversible process, represented by the following equation:

$$\Delta G_{ads} = \Delta H_{ads} - T\Delta S_{ads} \quad (4)$$

where ΔH_{ads} and ΔS_{ads} are the adsorption enthalpy and entropy changes respectively [88].

When adsorption or desorption happen, a small thermal signal is released, which can be related to the adsorption mechanism. So, through microcalorimetry, enthalpy measurements can be obtained providing useful information, which can help understanding adsorption mechanisms on the support [86, 88, 89]. Basically, microcalorimetric methods allow the measurement of the heat flow caused by the interaction during the adsorption process. More specifically, in the case of flow microcalorimetry, it allows the real-time measuring of the heat signal during the adsorption or desorption of the biomolecules who flow through the support. Due to this capacity, flow microcalorimetry provides an improved understanding of

the driving forces, mechanisms and kinetics involved in complete interaction processes. So, it simulates a packed-bed chromatographic system at the micro-scale and the results are expected to represent the mechanism that happen really in the chromatographic system [86, 88].

In figure 10 the schematics of a flow microcalorimetry system can be seen. Accordingly, micropump syringes are used to maintain a controlled constant flow rate through the system and the samples are injected into the line with a multiport valve system. This injection system has an adjustable injection loop supporting different sample volumes. The microcalorimeter cell, where the adsorbent is packed, has a total volume of 171 µL. Interfaced whit it there are two highly sensitive thermistors capable of detecting very small energy changes inside the cell with a short thermal response time. After the cell the effluent passes through the UV detector, allowing biomolecules output control.

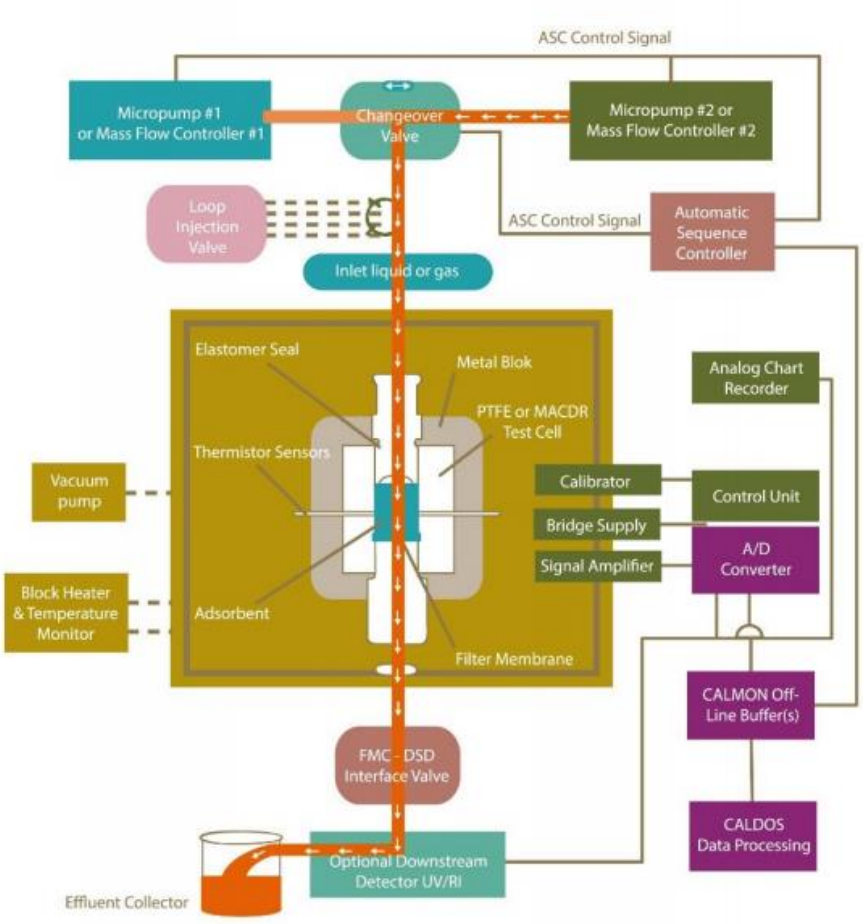

Figure 10: Schematics of a flow microcalorimetry system with all its elements.

A typical FMC thermogram (FMC output) can be seen in figure 11. Thermograms can present negative and positive signals which result respectively from energy absorption and energy release during the interaction. Namely, the endothermic events lead to a negative peak on the thermogram, since it registers a decrease of energy in the cell and the exothermic ones lead to a positive peak (Fig. 11), as it is listed an increase of energy [86, 88, 90]. The first exothermic peak in figure 11 is also the calibration peak, where a 30 µW heat impulse was induced for 500 s. This type of peak calibration is commonly used to correlate the signal generated with the energy impulse.

The data obtained from FMC can give us information about the kinetics of adsorption obtained under the condition of experiment, more properly, solution flow rate, volume, adsorbent bed packing density and temperature [91, 92]. Through the knowledge of the magnitude and chronology of thermal events during and after the biomolecule-adsorbent interaction, the adsorption mechanism may be elucidated [86, 88, 93].

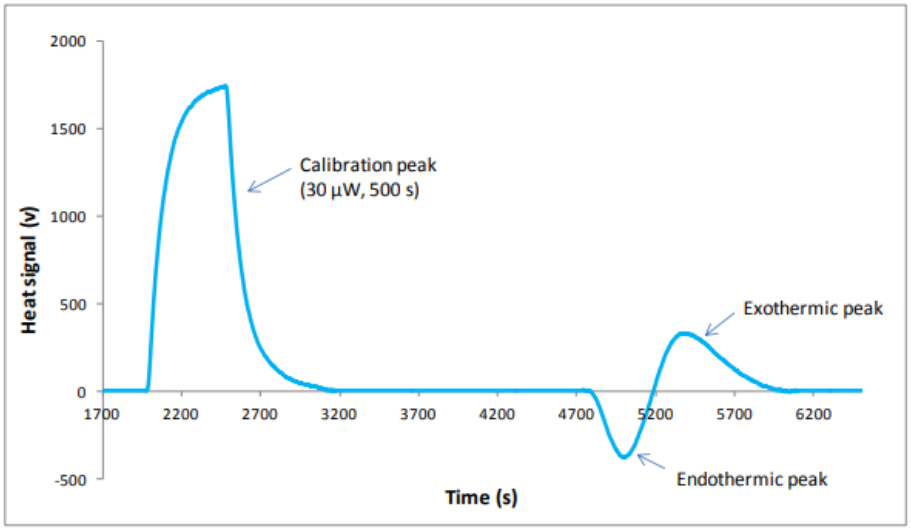

Figure 11: Example of a characteristic thermogram showing a calibration peak (electrical pulse given to the system) followed by an endothermic and exothermic peak, respectively.

1.3.3 Surface plasmon Resonance

Another technique used in the study is Surface Plasmon Resonance (SPR) using a biosensor to evaluate the binding affinity between ligands and biomolecules. It is used for analyses in real time, quick monitoring between drugs and biomolecules like nucleic acids and different proteins, antigen – antibody interactions, and receptor – ligand interactions, in different fields (like food, life sciences and medical testing and environmental monitoring) [94].

Defined as one kind of physical optics phenomena and produced with coupling of thin metal films, SPR can be find in several applications since its invention time, around 1960s, when Otto and Kretschmann [95] demonstrated optical excitation of surface plasmons by the method of attenuated total reflection. It was in 1982, when Nylander *et al.* [96] applied for the first time SPR on biosensing. Later, in 1983, Liedberg *et al.* [97] extended the use of SPR to immunosensing by studying and determining the interaction of immunoglobulin G with its antigen.

Due to the impact of SPR studies in different areas and due to the wide range of applications of SPR, some enterprises invested in this area and started to create commercial instruments. Accordingly, around 1990, Biacore AB created and launched the first SPR commercial platform, opening doors for an even more widespread application of the SPR technique.

1.3.3.1. SPR principle

In a wide range of fields, the system created by Kretschmann [98] is the most applied SPR sensor type. In all cases, SPR biosensors, are constituted by some common components: a light source, a detector, a thin metal film, a prism, a biomolecule and a flow system (Fig. 12) [98].

On its principle, the incident light that will come from the denser medium exposure to the light-thinning medium, at an appropriate range of incident angles, will lead to a total reflection creating some waves in the light-thinning medium. At the same time, the amplitude decays exponentially with depth penetration, leading to an electronic oscillation of the sample close the metal surface, forming a propagation density wave along the metal film and the sample near it, commonly named surface plasmon wave (SPW). When the incident light at

certain angle (critical angle) leads to minimum intensity of reflection spectrum, the SPR resonance angle is

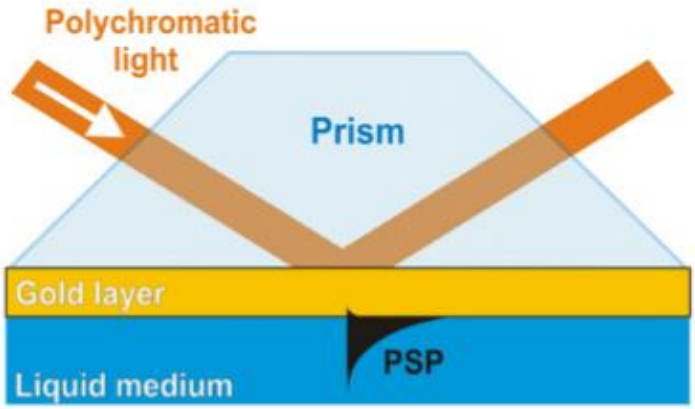

Figure 12: Kretschmann geometry of the attenuated total reflection method (ATR), representing a polychromatic light exciting propagating surface plasmons (PSP) [99].

obtained. Hereupon, any change at the refractive index or dielectric constant will conduce to a different position of the resonance peak (resonance angle or resonance wavelength) and the interaction information at the gold film will be obtained (Fig.13) [100]. Basically, if the analyte binds or get recognized (in the case of antigen-antibody) by the ligand coupled onto the metal film surface of the device, the refractive index of this interface would change. This refractive index modification would also modify the resonance angle of SPR and additionally it would be proportional to mass change of the biomolecules linked to the metal surface (Fig. 14) (the RIU – refractive index unit, is normally used as the SPR detection unit) [101]. In another words,

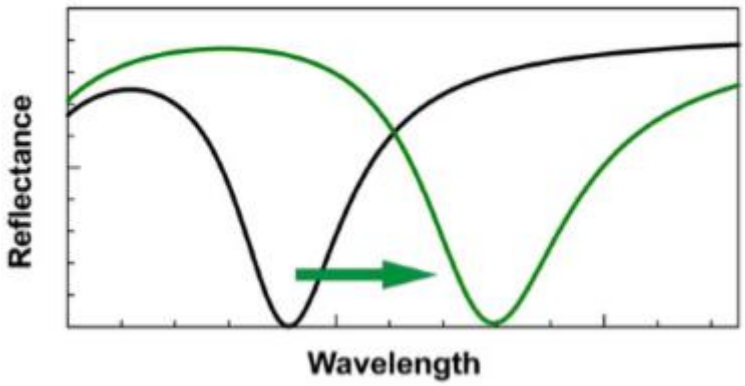

Figure 13: Spectrum of reflected light with a characteristic SPR dip for two different values of refractive index in a gold surface [99].

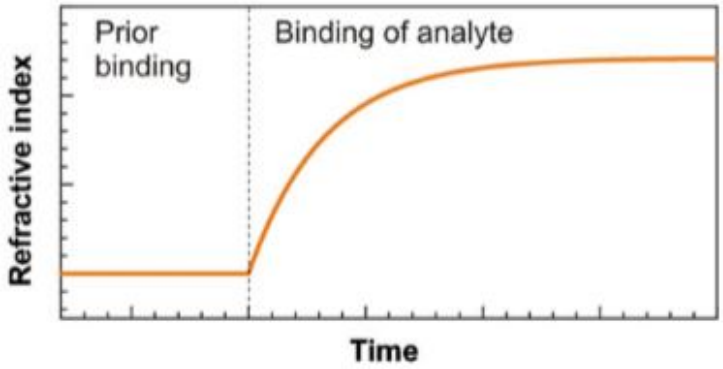

Figure 14: Example of evolution in the refractive index when the analyte is adsorbed and recognized by the surface [99].

SPR works with a special mode of the metal interface (dielectric), called surface plasmon, and it basically measure the change of the refractive index when an interaction between molecules happen in the surface of the sensor. These sensors applicate the surface plasmons on the planar metal face, propagating them on it and because of this they are sometimes known as propagating surface plasmons (PSPs). The PSP depth penetration, in this type of sensors, with a gold and dielectric frontier layer normally stays in a range between 100-600 nm (in visible and infrared wavelengths).

Important parameters in SPR biosensor performance to be considered, are sensitivity, linearity, accuracy, repeatability, dynamic range, resolution, and limit of detection (LOD). These last two ones distinguish from the others since they are considered key parameters to the SPR sensor performance evaluation [95].

Nowadays a wide number of SPR-based sensors have been and are commercialized. Being Biacore (now inside of Cytiva, US), the SPR device who has the highest refractive index resolution (measured values around $1x10^{-7}$ RIU), the most used nowadays, dominating the market. Since its first introduction as a SPR instrument, Biacore company developed a wide range of products as Biacore C, X100, T200, S200 and 8K, being its latest version the Biacore $8K^{+}$. These systems, can offer an observation of the biomolecular interactions in real-time, allowing the detection of molecular changes *in-situ* for every second without labeling [102].

1.3.3.2. SPR sensor chips

Depending on the model and purpose of using SPR there are many types of sensor chips. One of the most applied in different areas is the CM5 sensor chip. This sensor chip, as the particularity of having a coating layer of carboxymethyl dextran on the gold film and the capacity of being coupled with biomolecules and chemical groups like -NH_2, -SH, -CHO, -OH, -COOH, that bind covalently to the dextran's carboxyl group present on the gold surface. Additionally, flow cells in the sensor chip (more specifically 4) differ from macroscale flow cells in different points as: they can be controlled for independent responses separately; they are very small (around 60 nL), present reduced mass transport effects, as analyte is independent of diffusion to reach the sensor surface, leading to shorter kinetic measurements [102].

The correct immobilization of the antibody or of the antigen on the surface, is one of the crucial steps to achieve an immunosensor with good sensitivity, high specificity and the best detection limit possible [100]. The most rapid path of detection, is when the antibody is immobilized on the sensor surface and then the antigen binds directly to the antibody, resulting on a SPR response directly proportional to the concentration of the analyte in solution. One of the most used methods of immobilization is based on chemically preactivated surfaces followed by covalent amine coupling [103]. Nevertheless, this methodology takes to randomly antibody-oriented immobilizations, resulting in a low linkage of the antigens to the antigen-binding sites and because of it, reduced sensitivity of the immunosensor [104]. In order to solve this problem, many efforts were done to develop methods able to produce efficient antibody-based surface immobilizations on biosensors [105].

Other strategies to the antibody immobilization, pass through using tagged antibodies either by chemical modification or genetic engineering, this solution has the advantage of the existent high affinity between the ligand and their respective analyte. One example is the biotin-streptavidin pair, on this system the antibodies need to be previously biotinylated and then they can be strongly immobilized to the gold surface coated with avidin or streptavidin [103, 106]. Two cases of genetic engineered antibodies are the poly-histidine tagged antibodies, these have the particularity of high affinity to bind nickel-nitrilotriacetic acid (Ni-NTA) coated surfaces and the antibodies tagged with cysteine, that can bind to the gold film in thiolate (Fig. 15) or disulfide form [107].

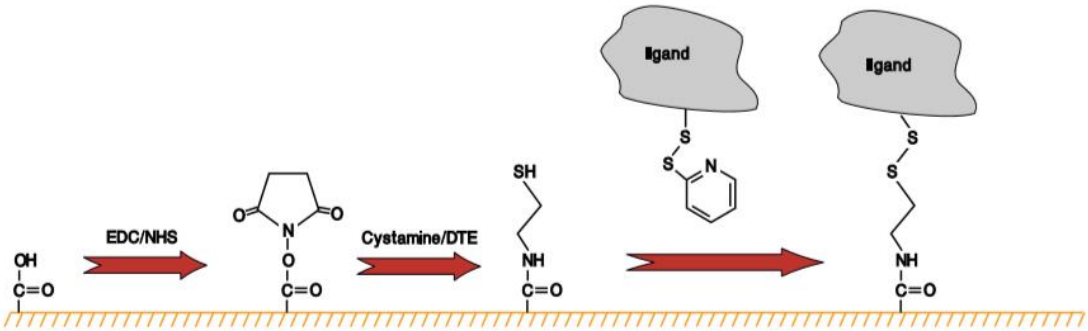

Figure 15: Surface thiol coupling of ligands to the surface. Took from Biacore Sensor Surface Handbook [108].

Another choice that could be used, overcoming the antibody modification, is the use of two known proteins of microbial origin before the introduction of antibodies. Proteins A and G link to the antibody by their Fc region, this means that the antibody's two FAb region remain accessible to antigen detection [109, 110]. Although, this alternative presents some drawbacks as: occupation problems, since bound antibodies will have steric complications with the protein if the four binding sites in Protein A or G are occupied (essentially because of their sizes); and correct protein immobilization, because the success of the antibody immobilization and forward immunoassay will be dependent on the density of well-oriented protein. To solve this, poly-cysteine tagged proteins A and G have been applied, because their use showed to be effective on the correct orientation linking through thiol adsorption to the gold film [105].

Nowadays, is already possible to isolate the recognizing peptides specific to the inorganic material, being used as molecular blocks to develop new applications, this is possible due to the development of combinatorial genetic techniques [111]. As example of this approach, specifically to the gold surface, there is a poly-peptide with sequence (MHGKTQATSGTIOS). This peptide is first selected by surface display and then is engineered to improve binding properties repeating it form three times and anchoring it to the gold film. The use of this peptide is relatively recent, and some works reported the construction of two recombinant antibody fragments [112, 113], although, the exact mechanism of the full process is not totally known, but it has kinetic parameters and binding energy comparable to the one observed in alkanethiols [114].

1.3.3.3. SPR main applications

The major application of SPR is biosensing and in the area of biomolecular analysis. The technique can be very useful in materials characterization, drug development, medical diagnosis and food quality assessment.

In materials characterization, the technique is very advantageous for monitoring film deposition, like Langmuir-Blodgett (LB) and layer-by-layer (LBL), once it is possible to convert the variation in the SPR angle to the thickness (*d*) of the film adsorbed on the sensor surface, by doing an angular scan after every deposition step and with the use of the Fresnel algorithm [115, 116]. There are two possible cases, if refractive index (*n*) is known and if the same is unknown. The first case is the easiest one, because when the refractive index is known or estimated the thickness of the films is easily determined by the linear relationship between *n*, number of layers and the calculated *d* [117]. When the reflection index is unknown, it is also possible to determine *d*, to do it there are two different ways to determine a unique value of *d* and *n*: do the SPR analysis in two different medias or do the analysis at different light wavelengths [117]. One example of the last path is expressed in Fig. 16, where four different wavelengths were used accoupled in two pairs (one pair 655 and 782nm, the other, 670 and 783nm) to perform the angle scans in air. With the same software, the relation between the *n* values and the corresponding *d* values was calculated [115].

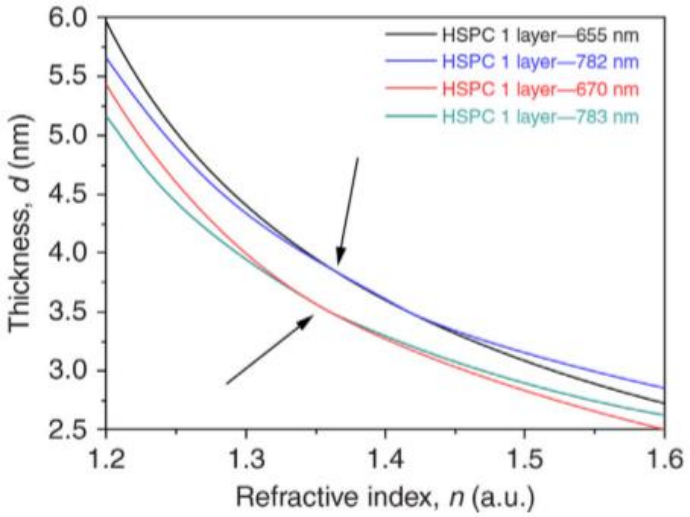

Figure 16: Example of intersection points (signed with arrows) finding from thickness (d) versus refractive index (n) of one monolayer of HSPC (hydrogenated L-α-phosphatidylcholine) in air with different wavelength method [115].

The SPR technique has also been considered a powerful tool for the pharmaceutical area in drug development for the selection and design of new therapeutic molecules, as SPR analysis gives information about biomolecular interactions kinetics and binding level by means of association and dissociation constants. When the binding kinetics is determined, it is possible to establish the duration of action and the chemical compound clinical benefit to a specific target. Additionally, this technique in this drug discovery field can identify the type of binding between two reactants, in real-time determine the affinity constants of the interaction process, calculate the rates of association and dissociation, and quantify the concentration of interacting molecules [118]. An example of these applications is a drug permeation study done by the immobilization of liposomes on a sensor chip. On this study, it was tested the affinity of two potential antimicrobial peptides with different lipid membranes, more properly, DMPC and DMPE. As can be seen in Fig. 17, the sensor response increases proportionally with "kalata" peptide concentration, it is also possible to see when at high concentrations the peptide binds more to DMPE than to DMPC, which is in accordance to the affinity values $9.98x10^3$ (to peptide-DMPC) and $43.4x10^3$ (to peptide-DMPE), obtained by simulation using a two-state reaction model. As the peptide showed high affinity for membranes containing phosphatidylethanolamine, like DMPE, it was suggest that "kalata" peptide will preferentially bind bacterial membranes [119].

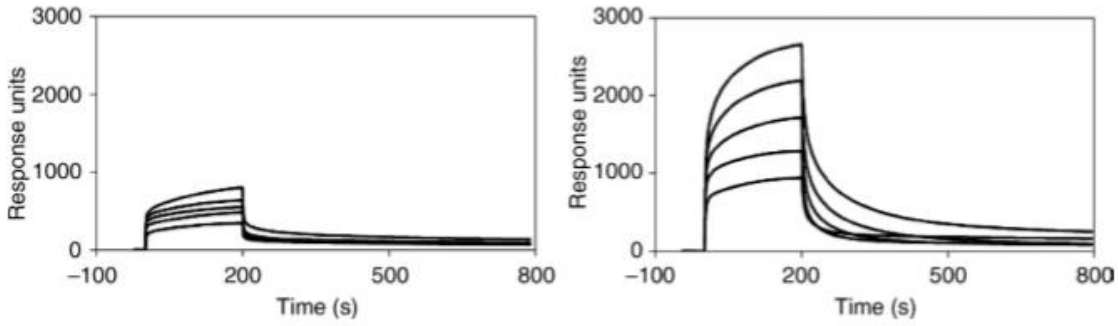

Figure 17: Sensorgrams for kalata B1 binding to DMPC (at the left) and DMPE liposomes immobilized on the surface (at right) [119].

Due to the capacity of real-time interaction monitoring and to be a label-free technique, SPR biosensors received a special attention for medical diagnosis, once the technique led to the production of high sensitivity and reproducibility analysis. Moreover, some modification at the surface level can be done to increase the sensitivity of the sensor and

consequently aiming a decrease in the detection limits. As example, there is the case of cardiac troponin T, which is immediately released in the bloodstream when the patient suffers an acute myocardial infarction (AMI) and it is also a cardio specific marker for myocardial cell damage [120]. Because of this marker importance, some studies have been done in order to know it better. Dutra and Kubota [120] developed a sensor based on the biotinylated anti-cardiac troponin T, which consists on a gold sensor coated by a dextran layer. The dextran's carboxylic groups allow it linkage to the streptavidin (second layer) via primary amino groups. The last step is the combination between the second layer and the antibody that is specific to the cardiac troponin T (third layer).

To improve the detection of biomarkers for disease diagnostics, multiplexed systems, surface plasmon resonance imaging (SPRI) (Fig. 18), have also been developed to allow the simultaneous detection of multiple DNA, RNA and proteins at the same electrode [121].

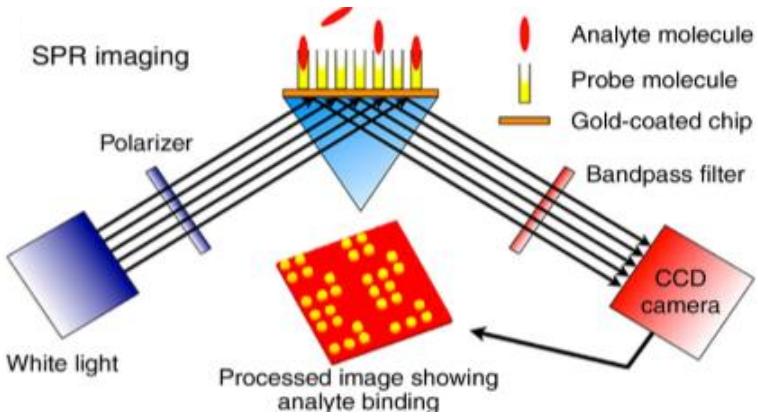

Figure 18: Schematic of SPRI experimental setup, the bio affinity adsorption leads to a local refractive index change. A difference in the monochromatic reflectivity image of the microarray will be noticed in the prism internal reflection geometry at the SPR angle [121].

SPR based biosensors have been likewise applied in some matters related with food quality, as pathogen detection, composition adulteration and environmental pollutants search, their use is essentially due to their demand's response like fast and reliable analysis to provide information about quality and safety to food industry and control authorities [122]. One example is a sensor developed for *Salmonella paratyphi* detection, which is a pathogenic microorganism in foodborne infections in humans, leading to diarrhea, fever and abdominal pain. The sensor basis consists on an Au sensor immobilized with protein G on the surface, in order to orientate correctly the against *S. paratyphi* antibodies [123].

Other case of these food quality sensors is a sensor to identify *staphylococcal enterotoxin* B (SEB), one of the ten most serological types of enterotoxins produced by *Staphylococcus aureus*, based on a sandwich-type antibody assay. On this format, after the first antibody layer been immobilized at the surface (capture antibodies), the antigen (target molecule) is passed through the sensor and captured by the first layer. Then a secondary antibody solution is put in contact with the sensor and it will bind to the captured antigen, increasing the sensor response by increasing the level of bound biomolecules [101]. It was proved that the sandwich assay increased the sensor response by 10 times more, with a sensor detection limit around 0.5 ng/mL on milk [124].

Chapter 2. – Aims of the study

Protein A affinity chromatography has been the most used purification method for therapeutic antibodies in industrial processes once it selectively purifies exploring molecular recognition and is an easy methodology. However, this type of chromatography has some cost-associated drawbacks and upstream titer limitations. This, coupled to the demand for high purity and quality requirements postulated by regulatory agencies and to the increasingly growth of monoclonal antibodies importance in therapeutic market, led us to develop some work with the purpose of getting a better performance of engineered protein A resins.

This study is part of a major aim where we intent to develop a Protein A monolithic column that shows better performance for the capture of antibodies from cell culture supernatant. In order to reduce the downstream costs, lead to a favorable scale-up and improve the performance of the process, every effort is worthwhile. In the present work our effort is focus in two main goals: the thermodynamic evaluation of matrix properties (2,5% QA monolith) by analyzing its response to the adsorption of a model protein (Bovine serum albumin (BSA)); and the capacity assessment of an engineered ligand for antibody capture.

Referring to the first goal where, as mentioned, a 2,5% QA monolithic matrix is used, multiple injections of different volumes of the same concentration of BSA were performed. Depending on the loop volume the column was submitted to different protein surface concentrations, leading to different responses and changes in volume linearity status. Also, multiple consecutive injections were performed in order to understand what happens under overloading conditions and to observe the point at which the monolith stops to adsorb. In this way, for the first time it was possible to analyze in the flow mode the thermodynamics of monolith convective media not limited by diffusion as particle-based resins. To perform this initial part of the work, it was used the Flow Microcalorimetric system, since it has the ability to give an improved understanding of mechanisms, kinetics and driving forces involved in the interaction process of biomolecules in their chromatographic systems adsorptions.

The second aim is subdivided in three different objectives: interaction study of protein A novel ligand, presenting eight binding domains, with an IgG antibody; optimization of different ligand immobilization procedures; and comparison of the novel ligand with the commercial already existent engineered Z form (four domains, MabSelect SuRe), in terms of antibody isolation potential. Two prototypes variants of the novel ligand with 8 B binding domains were used. One of them is marked with a poly-histidine tag (B8(RH_4)) and the other is

tagged with cysteine-lysine-cysteine-lysine tail (B8 cys-lys-cys-lys). These two are thought, as previously mentioned, to be used primarily in protein A chromatography, namely in the direct capture of monoclonal antibodies due to the high specificity of the antibody-protein A bind.

Therefore, and taking in mind the two new prototypes variants have the double binding sites of the well-known MabSelect SuRe, it is of interest the study of the relation between the number of binding sites and the quantity of antibodies captured, as well as to compare the amount of each other and see what conditions are affecting the results. In case the prototypes present highest values of antibodies captured, these could offer great improvements in terms of efficiency, since the percentage of return will be higher and the scale-up will happen with less losses.

To perform this last part of the work, it was used SPR biosensor (Biacore T200). The previous mentioned ligands were immobilized in two chips: Ni-NTA chip, containing nickel-nitrilotriacetic acid, which has high affinity for the B8(RH_4) poly-histidine tag and immobilizing due to a chelate formation; and CM5 chip, using a maleimide coupling kit for the immobilization (both by Biacore, now Cytiva Life Sciences). Afterwards, the amount of antibody in the surface was measured in response units and affinity.

Chapter 3. - Methods

3.1. Materials and Equipment

For the monolith study and characterization, BSA (from Sigma-Aldrich) was used as a model protein for the flow microcalorimeter analysis. Since BSA presented high aggregation level and consequently blocking drawbacks at the microcalorimeter monolith, BSA monomer purification was studied and optimized. For this purpose, were used three different chromatographic supports: it was used a CIMac^{TM} DEAE-0.1 mL disk-shaped monolith (diethylamine anion exchanger from BIA separations), kindly offered by Professor Ales Podgornik (University of Ljubljana, Slovenia); a CIMac^{TM} DEAE-0.2 mL disk-shaped monolith, also offered by Professor Podgornik; and a Toyopearl DEAE-650M resin. The collected BSA monomer was concentrated in 10 kDa concentrators (Corning® Spin-X® UF). After purified and concentrated, the real-time enthalpy measurements were performed with a flow microcalorimeter FMC 4 Vi, from Microscal Limited (London, U.K.). Data was collected and analyzed with CALDOS4 software, from Microscal Ltd (London, U. K.) and peak deconvolution were done using PEAKFIT software package (version 4.12, Seasolve Software Inc., San Jose, USA).

At the second main part of the work, a fully humanized IgG was chosen to be the analyte in the interaction of the two new ligand variants in study: B_8-$(RH)_4$ and B8-cysteine-lysine-cysteine-lysine protein A. Both protein A variants and the IgG were kindly offered by Professor Sonja Berensmeier (Bioseparation engineering group (Technical University of Munich, Germany)).

Different sensor chips were used for the immobilization of the different protein A variants and subsequent analyte analysis. Namely, for the B_8-$(RH)_4$ protein A immobilization, it was used a Serie S sensor chip NTA 28994951 from GE Healthcare (Uppsala, Sweden), since it has NTA on its surface that will interact with $NiCl_2$ and will form a chelate between the protein histidine tag and que Ni^{2+} that will coat the gold film surface, leading to the correct immobilization of the protein. On other hand, for the B8-cys-ly-cys-lys protein A immobilization, a Serie S sensor chip CM5 29104988 from GE Healthcare (Uppsala, Sweden) was used coupled with a Maleimide Coupling kit also from GE Healthcare (Uppsala, Sweden). Afterwards, IgG was passed through both of surface prepared chips. Additionally, to compare the response of the tested ligands to the already existent on the market MabSelectSuRe^{TM}, IgG was passed through a Serie S sensor chip Protein A 29127555 from GE Healthcare (Uppsala,

Sweden) that is ready to use and already has this protein immobilized on the surface. All the experiments were performed in Biacore T200 from Biacore (Uppsala, Sweden). Data was collected and analyzed by the evaluation software of the Biacore apparatus.

All the following reagents and salts were used in solutions and buffers in the development of this work: MOPS (Fisher scientific, Loughborough, U.K.), $Na_2HPO_4.7H_2O$ (AppliChem GmbH, Darmstadt, Germany and Panreac Química, Barcelona Spain), $NiCl_2.6H_2O$ (VWR, part of avantor, USA), $MgCl_2.6H_2O$ (labkem, Bacelona, Spain), Glycine (Fisher Scientific, Geel, Belgium), NaCl (labkem, Barcelona, Spain), EDTA (Panreac,, Barcelona, Spain), $H_2NaO_4P.H_20$ (Sigma-Aldrich, St Louis, USA), BSA (Sigma-Aldrich, St Louis, USA), Histidine , TRIS Base (NZYTech, Lisboa, Portugal) , NaOH (José Manuel Gomes dos Santos Lda., Odivelas, Portugal).

3.2. Bovine Serum Albumin Monomers Purification

3.2.1. Purification with different supports

With a volume of 0.1 mL, the CIM DEAE monolithic disk was inserted into a polypropylene housing (from BIA Separations) and posteriorly it was plugged to the ÄKTA Purifier system, where all the experiments were performed. It was passed through the system purified water (Mili Q), because the disk was stored at 20% ethanol, and before the sample injection the system was equilibrated with approximately 30 column volumes of 20 mM Tris buffer pH 8.0 at 2 mL/min flow rate. On the same buffer, 40 mg/mL sample was injected in a 100 µL loop, previously cleaned with buffer (3x loop volume). After the sample binding, the elution of the wanted BSA monomers was promoted by 3 minutes linear gradient from 0 to 12.5% of 2M NaCl in 20 mM Tris pH 8.0 (buffer B), after which BSA monomers were collected and stored. Later, the column was washed with 20 mM Tris 2M NaCl pH 8.0 for approximately 60 column volumes.

When needed, a cleaning-in-place (CIP) was proceeded with the following steps all performed at 2 mL/min flow rate; 1^{st}, 20 column volumes of purified Mili Q water; 2^{nd}, 40 column volumes of 1 M NaOH, 2M NaCl pH 8.0; 3^{rd}, 20 column volumes of purified Mili Q water; 4^{th}, 20 column volumes of 20 mM Tris buffer pH 8.0; and to finalize, again 20 column volumes of purified Mili Q water. It is important to say that all solutions were filtered and

degassed before passed through the system. Additionally, all the chromatographic data was collected and analyzed by UNICORN 6.1 software.

3.2.2. Sample Concentration

After some consecutive purification processes, the sample was concentrated and desalted with 10 kDa Corning® Spin-X® UF concentrators. The centrifugations were performed at a temperature of 4ºC and with a rotation of 800 G.

3.2.3. Sample Characterization

In order to characterize the sample after the purification, a size exclusion chromatography was performed. The Superdex 200 media (GE Healthcare) was packed in a column with a diameter of 1.6 cm, bed height of 30 cm and a bed volume of 60.32 mL. An isocratic gradient was kept with 20mM Tris buffer (pH 8.00). The chromatographic runs were carried out at 0.5 mL/min, at room temperature and the absorbance was continuously monitored at 280 nm. The chromatographic runs were performed in an AKTA Pure system (GE Healthcare, Buckinghamshire, UK) with UNICORN^{TM} 6.3 software.

3.3. Flow Microcalorimetry studies (FMC)

A QA monolith (by BIA separations) was packed into the FMC column, which as a volumetric capacity of 171 µL, with 96% ethanol solution. Afterwards, in order to remove all the residues of the previous solution, the system was overnight cleaned with ultra-purified Mili Q water at a 0.5 mL/h flow rate. Later, the equilibration step was made passing the respective buffer (20 mM Tris buffer pH 8.0) through the cell at a constant flow rate of 1.5 mL/h, using precision syringe pumps (Harvard Apparatus, UK).

Multiple injections were performed with loops of different volumes. Namely in this work, were used loops of 30 µL, 100 µL, 230 µL and 500 µL. Before and after each injection the loop was washed with ultra-purified Mili Q water (3x loop volume). To evaluate the adsorbed concentration (mg BSA/support volume), the flow through and the injected sample were read with a UV spectrophotometer at 280 nm (XMark, Bio-rad, Portugal). After each injection, 20 mM Tris 2M NaCl pH 8.0 was passed through the system in order to remove all the remain

impurities and retained adsorbed product. Then, the system was overnight washed with ultra-purified Mili Q water at 0.5 mL/h flow rate to get rid of cleaning solution remains and the equilibrium was restored passing the respective buffer through the cell at a constant flow rate of 1.5 mL/h. This process (Clean, wash and equilibrium) was performed between each injection. Additionally, consecutive injections were performed in order to submit the support to the maximum concentration possible, once this way it is possible to observe what changes occur at overloading conditions and determine the monolith maximum capacity.

Inside the cell, when the sample adsorption takes place in the monolith surface, enthalpy changes happened and those were measured by two thermistors interfaced in the FMC column. These are highly sensitive to heat changes in the order of 10^{-7}W and were calibrated by a specific outlet, that releases an energy pulse of 30 µW during 500 s. The calibration factor was later used to convert digitals to a heat signal (mJ).

All the data was acquired, stored, and processed with CALDOS 4 software. As mentioned before, peak deconvolution and area calculation were performed with PeakFit 4.12 software. Finally, the heat of adsorption was calculated from the area of the deconvoluted peaks and normalized by the amount of protein injected and adsorbed.

3.4. Bicinchoninic acid Protein Assay Kit

The Thermo Scientific™ Pierce™ BCA Protein Assay Kit contains: a BCA (bicinchoninic acid) reagent A, more specifically, containing sodium carbonate, sodium bicarbonate, bicinchoninic acid and sodium tartrate in 0.1M sodium hydroxide; BCA reagent B, which contain 4% cupric sulfate; and Albumin Standard Ampules, at 2mg/mL each in 0.9% saline and 0.05% sodium azide.

Before the assay procedure, the diluted Albumin (BSA) Standards (in a range of 2000 µg/mL to 0) and the Working Reagent (mixing 50 parts of BCA reagent A with 1 part of BCA reagent B) were prepared accordingly to the respective Kit protocol. This Kit has two different test procedures, the test-tube procedure, and the Microplate procedure. In this work we used the microplate one, so, the sample of Working Reagent solution (WR) was used in a ratio of 1:8.

In a well plate (Thermo Scientific™ Pierce™ 96-Well Plates), 25 µL of each standard and unknown sample replicate were distributed by different wells. Afterwards, for each one of

those wells was added 200µL of the WR solution and the plate was thoroughly mixed on a plate shaker for 30 seconds. Then, the plate was covered and incubated at 37ºC for 30 seconds. To finalize, the plate was cooled to room temperature and the absorbance at 562 nm was measured on a plate reader. With this procedure we could obtain the calibration curve for BSA at a maximum concentration of 2000 µg/mL, and consequently the real stock concentrations of the received analyte and ligand variants.

3.5. Surface Plasmon Resonance (SPR)

3.5.1. Protein A sensor chip

3.5.1.1 Analyte bound response

In this specific case, the sensor chip was already modified, since it consists in a carboxymethylated dextran matrix pre-immobilized with a recombinant Protein A (namely, the same molecule as in MabselectSure^{TM}), providing a ready-to-use means for convenient determination of antibody concentration. So, the analyte was passed through the sensor chip again in two running buffers (20mM phosphate pH 7.4 + 150 mM NaCl and 20mM MOPS pH 7.4 + 150 mM NaCl), with a concentration range from 0.032 g/L to 6.25x10^{-5} g/L, the data was recorded and analyzed using the software evaluation from Biacore.

3.5.2. NTA sensor chip

3.5.2.1. Ligand immobilization on the surface

As mentioned before, Serie S sensor chip NTA was used in the immobilization of B_8-$(RH)_4$ protein A. The process occurred due to a chelate formation between the histidine tag and the Ni^{2+} that is coating the gold film surface, that lead to the correct immobilization of the protein onto the surface. Accordingly, to the sensor instructions guide, immediately before the first analysis cycle in a run, the surface should be uniformized and conditioned. So, first regeneration solution (350 mM EDTA in running buffer (20 mM MOPS pH 7.4 + 150 mM NaCl) pH≈8.3) was passed through the surface in a 1-min pulse and to remove traces of the last solution, several washes with running buffer were performed. At this point, it was injected a one-minute pulse of Ni^{2+} solution (0.5 mM $NiCl_2$ in running buffer) to saturate the NTA with

Nickel and a wash was done with washing solution (3 mM EDTA in running buffer). Finally, the chip was ready to capture the ligand, and different concentrations of ligand in running buffer were tested, over the nickel activated sensor surface with a contact time of 3 min and a flow rate of 5 μL/min in order to optimize the concentration and reach the better capture level.

3.5.2.2. Analyte bound response

After the chelate formed and the ligand correctly captured onto the surface, the sensor chip was ready to measure the interaction between the ligand and the analyte. A concentration range of IgG in running buffer (20mM MOPS pH 7.4 + 150 mM NaCl), namely from 1000 μg/mL and 0.125 μg/mL, were passed through the surface of the sensor chip and the data was recorded and analyzed using the software evaluation from Biacore.

3.5.3. CM5 sensor chip

3.5.3.1. Ligand immobilization on the surface

The Serie S CM5 sensor chip was used in the immobilization of the B8-cys-ly-cys-lys protein A prototype. This type of sensor chip is already commercialized with a layer of carboxymethylated dextran matrix coating covalently to the gold thin surface, promoting the bound of ligands via carboxyl groups on the dextran. However, in this study the sensor chip was additionally coupled with a maleimide coupling kit, consisting in 5 main steps. First, the surface was activated with a mixture of EDC/NHS (1:1) for 6-7 min. Then, the amine groups were introduced by injecting ethylenediamine for 6-7 min. Afterwards, the maleimide groups were introduced by injecting sulfo-GMBS for 4 min. Later, the ligand was immobilized by injecting the solution for 6-7 min. To finalize, the excess of reactive groups was deactivated with the injection of cysteine/NaCl for 4 min.

3.5.3.2. Analyte bound response

After ligand captured onto the surface, the interaction level between the ligand and the analyte was measured. A concentration range of IgG in two running buffers (20mM phosphate pH 7.4 + 150 mM NaCl and 20mM MOPS pH 7.4 + 150 mM NaCl), namely from 1000 μg/mL to 1.07 μg/mL, were passed through the surface of the sensor chip and the data was recorded and analyzed using software evaluation program.

3.6. Polyacrylamide gel electrophoresis

This method is based in two different gels: the resolving gel (12% Acrylamide) prepared with, H_20, 30% Acrylamide (4ºC), 1.5M Tris pH 8.8, 10% SDS, 10% APS (-20ºC) and Temed (4ºC); and stacking gel (5% of recipe), composed by H_20, 30% Acrylamide (4ºC), 1.5M Tris pH 6.8, 10% SDS, 10% APS (-20ºC) and Temed (4ºC). First, the resolving gel was prepared mixing the ingredients with the APS and Temed as the last ones. The gel was charged into the glass apparatus and it was covered with isopropanol until the polymerization (around 30 minutes). Afterwards, the isopropanol was removed, the stacking gel was add covering the first gel and the combs were inserted until polymerization.

At this point the method has two different possible procedures, the non-reducing and the reducing PAGE, which includes a dithiothreitol (DTT) solution and a boiling step. In this work we used non-reducing conditions, without DTT, the sample was diluted 1:1 in sample buffer and at a volume of 10μL it was charged into the wells. The sample buffer without reducing agent is composed by: 125mM Tris pH6.8, SDS 4% (w/v), 20% (v/v) Glycerol and 0.004% bromophenol blue. Specifically, in this work it was used two different samples of B8-cys-ly-cys-lys protein A, resulting with the triplicates in 6 different working wells. Additionally, another well was charged with NZYcolour Protein Marker II (NZYTech, Lisbon, Portugal), covering a wide range of molecular weights, from 11 to 245 kDa.

The electrophoresis device was connected to the bath support mid-filled with running buffer and programed to run for approximately 120 minutes, with 160 V and 80 mA. The running buffer was prepared, mixing 25 mM Tris base with 250 mM Glycine and with 0.1% (w/v) SDS. After the end of the run, the gel was submersed in Coomassie Brilliant Blue staining solution and kept overnight, the solution composition was ethanol, Glacial acetic acid, H_20 and 0.05% Coomassie. Finally, the gel was passed to distaining solution (based on ethanol, glacial acetic acid and H_20) and the final result was photographically saved [125].

Chapter 4. – Results and Discussion

The results obtained in this work can be divided, according to their nature and objectives, in two main groups. The first group includes the study of a 2.5% QA monolithic matrix (properties and response) through the adsorption of a model protein (BSA). The second and last results collection explores the capacity of a novel ligand on the antibody capture.

4.1. Thermodynamic analysis of a monolithic column

Bovine serum albumin is one of the most frequently used model protein to study the adsorptive behavior in preparative chromatography using anion-exchange stationary phases due to its availability, stability, and low cost. Although, a majority of these studies have used BSA from commercial sources with nominal high purity (96 – 99%), heterogeneity of these protein samples remains a concern. Bovine albumins have long been known to exist in dimer and /or oligomer forms [126]. Noticeably, the presence of these forms affects the monolith performance as it can become clog, resulting in an increased pressure drop across the column, not good for the measurements using flow microcalorimetry, a technique that is very sensitive to changes in pressure during operation. Thus, to prevent the presence of aggregates in the injected sample and monolith blocking and clogging, different strategies for BSA monomer purification were tried.

4.1.1 Optimization of BSA monomer purification

- **CIM DEAE Monolith**

As a first tentative, it was used a CIM DEAE weak anion exchanger monolith from BIA separations (Slovenia). Initially, for this support, it was used a protocol where the column was equilibrated with 20mM TRIS pH 8.0 running buffer at a flow rate of 2mL/min, followed by an injection of BSA 40mg/mL, later eluted with a 3 minutes linear salt gradient from 0 to 12.5% of 2M NaCl prepared in 20mM TRIS- pH 8.0. However, the described protocol was not able to correctly separate the monomers from the rest of unwanted isoforms and aggregates as can be seen from Fig. 19. Comparison of our results with the ion exchange results from Amartely *et al.* [127] based on multi-angle light scattering (MALS) detection, confirm that the shoulder

observed in the elution peak has a molecular mass around 130 kDa corresponding to the BSA dimer, and the first part of the elution peak corresponds to the monomer with a molecular mass of 66.8 kDa. Also, the amount of protein recovered was not high and monolith capacity was exceeded once we observed a flow through peak during injection. In face of these results, different strategies were used to increase the resolution and improve the peak separation.

By changing different parameters is possible the optimization of the proposed IEX method, namely [127]:

- a decrease in the flow rate may improve peak separation;
- the adjustment of buffer capacity may increase the charge variation between the protein populations in the sample and improve the separation between variants;
- the change in the gradient slope and length may result in better resolutions. Short gradients with high slopes provide intense peaks with less separation, while long gradients with mild slopes provide lower peaks with better separation.
- the use of a stepwise salt concentration profile for the elution may help to collect the target protein.

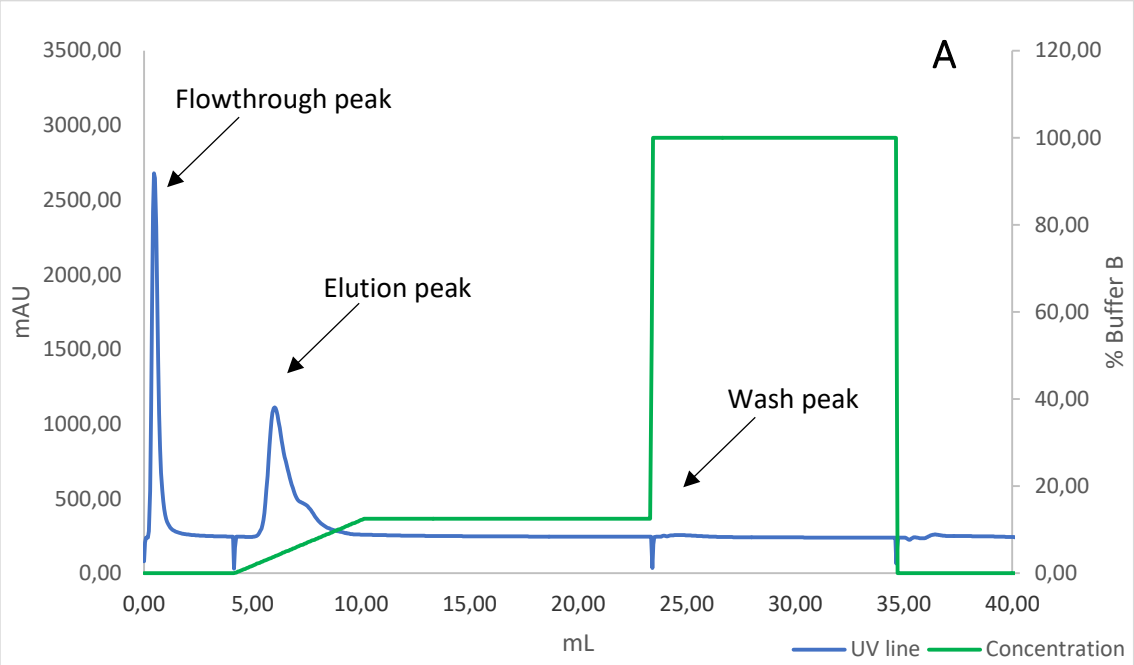

Figure 19: BSA purification chromatogram resulting from application of the initial described protocol. For an easier understand additionally to the UV line, the elution buffer concentration line is presented.

Table 4 presents the different applied strategies, where different flow rates, buffer concentrations, linear elution salt gradients, and sample injection concentrations were tested in different trials.

Table 4:

Trial	Buffer concentration	Flow rate	Gradient	Injection concentration
A	20mM TRIS	2mL/min	0 to 12.5% buffer B, 3min	40mg/mL
B	20mM TRIS	0.5mL/min	0 to 12.5% buffer B, 3min	40mg/mL
C	500mM TRIS	0.5mL/min	0 to 12.5% buffer B, 3min	40mg/mL
D	20mM TRIS	1mL/min	0 to 12.5% buffer B, 3min	15mg/mL
E	20mM TRIS	1mL/min	0 to 11.5% buffer B, 3min	15mg/mL
F	20mM TRIS	1mL/min	9.20% buffer B, 0min 12.5% buffer B, 3min	15mg/mL

Performed trials and respective used IEX method parameters (Buffer B - 2M NaCl in 20 mM Tris pH 8.0).

From table 4 it can be seen that the 2nd trial involved a change in the flow rate, maintaining all the other parameters. As can be seen from Fig. 20.B, even with a taller elution peak, the protein concentration injected was too high for the monolith capacity, explaining the presence of the flowthrough peak during injection. Another drawback from this trial is the time needed, since we wanted to purify a considerable amount of monomer, we needed a relatively faster procedure.

In the 3rd trial the salt buffer concentration was increased maintaining the rest of the parameters used in the 2nd trial (Fig. 20.C). It is known that buffer provides a larger buffering capacity (stabilizing pH, and so protein binding strength) at a higher concentration of the buffer itself, yet protein binding strength during ion exchange chromatography is pH-dependent and decreases with increasing ionic strength of the buffer solution. In the present case the peak of interest disappeared, accompanied by an increase of the flowthrough peak, showing that no binding occurs (Fig. 20.C). An ideal buffer is one that provides a high buffering capacity while still not decreasing protein binding too much, which was not verified in the present case. As such, and to minimize the ionic strength effect of the buffer, TRIS concentration was fixed to 20 mM [63].

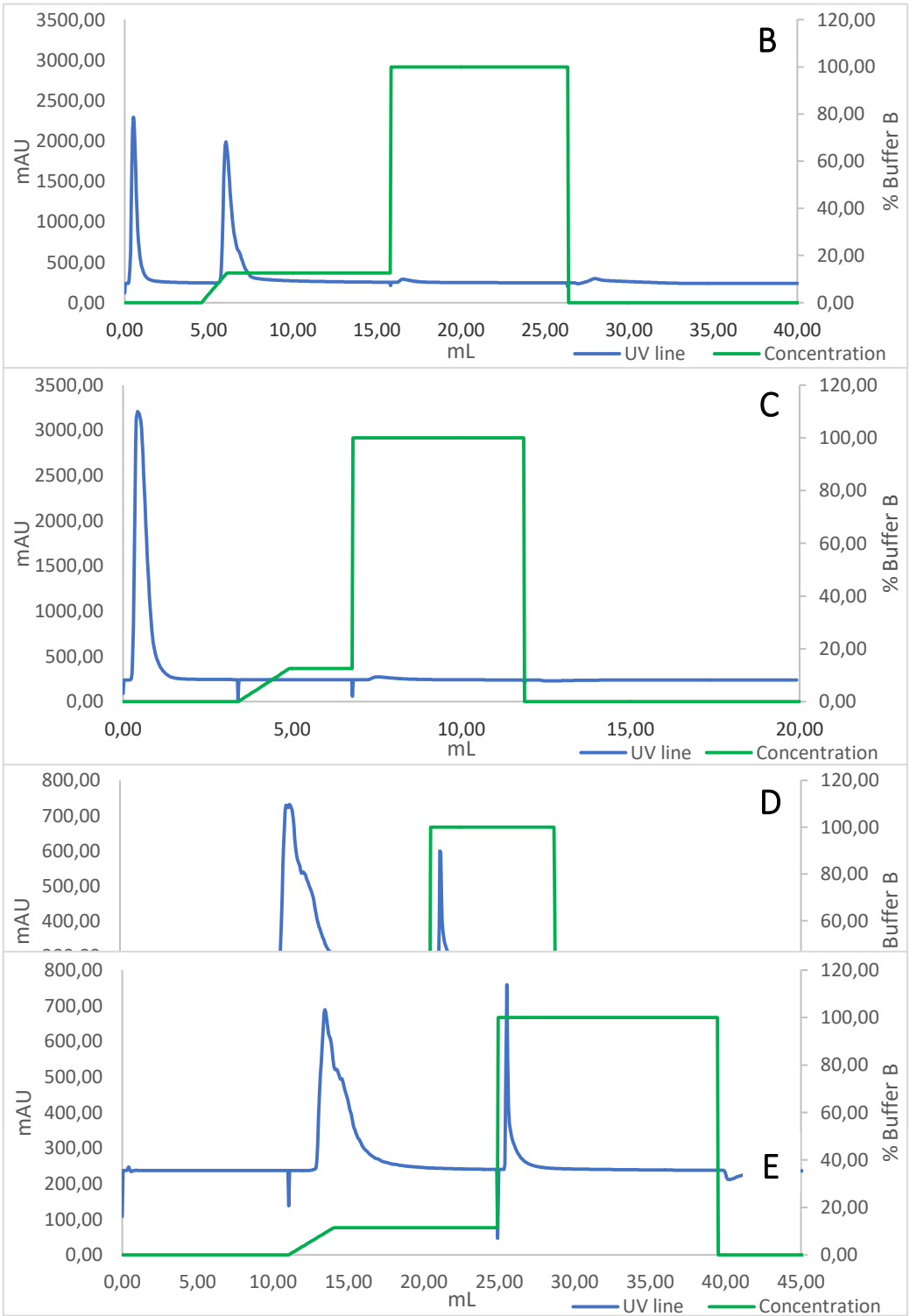

Figure 20: Chromatograms resulting from trials indicated on table 4.

Based on the previous results, the 4th trial involved the increase of flow rate to 1 ml/min for a faster purification and the reduction in the concentration of injected sample (15 mg/mL), not to overload the monolith. As can be seen from Fig. 20.D, the flowthrough is almost inexistent and the peak of interest can be identified, but it still presents a shoulder. The next step was the change in the gradient slope (Fig. 20.E). Although the resolution did not suffer a great increase, at least it was possible to identify the concentration point of the gradient at which the maximum of the monomer peak occurs. Taking this information, a step elution was tried at the identified salt concentration (9.2% buffer B = 18.4 mM NaCl), followed by 3 minutes linear gradient from 0 to 12.5% buffer B. As can be seen from Fig. 21, the peak of interest was eluted separately from dimers and oligomer forms, eluted later by the linear gradient. After this step the rest of the impurities were removed from the column with a washing step using 2M NaCl, 20mM TRIS - pH8.0, getting the column ready to a new injection, after an equilibration with running buffer. Finally, the observed tailing in monomer peak (Fig. 21) may be related to a component closely associated with the BSA monomer, perhaps a BSA variant as advanced by Carta and co-workers [126].

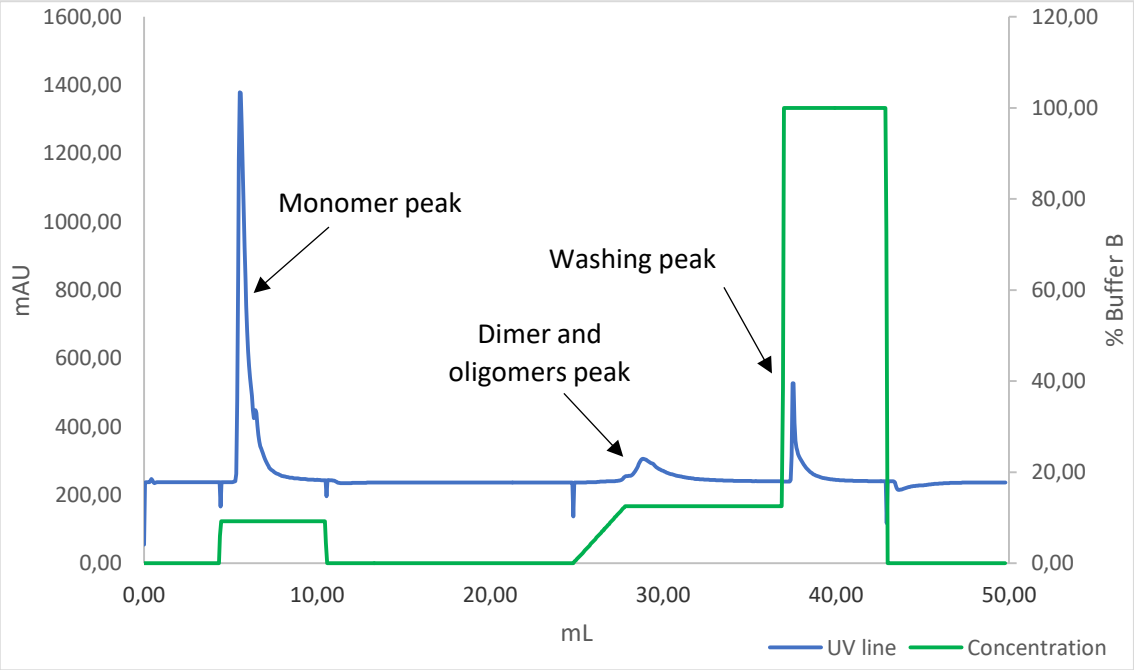

Figure 21: Final optimized protocol. A step elution (9.2% buffer B) is combined with a linear gradient from 0 to 12.5% buffer B and a washing step with 100% buffer B.

To further confirm that the eluted peak was the BSA monomer, a gel filtration chromatography was performed using a Superdex 200 size exclusion column according to the

procedure described in the Methods section (3.2.3. Sample Characterization). Two samples were used, the purified BSA monomer and an old unpurified BSA sample composed of BSA monomers, oligomers, and isoforms. From Fig. 22 it can be confirmed that the purified BSA sample corresponds to the monomer, as in the chromatogram of the unpurified sample an extra peak can be seen before the elution of the monomer peak (the major component in the sample).

Also, on this chromatogram a peak due to the presence of salt can be observed.

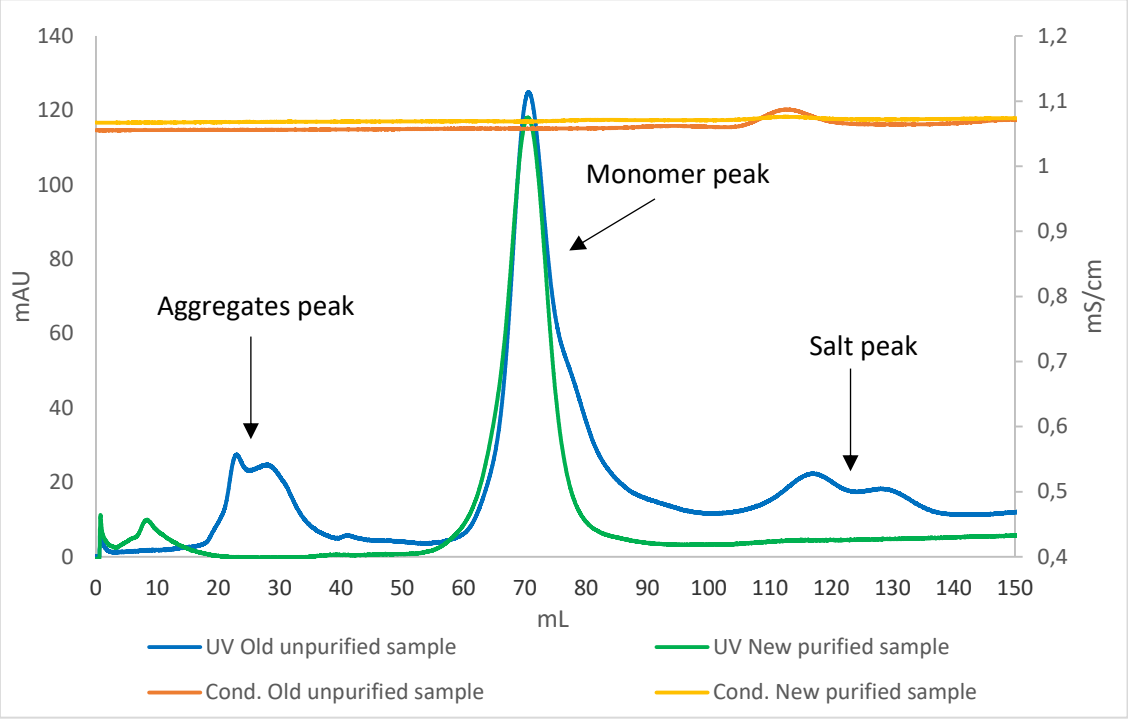

Figure 22: Analytical size exclusion chromatography of BSA purified and unpurified samples.

Based on the IEX optimized protocol, we proceeded with the purification of BSA monomers by step elution at 9.2% buffer B, being the rest of the undesired adsorbed products eluted in the washing step.

A big volume of BSA monomer solution is required, once each sample injection for microcalorimetric studies needs at least 100 µL of BSA monomer with a concentration around 20 mg/mL. However, after several injections, the chromatographic profile in this monolith has started to change. As can been seen from Fig. 23, as the number of injections increase the flow through peak started to increase and at the same time the elution peak started to decrease proportionally. When this was noticed, cleaning-in-place (CIP) and column regeneration were performed multiple times, in order to get rid of aggregates that could be blocking the monolith

and try to restore the co-ions present in the monolith surface, unfortunately all the efforts did not solve the loss of sample adsorption and the pressure drop problem. To sum up, with the

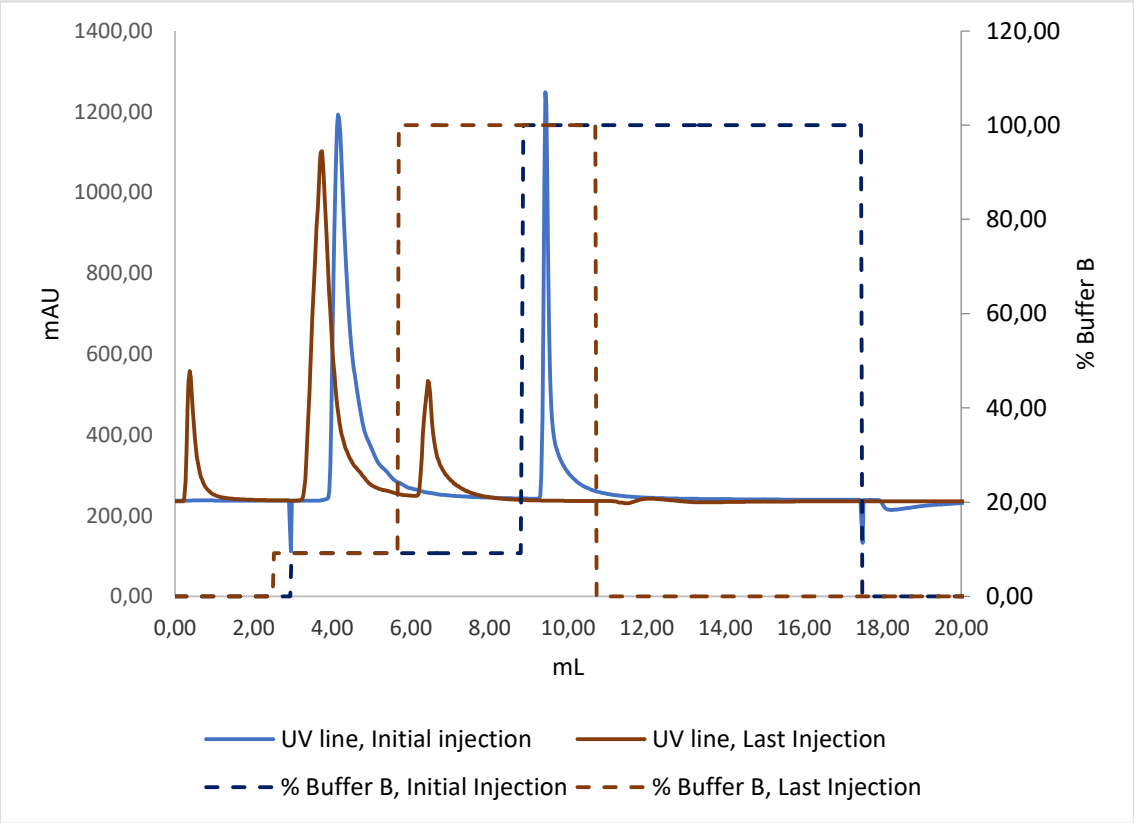

extensive use, this monolith showed a capacity loss.

Figure 23: Change in chromatographic profile resultant from multiple BSA injections in the monolith.

- **CIM DEAE Monolith (Double volume)**

In order to increase the volume of purified BSA monomer, another approach was tried, again using a CIM DEAE weak anion exchanger monolith from BIA separations, but with the double of the volume and column length. So, in first place it was checked if the monolith response was the same using the previous optimized protocol, in presence of the same concentration of injected sample. As the response was pretty much the same and capable of purifying protein monomers (Fig. 24. A), theoretically the double volume monolith would be also able to adsorb and purify the double of the protein quantity. So, after this first test, scale-up trials at higher BSA concentrations (20, 30 and 40 mg/ml) were performed.

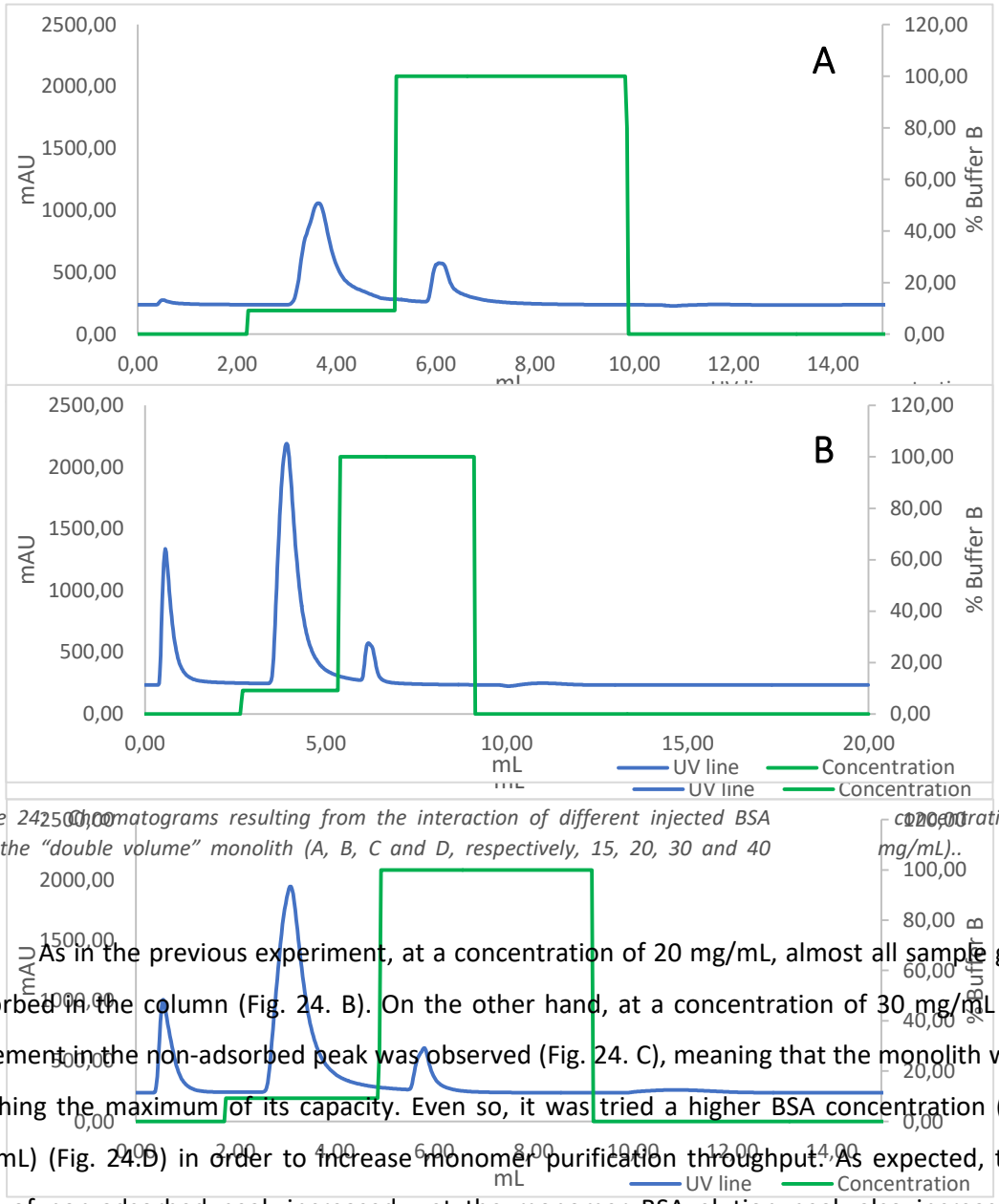

Figure 24. Chromatograms resulting from the interaction of different injected BSA concentrations with the "double volume" monolith (A, B, C and D, respectively, 15, 20, 30 and 40 mg/mL)..

As in the previous experiment, at a concentration of 20 mg/mL, almost all sample got adsorbed in the column (Fig. 24. B). On the other hand, at a concentration of 30 mg/mL an increment in the non-adsorbed peak was observed (Fig. 24. C), meaning that the monolith was reaching the maximum of its capacity. Even so, it was tried a higher BSA concentration (40 mg/mL) (Fig. 24.D) in order to increase monomer purification throughput. As expected, the area of non-adsorbed peak increased, yet the monomer BSA elution peak also increased.

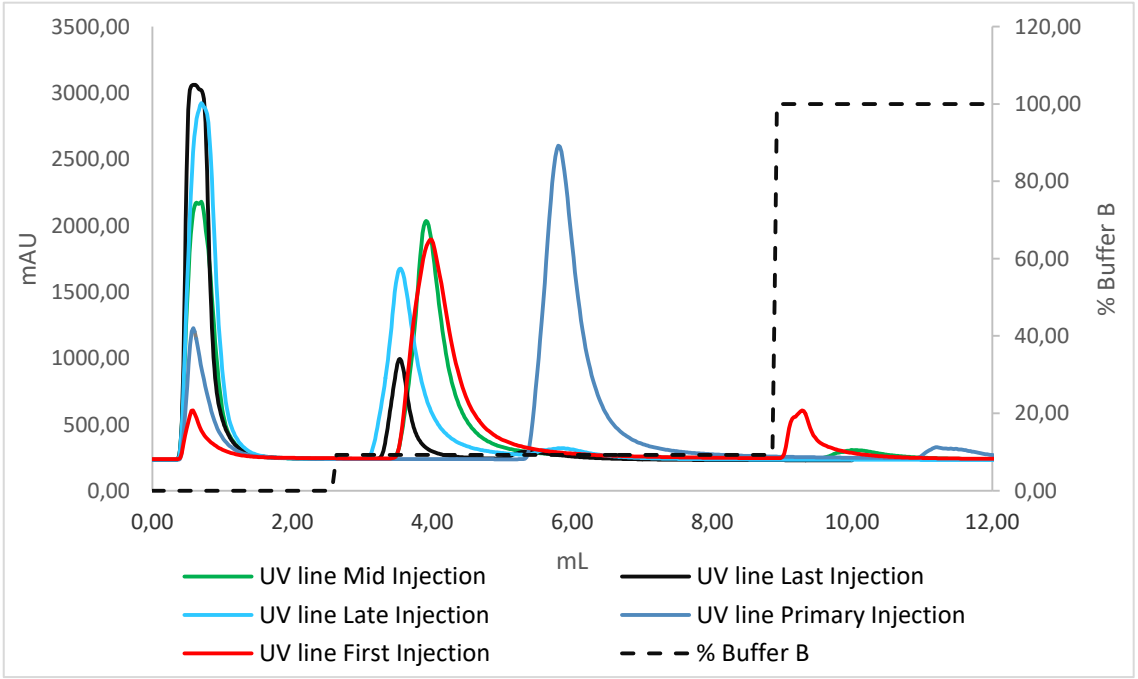

Accordingly, following injections were performed using a BSA sample concentration of 40 mg/ml.

Figure 25: Injection profile change resulting from monolith re-use.

This arrangement of monoliths presented a longer life-time when compared to the use of only one monolith, leading to a higher number of injections and consequently to a higher volume of purified BSA monomer, however after exhaustive use it reached the same point of capacity loss as the previous one. As can be seen in figure 25, when the monolith was working normally, like in the primary injection, the first peak correspondent to non-adsorbed sample was low (around 1200 mAU) and when the gradient was applied the desired peak, the one with the monomer, was very high (around 2500 mAU). But as it can be also observed along the injections, from the first to the fifth, there is a reverse growth proportional tendency between the flowthrough peak and the purified monomer peak. Namely, whenever an injection is performed the first peak tends to grow and the second one to decrease, meaning every time the column is used less it can adsorb after each injection and less monomer will be purified from the protein injected solution (a mixture of aggregates, monomers and other BSA isoforms).

Again, multiple cleaning-in-place (CIP) and regenerations tries were performed in order to recover the column, but without success, which lead to the application of a new approach as the protein purification needed to continue.

- **Toyopearl DEAE- 650M resin column**

This time a resin was used instead of the monolith. As mentioned before, this type of support is formed by spherical structures, named beads, in a fluidic solution. The main difference to monoliths, is that monoliths are closed solid compact structures and the resins are fluidic solutions, so they can be easily resuspended and recovered and are less prone to fouling and clogging.

In the present study a Toyopearl DEAE - 650M weak anion exchanger from Tosoh was used to pack a 4.71 cm^3 column. The pervious optimized IEX protocol was also used with this resin once it presents the same ligand and is expected to have the same behavior of the previous studied DEAE monolith in BSA monomer separation. Although, as it can be seen from

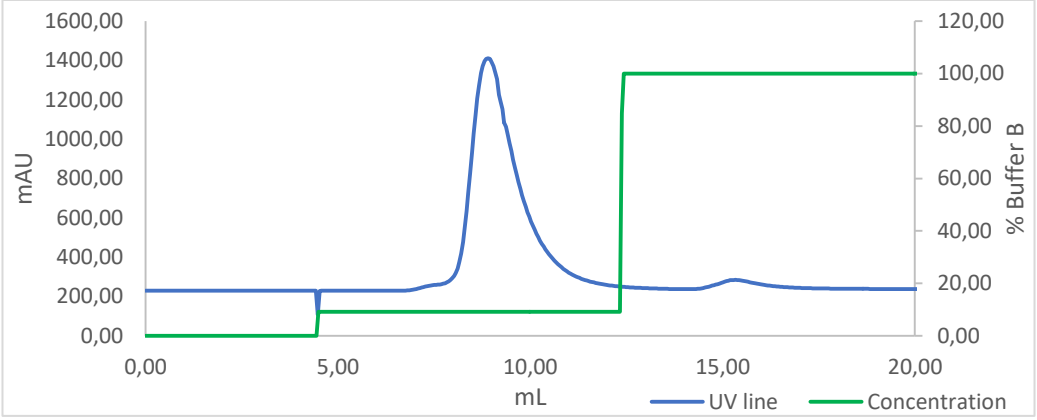

Fig. 26.A, this protocol was not totally capable of BSA monomers separation from the rest of the mixture since it can be observed a shoulder at the beginning of the peak. Thus, further optimization was done, this time we tried to do a 30 minutes linear salt gradient from 0 to 50% of 2M NaCl prepared in 20mM TRIS - pH 8.0, which revealed to be a satisfactory protocol (Figure 26.B). Additionally, to reduce the time of purification, a lower slope gradient was performed in less time, resulting in the successful separation of the BSA monomer peak, as it can be seen from Fig. 26.C. Accordingly, following purifications were performed using this protocol.

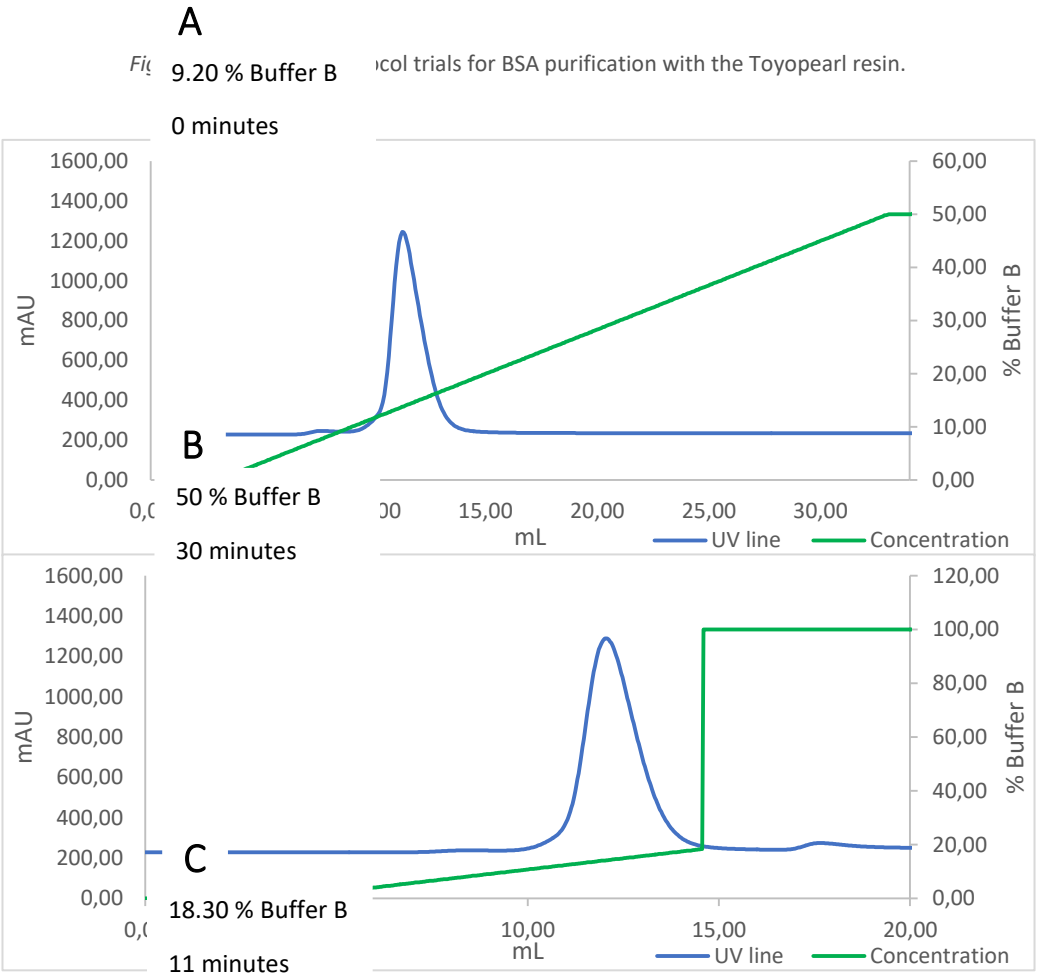

4.1.2 BSA monomer adsorption onto a QA monolith analyzed by flow microcalorimetry

As mentioned before, in the present study our effort focuses on the thermodynamic evaluation of a 2.5% quaternary ammonium monolith by analyzing its response to the adsorption of a model protein (BSA), through flow microcalorimetry. For the referred monolith, different injections were performed, as described in the methods section (3.3), using four distinct loops to reach increasing protein surface concentrations (30 µL, 100 µL, 230 µL and 500 µL) (Fig. 27).

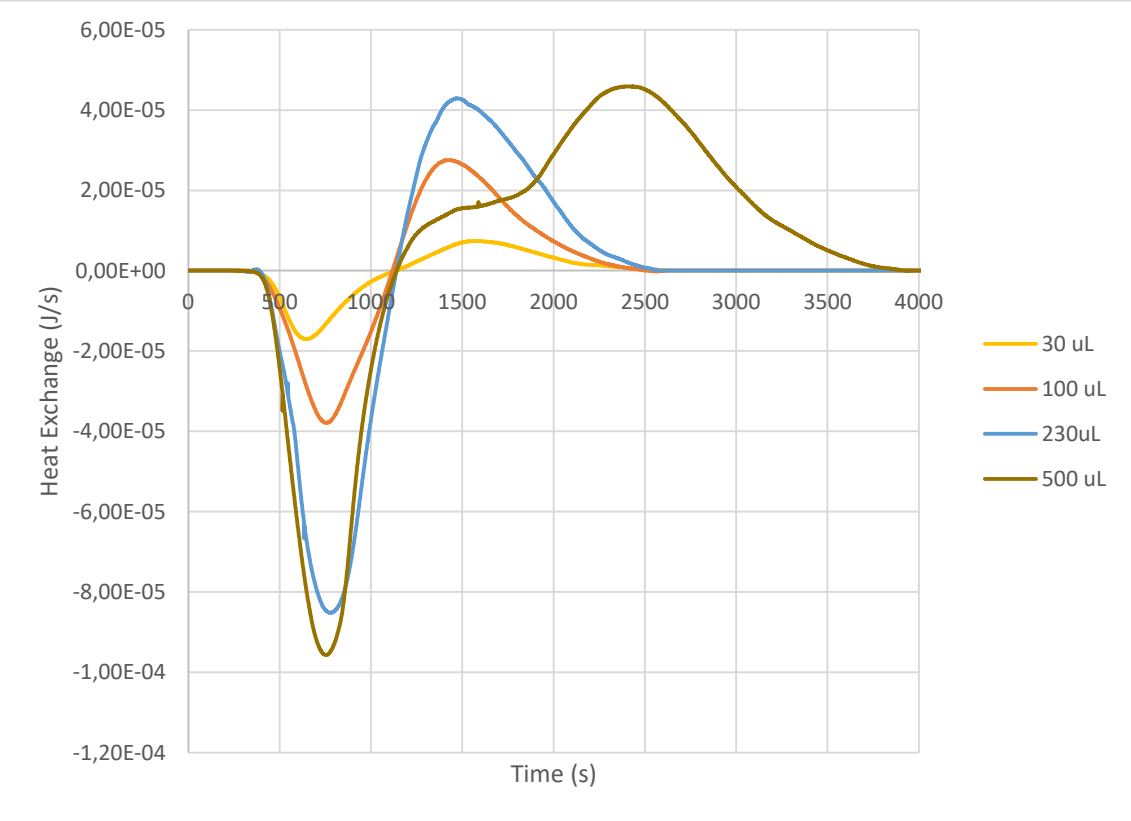

Figure 27: Thermograms for BSA monomer adsorption (20 mg/mL) onto a 2.5% QA monolith at pH 8.0. Injection loop volume: 30 µL (yellow line), 100 µL (orange line), 230 µL (blue line) and 500 µL (brown line). Flow rate 1.5 mL/h.

As it can be observed from Fig. 27, different events are present in the thermograms, first were observed endothermic peaks and next to them exothermic signals. Yet, these events might be occurring simultaneously or sequentially. Therefore, all the data was analyzed with PeakFIT software, which allows the de-convolution of heat signals, and allows to discriminate between the different subprocesses occurring during the adsorption process, taking in account also the apparently masked energetic events (Fig. 28 A, B, C and D).

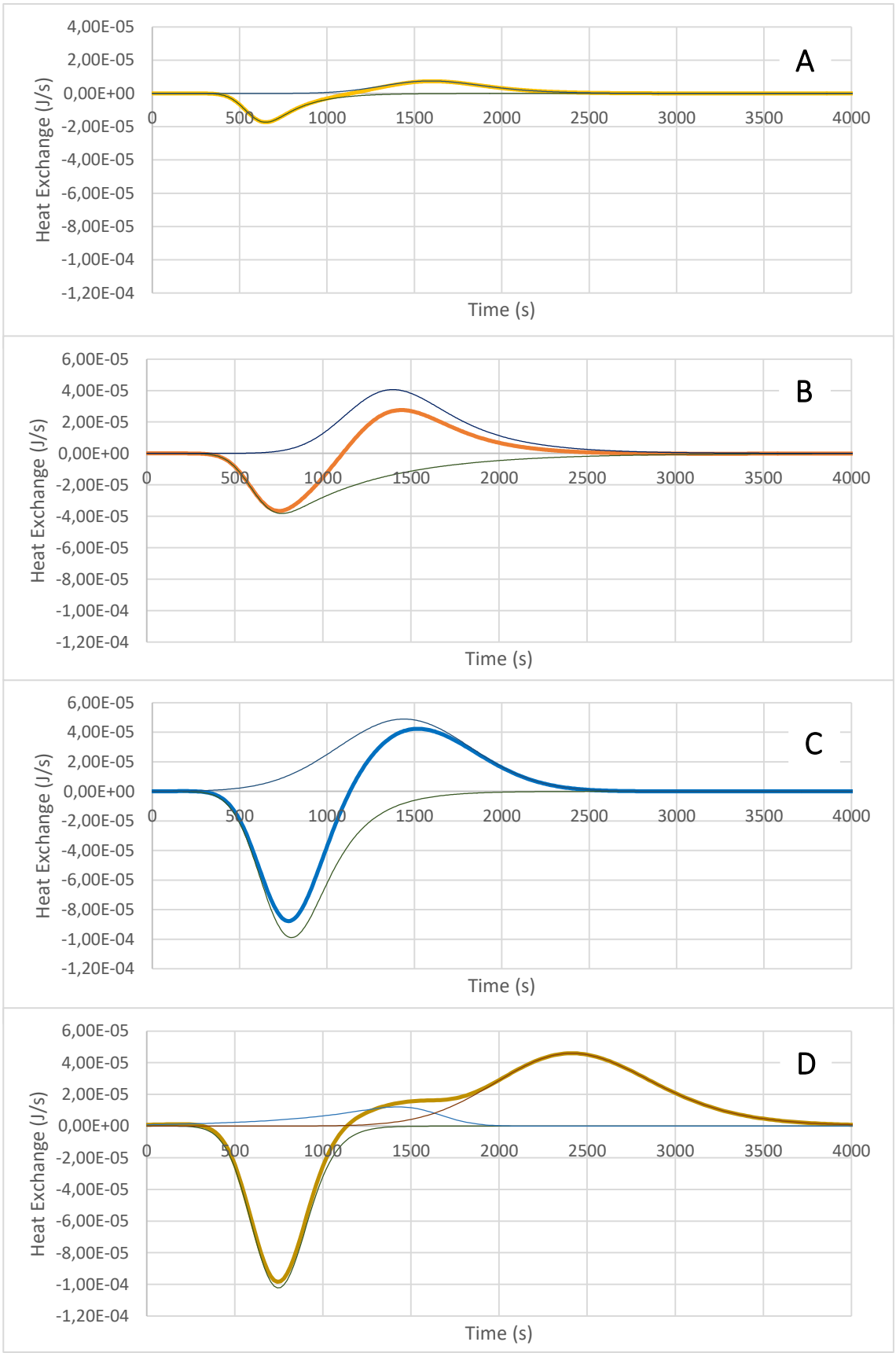

Figure 28: De-convolution of thermograms resulting from BSA (20 mg/mL) adsorption onto a 2.5% QA monolith at pH 8.0 (20 mM Tris). Injection loop volume: 30 µL (yellow line – A), 100 µL (orange line – B), 230 µL (blue line – C) and 500 µL (brown line – D). Flow rate 1.5 mL/h.

Thermograms in Fig. 28 A – D show the de-convolution of the heat signals for experiments using the different injection loops. From them, it can be observed that the endothermic and exothermic signals overlap. Also, as the BSA loading concentration increases the endothermic and exothermic events on each thermogram increase in magnitude (Fig. 28 and Table 5). Differences in whole interaction length and at the time at each event take place can also be noticed in the thermograms. All the aforementioned results are expected since a higher quantity of protein is in contact with the adsorbent as the injection loop increases. A similar behavior was observed by Dias-Cabral and co-workers for the adsorption of Lysozyme onto a 1st generation cation exchanger (CMC) [88].

Thermograms resulting from injections with the 30, 100 and 230 μL loop (Fig. 28 A, B and C) present a similar profile, one endothermic signal overlapped with an exothermic signal. On the other hand, the thermogram resulting from the injection with the 500 μL present in addition to the endothermic peak, two exothermic overlapping peaks. This profile was expected, as in the presence of this higher loop, the adsorption happens under volume overloading conditions. The difference between these two cases is the fact that when using the lower volume loops for injection, the injected sample can be considered as a pulse. Oppositely, as the FMC column volume is 171 μL, when the 500 μL loop is used, the injected sample is feeded continuously trough the packed bed, influencing the adsorption mechanism. Taking this in mind, after the first 171 μL of injected sample pass through the column another 329 μL still has to pass through it, which interferes with the equilibrium already established by the adsorbed biomolecules.

To analyze the de-convoluted thermograms (Fig. 28 A – D), it is also important to consider the mechanism proposed by Yamamoto and co-workers for ion exchange adsorption. Accordingly, the process can be sub-divided in five sequential sub-processes: water molecules and ions release from the biomolecule surface (I); water molecules and ions release from the adsorbent surface (II); electrostatic and/or hydrophobic interactions between the biomolecules and the exchanger (III); structural conformation rearrangement and reorientation of the adsorbed biomolecules (IV); and rearrangement of the excluded water molecules and ions in the solution (V) [128]. Therefore, the exothermic event can be related to the sub-process (III) and the endothermic heat signal to sub-processes (I), (II), (IV) and (V) [88]. Considering the net heat of adsorption (Table 5), which is the sum of all contributions to heat, the overall adsorption process, with exception of the injection made with the 500 μL loop, is endothermic. More specifically, since the Gibbs free energy is negative in favorable adsorption conditions, for the injections using the lower volume loops, the adsorption process has to be

entropically driven. This is against what is expected for adsorption by electrostatic interactions that is supposed to be an exothermic process [88], attraction of oppositely charged target molecules and stationary phase, releases energy making it an exothermic interaction. Nevertheless, as discussed, it cannot be forgotten that the IEC adsorption mechanism consists of several subprocesses, with some of them contributing to an overall endothermic signal, namely: repulsive interactions between adsorbed proteins, between protein hydrophobic surface groups and adsorbent surface hydrophilic moieties, between same charged groups on the protein surface and on the adsorbent; protein conformational changes and protein reorientation on the surface; and ions and water release from the surface of the adsorbent and the protein [129]. Taking in mind the five sub-processes previously mentioned, and the fact that when using the lower volume loops for injection we were quite far from the monolith capacity it seems that the desolvation process during the interaction between the biomolecule and the monolith, including the dehydration and counter ions release from biomolecules and adsorbent surfaces might be the main reason for the overall endothermic signal. Due to desolvation, the endothermic heat is compensated by water and ions releasing entropy gain, ensuring the adsorption of the biomolecule to the monolith [130, 131].

Table 5: Heat of adsorption for BSA adsorption onto 2.5% QA monolith at pH 8.0 using different volume injection loops; flow rate: 1.5 mL/h. Enthalpies were determined from the deconvoluted thermograms.

Loop (μL)	Feed (mg)	BSA loading (mg/g)	Endothermic Peak (J)	Exothermic Peaks (J)			Net heat of adsorption (J)	Net heat of adsorption (kJ/mmol)
			ΔH^{I}	ΔH^{II}	ΔH^{III}	$\Delta H^{II}+\Delta H^{III}$	ΔH^{Total}	
30	0.8633	10.128	0.0065	-0.0056	---	-0.0056	0.0010	0.83
100	2.4103	30.637	0.0331	-0.0309	---	-0.0309	0.0022	0.60
	2.8777	35.039	0.0163	-0.0139	---	-0.0139	0.0024	0.57
230	5.5436	74.053	0.0870	-0.0819	---	-0.0819	0.0050	0.63
	6.6188	80.165	0.0680	-0.0720	---	-0.0720	0.0040	0.41
500	12.0513	137.130	0.0410	-0.0106	-0.0524	-0.0630	-0.0220	-1.35

As stated above, more than a change in the heat signal magnitude and length, the transition from a pulse injection (Fig. 28 C) to a continuous feed (Fig. 28 D) influences the heat signal profile, suggesting the presence, in the adsorption mechanism, of an additional sub-process. In this case, to analyze the thermograms, it should be also considered the interaction between adsorbed BSA molecules and free BSA molecules in the feed solution. Despite of some repulsion between these molecules, this interaction may promote the early reorientation and subsequent secondary adsorption of already bound biomolecules, leaving free space for BSA in solution to adsorb and in this way increasing the overall exothermic contribution on the adsorption process. This behavior presents similarities with the one observed by Dias-Cabral and co-workers when studying the adsorption of pDNA onto Fast Flow (FF) Q-Sepharose [87].

Finally, in order to evaluate 2.5 % QA monolith response under overloading conditions and access its adsorption capacity, several injections were performed consecutively. As it can be seen, in Fig. 29, four thermograms were obtained with the 230 μL, resulting from consecutive injections. By analyzing the obtained profiles, it is possible to observe that the endothermic and exothermic peaks, both decrease in magnitude as the protein loading increases. It is also clear the presence of overlapping peaks, which could be confirmed by heat signals de-convolution (Fig. 30 A – D), using PEAKFIT software. As in the single injection with the 500 μL, the thermograms from the 3rd and 4th consecutive injections also present two exothermic heat signals following an endothermic one.

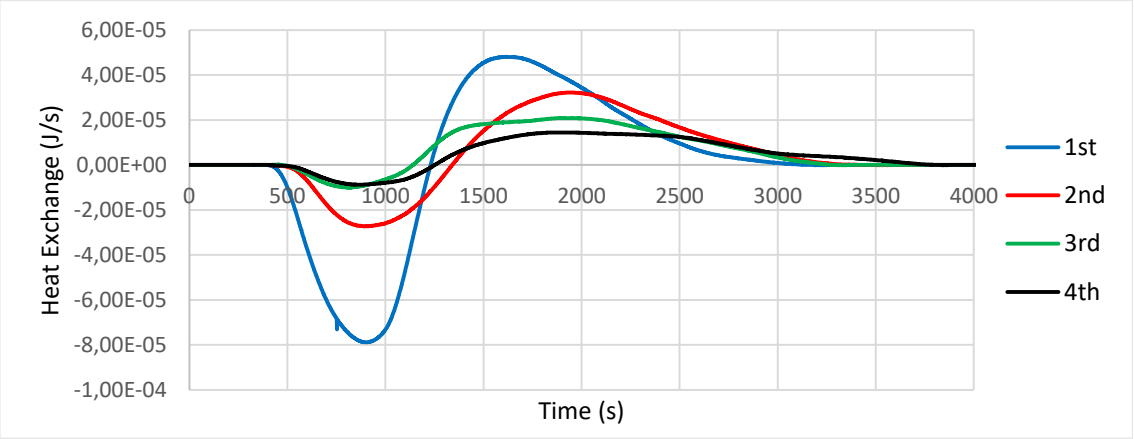

Figure 29: Thermograms resulting from consecutive injections of BSA monomer (20 mg/mL) onto a 2.5% QA monolith at pH 8.0 (20 mM Tris). Flow rate 1.5 mL/h. Injection loop 230 μL.

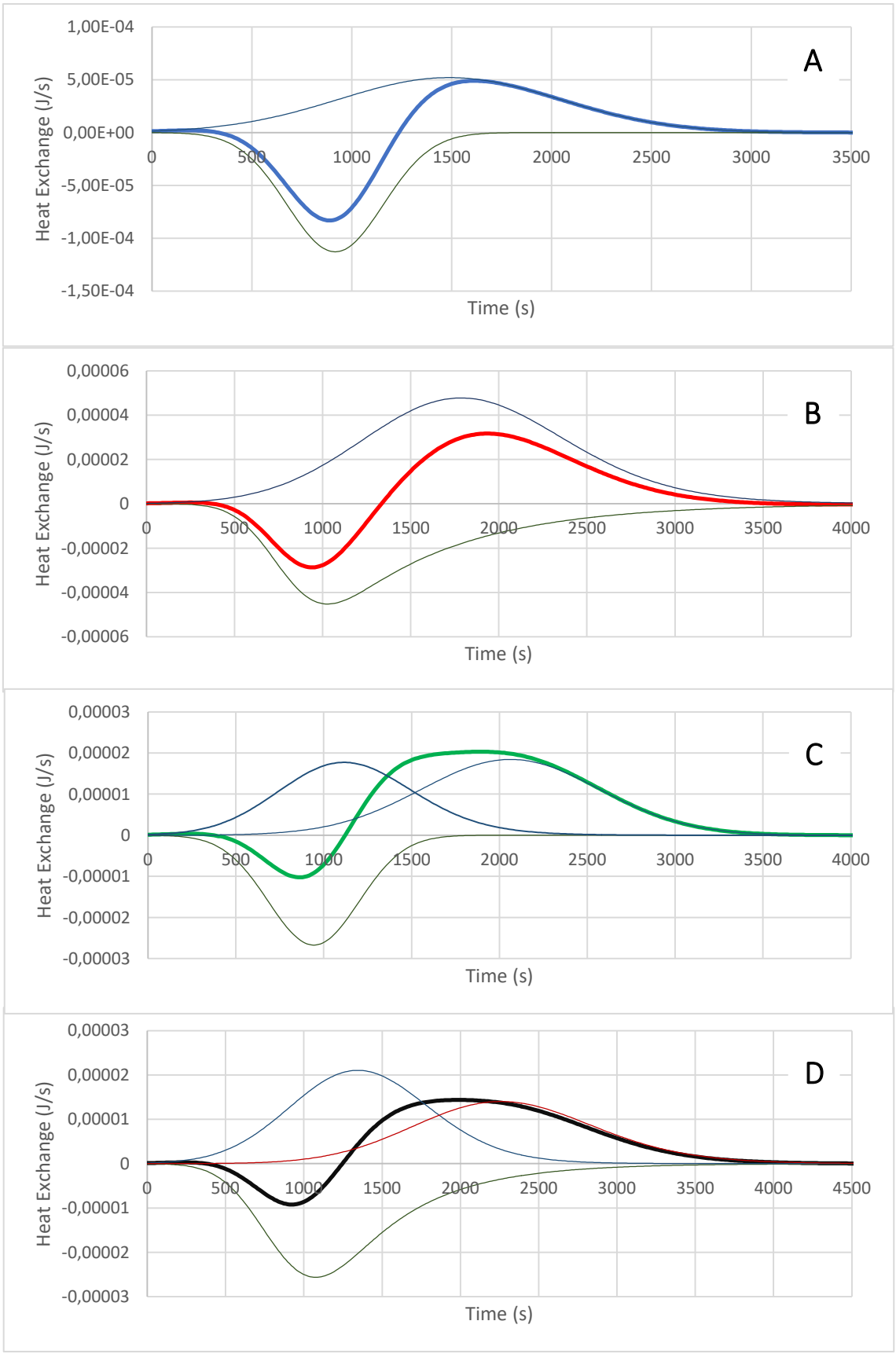

Figure 30: De-convolution of thermograms resulting from consecutive injections of BSA (20 mg/mL) onto a 2.5% QA monolith at pH 8.0 (20 mM Tris). Injection loop volume: 230 µL. A – 1st injection, B – 2nd injection, C – 3rd injection and D – 4th injection.

The enthalpy changes determined from the deconvoluted thermograms for each step in the process by which BSA adsorbs onto the 2.5% QA monolith are summarized in Table 6.

Table 6: Heat of adsorption from consecutive injections of BSA onto a 2.5% QA monolith at pH 8.0 using a 230 μL loop; flow rate: 1.5 mL/h. Enthalpies were determined from the deconvoluted thermograms.

Loop (μL)	Order	Feed (mg)	BSA loading (mg/g)	Endothermic Peak (J)	Exothermic Peaks (J)			Net heat of adsorption (J/mol)	Net heat of adsorption (kJ/mmol)
				ΔH^{I}	ΔH^{II}	ΔH^{III}	$\Delta H^{II}+\Delta H^{III}$	ΔH^{Total}	
230	First	6.6188	80.165	0.0680	-0.0720	---	-0.0720	0.0040	0.41
	Second		152.844	0.0516	-0.0699	---	-0.0699	-0.0183	-2.05
	Third		203.955	0.0172	-0.0171	-0.0234	-0.0405	-0.0233	-3.71
	Fourth		263.145	0.0272	-0.0236	-0.0204	-0.0440	-0.0168	-2.31

From Table 6 it can be seen a similarity in terms of net heat of adsorption to what happened when the 500 μL loop was used. In the first 230 μL consecutive injection, similarly to the 30, 100 and 230 μL single results, a positive net heat of adsorption was noticed meaning the overall adsorption is endothermic and consequently entropically driven, as mentioned before. In terms of profile, it showed the biggest event magnitude and exothermic and endothermic peaks overlapped. The second injection also presented the two event peaks overlapped. However, their magnitudes were smaller than in the last case and the net heat value obtained was negative. So, oppositely to the first injection, in this case the overall adsorption is exothermic and consequently enthalpically driven.

The two last cases (third and fourth injections), presented even more negative values of net heat of adsorption, since like in the study with different loop injections this one followed a tendency to negative values with protein surface increasing. Similarly, to what happened with the 500 μL loop, these two injections after de-convoluted, presented one endothermic peak and two exothermic peaks overlapped. Confirming also what was explained before about the early reorientation and subsequent secondary adsorption of already bound biomolecules leaving free space for BSA in solution to adsorb.

4.2. Novel ligand evaluation for antibody capture

The second part of my study, as mentioned before, uses Surface Plasmon Resonance to explore the capacity of a novel ligand for IgG antibody capture. Two prototype variants of the novel ligand with eight binding domains were used. One marked with a poly-histidine tag (B_8-$(RH)_4$) and the other tagged with cysteine-lysine-cysteine-lysine tail (B8-cys-lys-cys-lys).

The first step in the present study was the procedure optimization for the immobilization of each ligand variant onto the sensor chip. After this, a comparison of the novel ligand with an already existent commercial Protein A engineered Z form (four domains, MabSelect SuRe), in terms of antibody isolation potential was performed.

A fully humanized IgG was chosen to be the analyte in the interaction with the two new ligand variants. This analyte choose, was essentially made due to the fact that this work is being developed in collaboration with Prof. Berensmeier group from Technical University of Munich (Germany) and previous work was also performed with this antibody. Also, IgG is one of the antibodies with most impact in the therapeutic market.

Before any study, it was necessary to proceed with the quantification of antibody and engineered Protein A in the samples received from Munich.

4.2.1. Protein quantification

Taking in mind the volume of each sensor chip flow channel is very small, around 60 nL, it is important to have the sample concentrations well defined. The amount of ligand to immobilize for any application depends in the first place on the relative molecular weights of the ligand and analyte and on the sensitivity of the Biacore system. Since the SPR response is directly proportional to the mass concentration of material at the surface, the theoretical analyte binding capacity of a given surface is expected to be related to the amount of ligand immobilized. However, in practice, the maximum observed response is affected by the activity of the ligand, the kinetics of analyte binding and limitations on the maximum contact time and available analyte concentration [108]. Thus, it is important to control the ligand and analyte concentrations, in order to reduce the probability of error in concentrations, that eventually could lead to immobilization and interactions different from what is expected. Hence, in order to confirm the concentration of the received antibody and ligands variants, before SPR development, a BCA assay was used, accordingly to what was described in section 3.4.

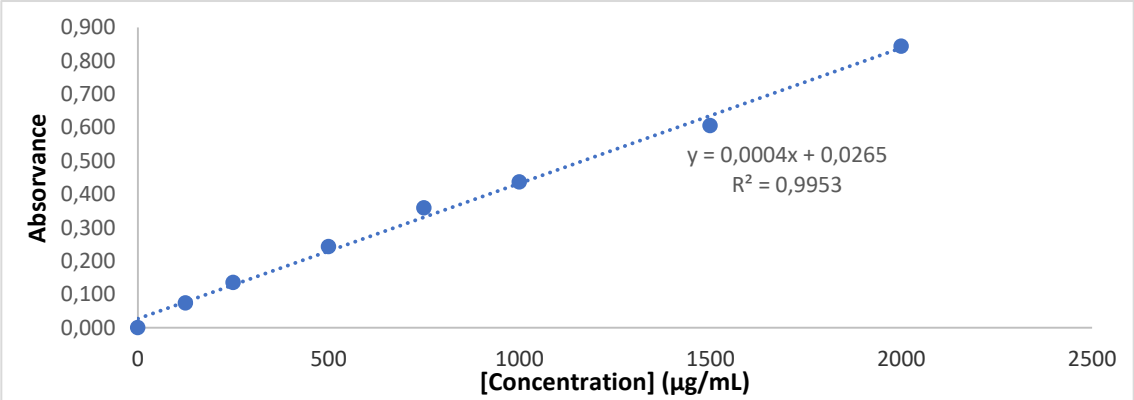

Figure 31: Standard BSA calibration curve in a range of concentrations between 0 and 2000 µg/mL.

As can be observed from Fig. 31, a calibration curve was constructed within the working range for standard BSA values from 0 to 2000 µg/mL. In the same figure, can be observed the equation and correlation factor for the standard curve, which indicates a good fitting to the model. Based on the previously mentioned curve, all the samples concentrations were checked. Results are presented in Table 7, where it is possible to observe that the concentration of each protein stock solution is more or less the same. Although, differences were noticed, so, with these values it was possible to correct the concentration for each sample and consequently reduce errors.

Table 7:

Sample	Absorbance (280 nm wavelength)	Mean	[µg/mL]	Dilution	[stock] mg/mL
IgG #1	0.630	0.618	1478.8	**15**	22.18
	0.607				
IgG #2	0.582	0.603	1440.0	**15**	21.60
	0.624				
B8 Cys #1	0.449	0.462	1087.5	**5**	5.44
	0.475				
B8 Cys #2	0.420	0.430	1007.5	**5**	5.04
	0.440				
B8 RH4 #1	0.632	0.645	1545.0	**3.75**	5.79
	0.658				
B8 RH4 #2	0.665	0.677	1625.0	**3.75**	6.09
	0.689				

Concentrations obtained from BCA Assay Kit test, for two different tubes of each proteins.

4.2.2. Interaction study between protein A commercial form and IgG by SPR biosensor

As mentioned before for the SPR studies, protein A sensor chip has already the commercial Protein A ligand immobilized on its surface, meaning it was ready-to-use. The analyte (IgG) was passed through the sensor chip, after optimization of concentration. Multiple trials were performed with different concentration ranges in order to establish the concentration value that saturate the ligand surface. Additionally, two different running buffers were tested during analyte adsorption: 20 mM phosphate + 150 mM NaCl pH 7.4 and 20 mM MOPS + 150 mM NaCl pH 7.4.

Accordingly, to the method already described (section 3.5.3) and using 20 mM phosphate + 150 mM NaCl pH 7.4 as running buffer, cyclic injections of IgG with concentrations ranging from 62.5 μg/L to 32.0 mg/L were used. In order to access steady state affinity constant for the antibody adsorption, a plot of the observed R_{eq} against IgG concentration was fitted to a model representing a 1:1 binding equilibrium; however, the response was not favorable to the isotherm fit and have a high Chi^2. Also, the response was too high (around $2.971x10^4$ RU for the higher concentration), indicating that this concentration range was not suitable for a reliable evaluation.

Table 8: Affinity results obtained by SPR for IgG adsorption onto a Protein A sensor chip in presence of 20 mM phosphate + 150 mM NaCl pH 7.4. IgG concentrations ranging from 62.5 μg/L to 32.0 mg/L.

K_D (M)	R(maximum)	Chi^2
$6.284x10^{-7}$	$2.971x10^4$	$3.67x10^4$

Another attempt was tried in order to reduce the achieved Chi square value in another flow cell and with a lower concentration range of analyte. More specifically, concentrations from 0.25 μg/mL to 250 μg/mL were passed through the surface with regeneration step between each injection. This concentration range was selected according with instructions guide (Instructions 29-1383-03 AA).

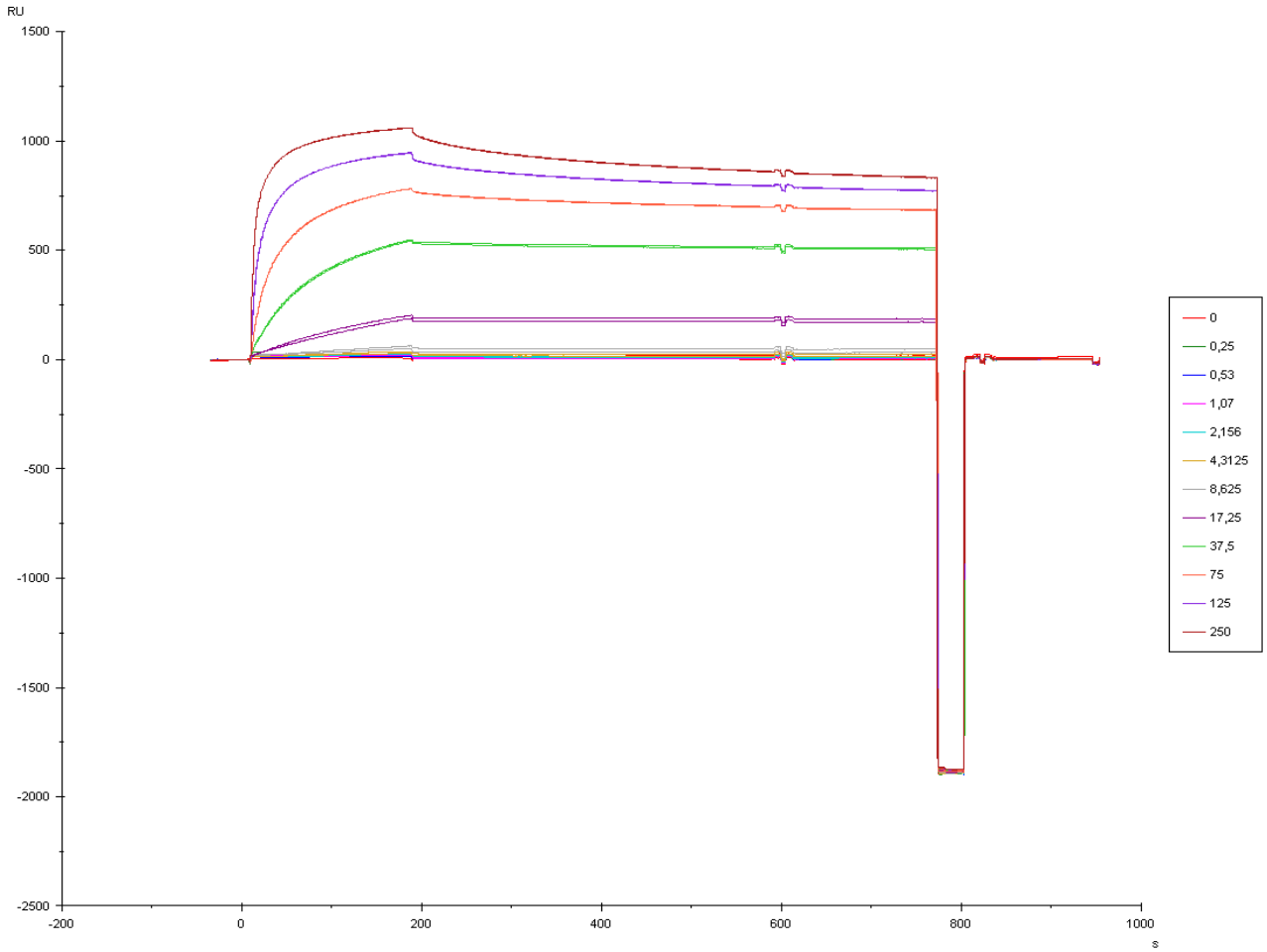

Figure 32: Response (RU) of a Protein A chip surface to a range of IgG concentrations as function of time (s) in presence of 20mM phosphate + 150 mM NaCl pH 7.4. IgG concentrations ranging from 0.25 μg/L to 250 μg/L.

The response obtained in Fig. 32, shows a decrease in response units (RU) with this range concentration reduction. Namely, comparing maximum responses from Table 8 and 9, a

drop from $2.971x10^4$ RU to 1551.68 RU can be detected. Overall, Chi^2 values dropped and the K_D remained in the same order of magnitude for all the flow channels.

Table 9: Affinity results obtained by SPR for IgG adsorption onto a Protein A sensor chip in presence of 20 mM phosphate + 150 mM NaCl pH 7.4. IgG concentrations ranging from 0.25 μg/L to 250 μg/L. The four sensor chip flow channels were used.

	K_D (M)	R (maximum)	Chi^2	Excluded points: 0.25; 0.53; 1.07; 2.16; 8.53 and 17.5 μg/mL
Fc1	$2.73x10^{-7}$	1361.23	177.46	
Fc2	$2.85x10^{-7}$	1329.75	211	
Fc3	$2.77x10^{-7}$	1558.14	281.78	
Fc4	$2.99x10^{-7}$	1551.68	389.69	

Chi-squared values remained large compared to the values that should be achieved or expected, error should be low in relation to the maximum measured response. As a rough guideline, acceptable chi-squared values should be less than about 5% of the response reached at the end of the sample injection at the lowest flow rate [132]. In terms of fit, the model adjusted better to the present range of IgG concentrations studied (Fig. 33), for the 1:1 fitting (Table 9).

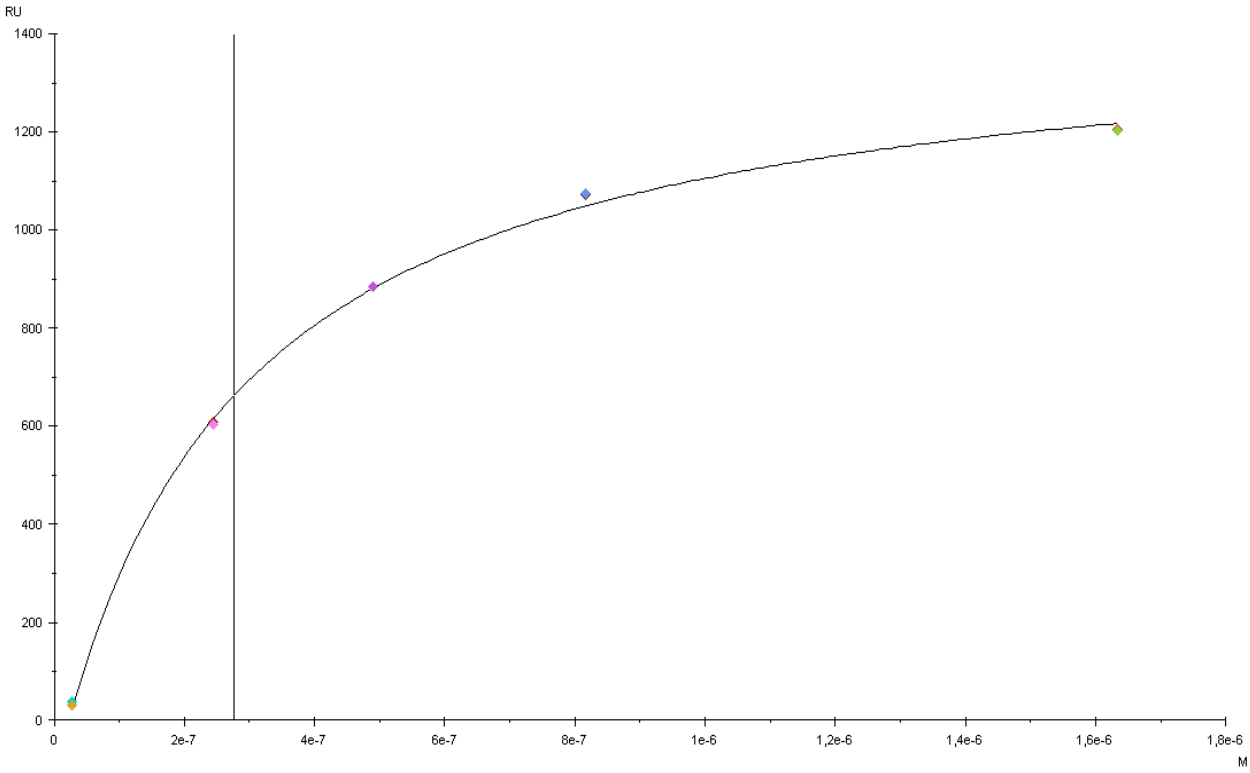

Figure 33: Affinity results obtained by SPR for IgG adsorption onto a Protein A sensor chip in presence of 20 mM phosphate + 150 mM NaCl pH 7.4. IgG concentrations ranging from 0.25 μg/L to 250 μg/L. Although this isotherm belongs to sensor chip flow channel 2, the other three channels expressed similar dispersion profiles.

The reported K_D value is marked on the plot (Fig. 33) as a vertical line. For a 1:1 interaction, K_D is the same as the analyte concentration at a response equal to half R_{max}. Thus, if the reported value is higher than half the highest concentration used, this is a warning that the value may be unreliable because the plot does not flatten out sufficiently, however this was not the case in the present analysis. Accordingly, another explanation has to be found for the significant chi-squared values. A possibility is that the adsorption between IgG and the Protein A ligand does not follow a 1:1 stoichiometry. In fact, from previous studies using MabSelect SuRe resin (from GE), a resin that has the same Protein A ligand as the Biacore Protein A sensor chip, it was proved that in the saturation region, a 2:1 stoichiometry is more likely to occur, being favored a 1:1 ratio, with the antibody binding to the outer domains in the protein A chain at very low and high concentrations in the linear range of the isotherm [133].

The interaction of IgG with protein A was also evaluated with 20 mM MOPS + 150 mM NaCl pH 7.4 running buffer (Fig. 34), which allowed to compare the commercial Z form protein A ligand with the new engineered eight binding domains protein A ligand. The sensorgram response, showed a maximum response slightly higher, with an increment around 250 RU compared to the last running buffer. Similarity to the other approaches, the data was fitted to a 1:1 binding stoichiometry model and presented in Fig. 35. The dissociation constant was slightly decreased, but the value remained in the same order of magnitude, indicating higher affinity between IgG and protein A. Also, the chi-squared decreased to acceptable values (less than 2.5% of the response), except for the flow cell 4.

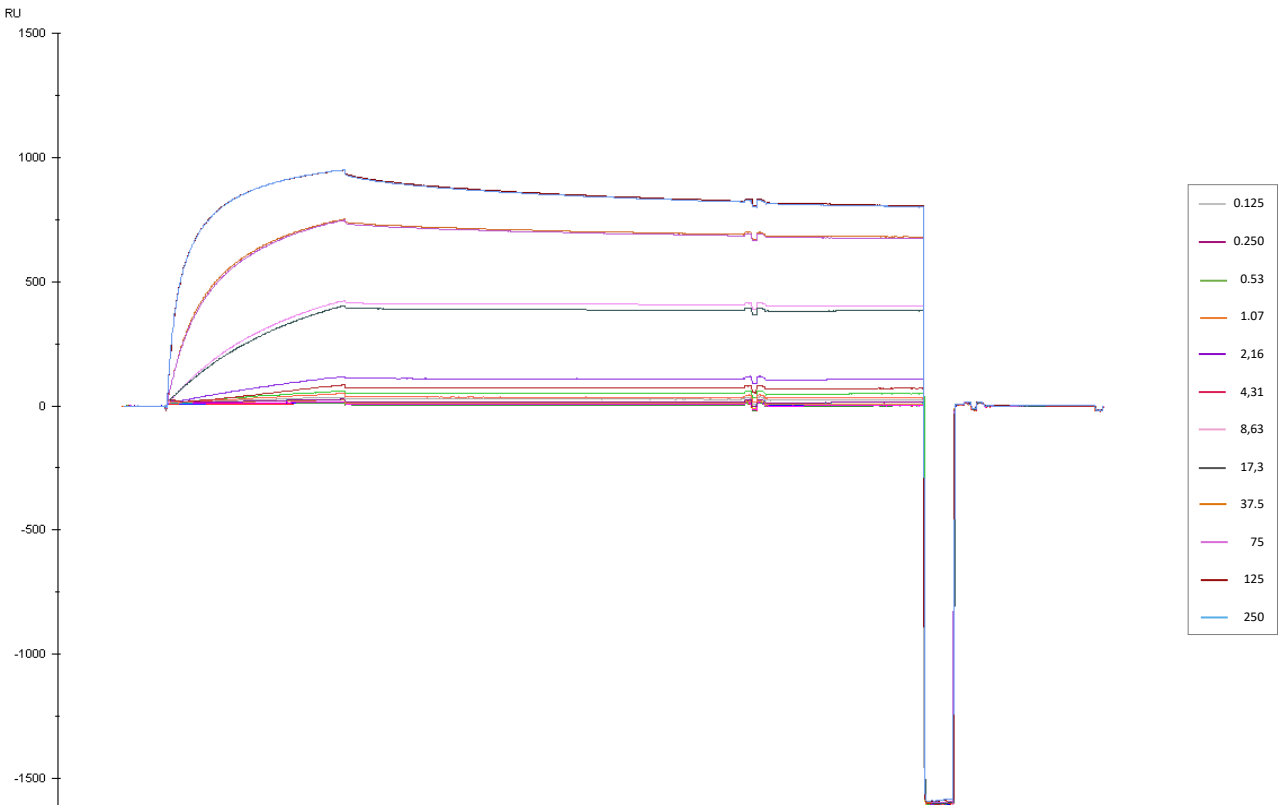

Figure 34: Response (RU) of a Protein A chip surface to a range of different IgG concentrations as function of time (s) in presence of 20 mM MOPS + 150 mM NaCl pH 7.4. IgG concentrations ranging from 0.25 μg/L to 250 μg/L.

Table 10: Affinity results obtained by SPR for IgG adsorption onto a Protein A sensor chip in presence 20 mM MOPS + 150 mM NaCl pH 7.4. IgG concentrations ranging from 0.25 μg/L to 250 μg/L. The four sensor chip flow channels were used.

	K_D (M)	R (maximum)	Chi^2	
Fc1	$2.38x10^{-7}$	1568.52	38.37	Excluded points: 0.25, 0.53, 1.07, and 8.53 μg/mL
Fc2	$2.45x10^{-7}$	1524.55	34.98	
Fc3	$2.34x10^{-7}$	1822.20	42.99	
Fc4	$2.51x10^{-7}$	1851.98	224.30	

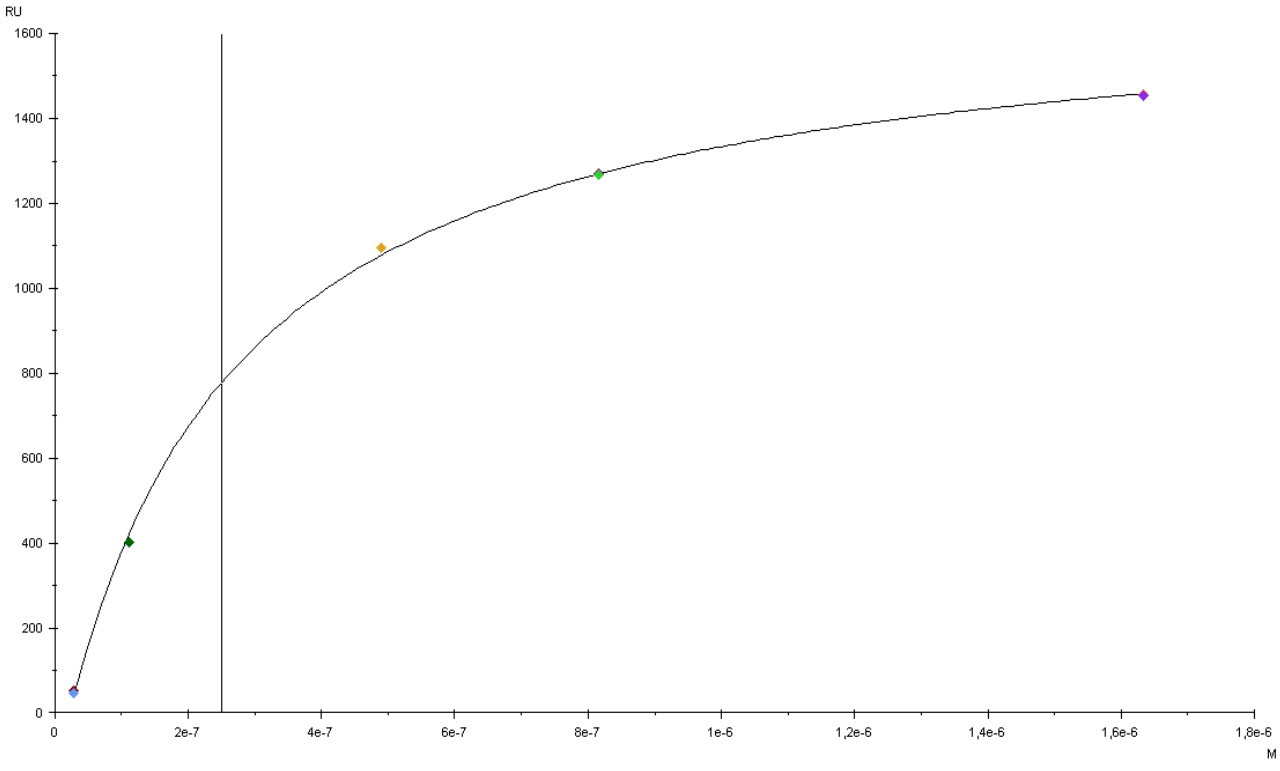

Figure 35: Affinity results obtained by SPR for IgG adsorption onto a Protein A sensor chip in presence of 20 mM MOPS + 150 mM NaCl pH 7.4. IgG concentrations ranging from 0.25 μg/L to 250 μg/L. Although this isotherm belongs to sensor chip flow channel 2, the other three channels expressed similar dispersion profiles.

In short, for protein A sensor chip, the concentration range used must be 0.25 μg/mL to 250 μg/mL. The lowest concentrations must be removed since the response was less than 5 RU. In both buffers this was the approach that led to the lowest chi-squared values. This suggest that probably the sensor limit of detection (LOD) was reached, or that the used model does not properly fit to the results. It is believed that the last hypothesis is the one that justifies the observed behavior, as in previous studies it was proved a heterogeneous binding mechanism favoring different stoichiometry at the different regions of the isotherm [134].

In terms of running buffer influence, the dissociation constant and maximum response achieved were similar. Although, taking in mind the error associated and comparing both buffers chi-squares, it can be noticed that the minor error is reached when the analyte is injected in 20 mM MOPS + 150 mM NaCl at pH: 7.4, indicating that this buffer may favor the analyte pre-concentration on the sensor surface, promoting the IgG-ligand interaction.

4.2.3. Optimization of ligand variants immobilization and respective IgG interactions

- **NTA sensor chip**

Contrary to the previous sensor chip, the NTA sensor chip has no ligand immobilized on its surface. Therefore, a ligand immobilization step must be performed. As described in section 3.5, the protocol consists of five steps, conditioning of the surface with regeneration solution, wash with running buffer to remove the traces of the last solution, preparation of the surface with a Ni^{2+} pulse in running buffer, removal of nickel excess with washing solution and ligand capture, reached by the chelation of the Ni^{2+} between the NTA on the surface and the histidine tag on the ligands.

A key parameter on the ligand immobilization step is the concentration. Thus, an optimization of this step was done, using different concentrations of ligand (all in MOPS buffer, since it was the ligand buffer). First, it was tried an injection of 30 μg/mL, passing 5 μL/min for 3 min. The response profile can be seen in Fig. 36 and the final response value was 214.7 RU.

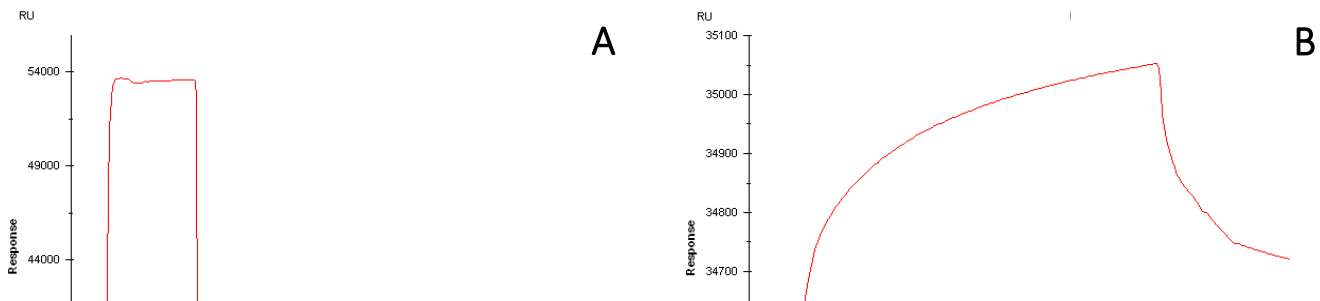

Figure 36: Ligand immobilization response (RU) as function of time (s) on NTA sensor chip surface in presence of 20 mM MOPS + 150 mM NaCl pH7.4. 30 μg/mL ligand injection. A – Sensor chip conditioning and preparation; B – Ligand capture.

Specifically, Fig. 36 A is subdivided in two parts: conditioning of the surface with regeneration solution is presented in the first peak (Fig. 36.A) and the preparation of the surface with nickel in the second small peak. Figure 36.B presents the ligand capture isotherm leading to the end of the immobilization process. After this attempt other ligand concentrations were injected and are summarized in Table 11.

Table 11: Immobilization protocols tried on the NTA sensor chip in presence of 20 mM MOPS + 150 mM NaCl pH7.4 and respective immobilization final responses.

	Ligand concentration	Flow rate	Interaction time	Final Response (RU)
A	30 μg/mL	5 μL/min	3min	214.7
B	90 μg/mL	5 μL/min	3min	293.7
C	500 μg/mL	5 μL/min	3min	616.8
D	750 μg/mL	5 μL/min	3min	935.5
F	1000 μg/mL	5 μL/min	3min	625.7

Based on the results of Table 11, the optimized ligand concentration is 750 μg/mL, since the final response was higher than the remaining injections. Although, in order get higher final response values, consecutive immobilizations were performed and no regenerations were made, to saturate the surface with ligand. Repeated injections of analyte without regeneration can be used to estimate the maximum analyte binding capacity of the surface. Three

consecutives immobilizations were made, the first one with 1000 μg/mL, followed by the second and third with 750 μg/mL ligand injections. The three injections were performed in flow cells FC1 and FC2 lines and their final response values are presented on Table 12.

Table 12: Consecutive immobilization protocol tried on the NTA sensor chip in presence of 20 mM MOPS + 150 mM NaCl pH7.4 and respective immobilization final responses

		Ligand concentration	Flow rate	Interaction time	Final Response (RU)
FC1	First	1000 μg/mL	5 μL/min	3min	516.6
	Second	750 μg/mL	5 μL/min	3min	333.9
	Third	750 μg/mL	5 μL/min	3min	342.7
FC2	First	1000 μg/mL	5 μL/min	3min	688.1
	Second	750 μg/mL	5 μL/min	3min	443.2
	Third	750 μg/mL	5 μL/min	3min	392.7

By analyzing the final response after the second and third immobilizations which are much higher than expected, this approach was not leading to the estimation of the maximum binding capacity. The consecutive immobilizations were supposed to fill consecutively the nickel surface and unfilled sites between each bonded nickel-ligand complex, left by the two first ones. It was expected a stop in capture tendency, due to limited number of binding sites. Yet, it was seen a constant binding from the ligand during the second and third consecutive injections, which led to the existence of non-specific interactions. Nevertheless, analyte was passed through this surface system in order to try understanding what was happening. The sensorgram showed a bigger dispersion of signals and some of the points were excluded not to interfere with the model fit. Again, in order to access steady state affinity constant for the antibody adsorption, a plot of the observed R_{eq} against IgG concentration was fitted to a model representing a 1:1 binding equilibrium (Fig. 37). However, the point distribution was not

suitable to the isotherm fit, and as a consequence the reported K_D was shown to be higher than half the highest concentration used (red dashed vertical line in Fig. 37). Also, the isotherm presents a "S shape" that was already proved to be characteristic when certain places on the adsorbent surface are filled after only a few adsorption layers are formed [135], confirming the presence of different protein layers onto the surface and non-homogeneity of the binding sites (Fig. 37).

Concluding, this last attempt did not work as predicted and the most profitable immobilization (750 μg/mL of ligand, Table 11) was the one chose to proceed with the study.

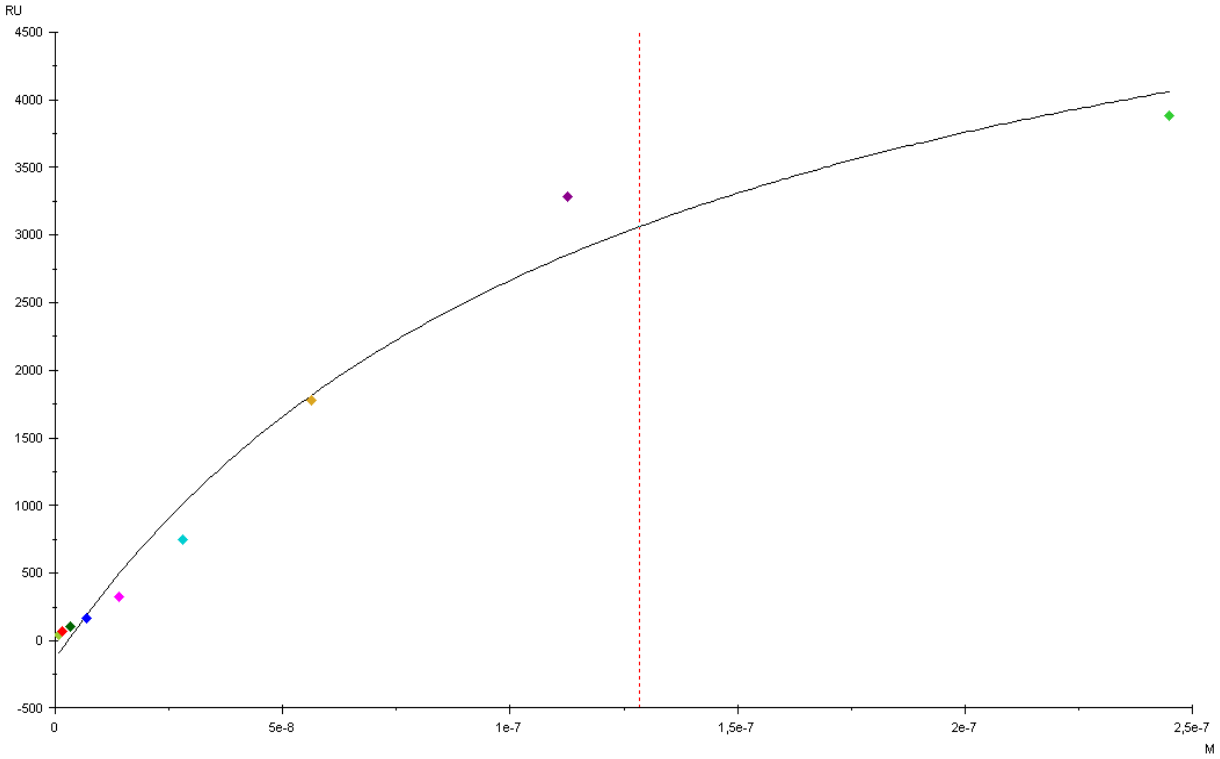

Figure 37: Affinity results obtained by SPR for IgG adsorption onto a modified *NTA sensor chip after three consecutive* Protein A *immobilizations* in presence of 20 mM MOPS + 150 mM NaCl pH 7.4. IgG concentrations ranging from 0.125 μg/L to 1000 μg/L. Although this isotherm belongs to sensor chip flow channel 2, the first channel expressed similar dispersion profile.

After optimization of ligand immobilization, the next step was optimizing the analyte injection and regeneration steps. Some approaches were performed with different regenerations solutions, as can be seen from Table 13.

Table 13: Protocols for optimizing analyte analysis and regeneration between each cycle on the modified NTA sensor chip in presence of 20 mM MOPS + 150 mM NaCl pH7.4.

	Regeneration solution	Blank procedure
1st approach	10 mM Glycine-HCl pH1.5	Without Nickel
2nd approach	3.6 M $MgCl_2$	Without Nickel
3rd approach	100 mM Glycine-HCl pH3	Without Nickel
4th approach	2x (100 mM Glycine-HCl pH3)	Without Nickel

1st approach

On the first approach, the solution used for regeneration, was 10 mM Glycine-HCl pH1.5. It is important to reinforce that, a blank flow cell is necessary to subtract the non-specific interactions to the working line, in order to obtain the correct K_D value. In this case, nothing was injected on reference line according to the supplier sensor chip protocol (Instructions 22060737 AH). Basically, nickel should not be injected on the reference surface, except when a negative protein will be used.

Taking this in mind the pervious optimized conditions, the ligand 750 μg/mL was injected through FC2 line at a flow rate of 5 μL/min for 3 min. The response value was 598.6 RU. FC1 was kept as a reference and only regeneration solution was injected, this means without any ligand or Nickel captured after the surface conditioned. After that, analyte was injected through both flow cells (FC1 and FC2), in a range between 0.125 μg/mL and 1 mg/mL. The response in FC1 was higher than the response from the working line (FC2), leading to a negative sensorgram. The higher response in FC1 could be explained by the interaction between the nitrilotriacetic acid pre-immobilized on the sensor surface and the analyte.

Additionally, the analyte was injected through the surface starting on the lowest concentration until the highest ones. After analyzing the sensorgrams we conclude that the regeneration solution did not remove the analyte at higher concentration, since the baseline between each cycle did not returned to the previous value.

2nd approach

In this approach we tried to optimize the regeneration step using $MgCl_2$ solution. FC1 was kept again as reference flow cell and in FC2 was immobilized the ligand at 750 μg/mL, presenting response values of 1705.8 RU. Then, the analyte was injected at concentrations range from 1 mg/mL to 0.25 μg/mL in both flow cells as well as regeneration solution that was 3.6 M $MgCl_2$ between each analyte cycle. After analysis of sensorgram we conclude that $MgCl_2$ removed the analyte and also the ligand because the baseline did not return to the first value.

3rd approach

A third different regeneration solution was tested that is 100 mM Glycine-HCl pH3. This solution have already been used for protein A [134]. FC1 was left as reference cell and in FC2 was immobilized 750 μg/mL of $B_8(RH)_4$ protein A ligand at a flow rate of 5 μL/min for 3 min. The response value was 627.6 RU.

The analyte was injected through both channels (FC1 and FC2), in a range between 0.5 mg/mL and 1.172 μg/mL, starting from the lowest to the highest concentration. The response remained positive when the baseline was subtracted, being only noticed analyte negative responses at the lowest concentrations (Fig. 38).

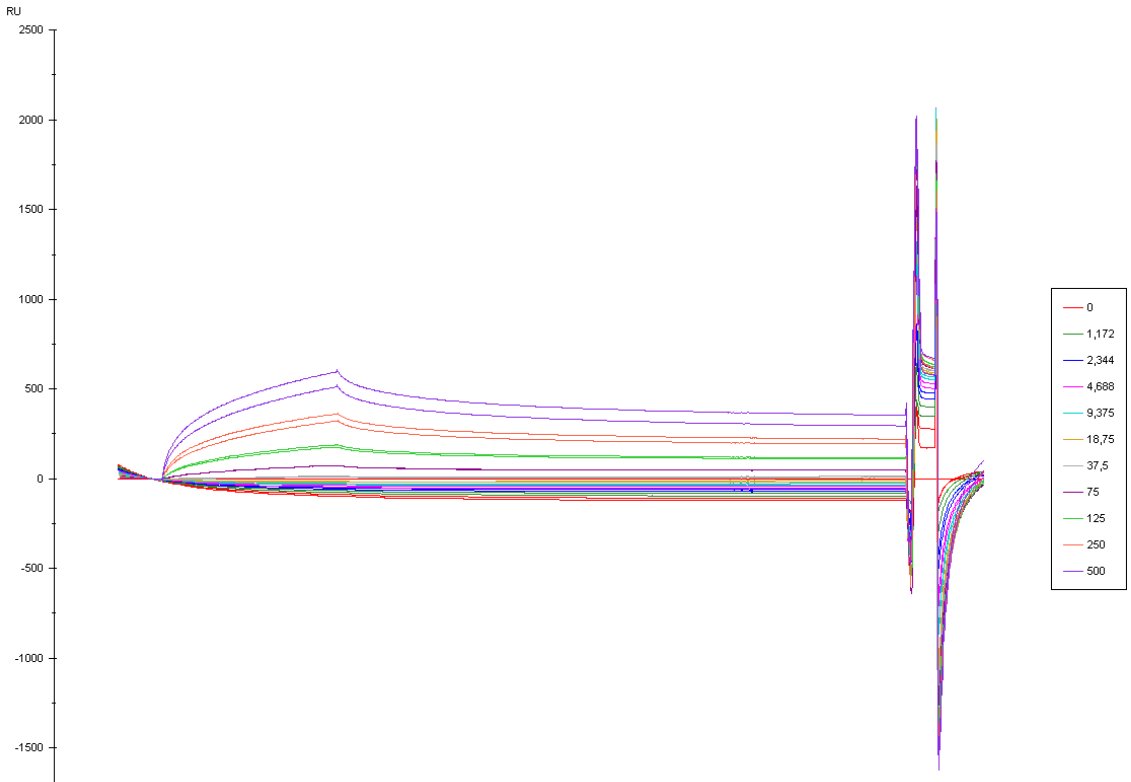

Figure 38: Response (RU) of different IgG concentrations per time (s) on Second flow channel of modified NTA sensor chip surface in 20 mM MOPS + 150 mM NaCl pH7.4. *100 mM Glycine-HCl pH 3* used as regeneration solution.

Figure 38 shows that the baseline did not had enough time to stabilize between cycles. Additionally, looking to the purple line (500 μg/mL), the baseline did not return to the same point as the others. Also, the replicates for the highest concentrations are different. Suggesting that the regeneration solution does not has the strength to strip the analyte from the ligand for the analyte highest concentrations.

Even so, the affinity study was performed, and observed response fitted to the previous mentioned 1:1 binding equilibrium model. Yet, even with some points removed the fit was not the better and the chi square value huge.

Table 14: Dissociation constant, maximum response and error (Chi square) obtained from the modified NTA chip Sensorgram when using *100 mM Glycine-HCl pH 3* as regeneration solution.

	K_D (M)	R (maximum)	Chi^2	Excluded points
FC2	$3.24x10^{-6}$	1258.08	698.74	1.2; 2.3; 4.7; 9.4 and 18.8 μg/mL

4th approach

In this last approach it was used the same regeneration solution; however, two pulses were made between each analyte cycle instead of one. A FC1 was kept as reference cell line and in FC2 was immobilized the ligand at 750 μg/mL with flow rate of 5 μL/min for 3 min. The final response was 579.3 RU.

The analyte was injected through both flow cells (FC1 and FC2), in a range between 1 mg/mL and 1.172 μg/mL, starting from the lowest to the highest concentration. Two pulses of regeneration solution were applied in each cycle, with the stabilization period after these pulses were increased to 300 s, since in the last approach the baseline did not have enough time to stabilize (Fig. 39).

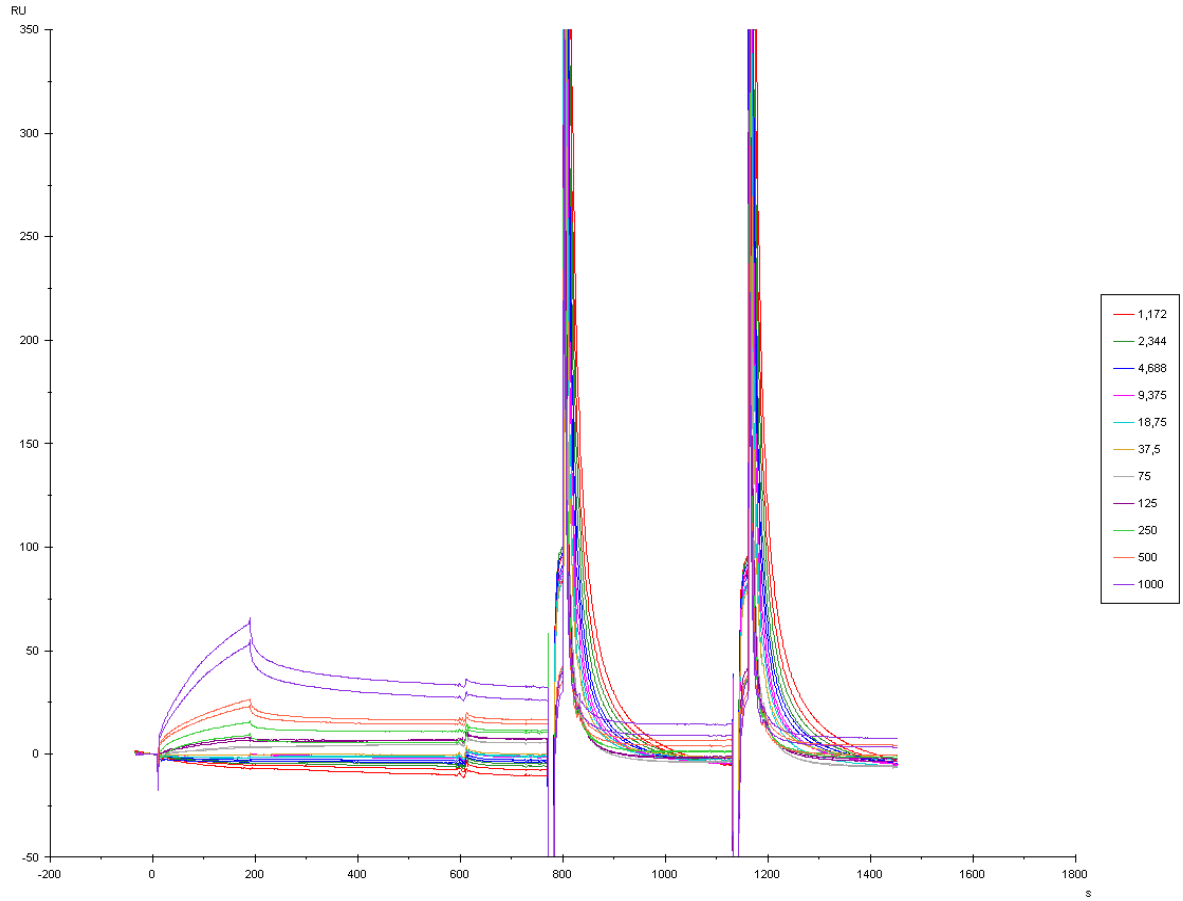

Figure 39: Response (RU) of different IgG concentrations per time (s) on Second flow channel of modified NTA sensor chip surface in 20 mM MOPS + 150 mM NaCl pH 7.4. The two last peaks represent the regeneration pulses with 100 mM Glycine-HCl pH 3.

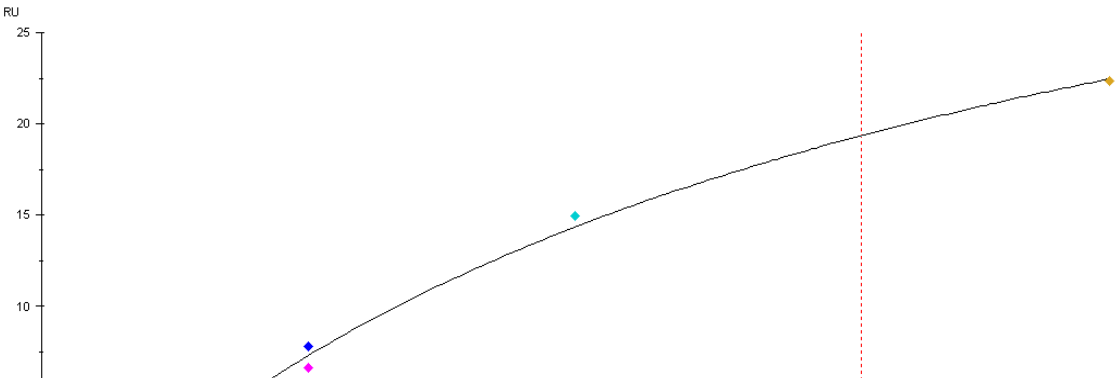

Figure 40: Affinity results obtained by SPR for IgG adsorption onto a modified NTA sensor chip in presence of 20 mM MOPS + 150 mM NaCl pH 7.4. IgG concentrations ranging from 1.172 μg/L to 1000 μg/L. Two pulses of regeneration solution (100 mM Glycine-HCl pH 3) were used between each cycle. Results from sensor chip flow channel 2.

After analyzed the sensorgram (Fig.39), the baseline had enough time to stabilize and differences between duplicates were reduced, being just noticed at 500 and 1000 μg/mL; this is related to the fact that regeneration was not completed at these two concentrations. The affinity studies were performed, and the fitting was improved. The dissociation constant was determined and is in the same order of magnitude. Maximum response value changed from 1260 to a value around 48 response units, and Chi^2 was improved from around 700 to 0.336, which is very positive. However, the reported K_D value was higher than the analyte concentration at a response equal to half R_{max} (considering a 1:1 interaction), which is a warning that the obtained value for K_D may be unreliable because the plot does not flatten out sufficiently.

Table 15: Dissociation constant, maximum response and error (Chi square) obtained from the modified NTA chip Sensorgram when using *100 mM Glycine-HCl pH 3* as regeneration solution.

	K_D (M)	R (maximum)	Chi^2	Excluded points
FC2	$2.51x10^{-6}$	47.4	0.336	500 and 1000 μg/mL duplicates

Summarizing, for NTA sensor chip, the optimized regeneration solution is 100 mM glycine-HCl pH 3 using two regeneration pulses between each cycle and 300 s of stabilization after each pulse (4^{th} approach). The analyte concentration range 1.172 μg/mL to 1 mg/mL. Even with some drawbacks in the regeneration at the highest concentrations of analyte, this

protocol led to the lowest Chi^2. Nevertheless, some caution has to be taken when considering the reached K_D, as the plateau characteristic of a 1:1 binding isotherm has not been attained.

The running buffer used was 20 mM MOPS + 150 mM NaCl at pH 7.4, the buffer was maintained since it was the ligand buffer.

- **CM5 sensor chip**

As mentioned before, this sensor chip explores a different ligand immobilization process. Instead of a chelate formation between Ni^{2+}, NTA and histidine, on CM5 the ligand was immobilized using maleimide coupling kit, namely, sulfo-GMBS. The buffer used was 20 mM MOPS + 150 mM NaCl pH 7.4. The immobilization was performed with a mixture of EDC/NHS (1:1) to activate carboxyl-dextran groups for 7 min with a flow rate of 10 μL/min. To introduce amine groups, ethylenediamine was injected using the same parameters. Afterwards, maleimide groups were introduced by the injection of sulfo-GMBS for 4 min. The ligand solution at 50 μg/mL was injected, and the reactive groups were deactivated with a 4 min injection of cysteine/NaCl. In Fig. 41, presents the sensorgram of ligand immobilization.

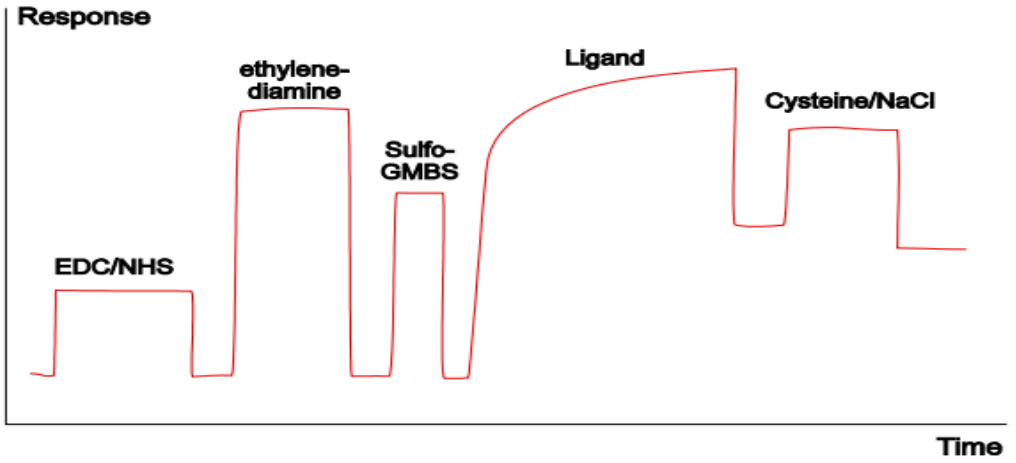

Figure 41: Typical sensorgram of a ligand immobilization by maleimide coupling using sulfo-GMBS (Laboratory Guideline BR-2001-24 AC).

The final immobilization response was lower about 325 RU and the run profile was different from the typical immobilization sensorgrams. A difference in the third and fourth steps was observed, when compared to figure 41. In the first case, the sulfo-GBS value was higher than the one at a typical sensorgram; in the second case, the ligand isotherm was almost inexistent compared to the typical sensorgram. The first flow channel of the sensor chip was maintained as blank line.

In FC3 was immobilized the ligand at 750 μg/mL. The final response value was 275.9 RU, even lower than the last one. In terms of immobilization profile, it showed the same profile and drawbacks of the previous one (50 μg/mL), showing a low interaction of the ligand with the system. Even so, analyte was injected through the immobilized ligand on flow channel 2, once the final response in this one was higher than in channel 3, previous surface plasmon resonance studies on engineered Z domain Protein A ligands got good results with ligand immobilizations in the order of 25 to 100 RU [125].

The run was performed with injection concentration range 1 mg/mL to 1.07 μg/mL and regenerating with Glycine-HCl pH 1.5 between each injection. The results are in figure 42. Overall, the response was low and the sensorgrams at lowest concentration had negative responses and at the highest it presented a negative slope near the maximum of the isotherm. Additionally, it was noticed that the maximum response was too low since the highest concentrations only reached responses around 10 response units. Even so, affinity was studied and the dissociation constant, maximum response (R maximum) and Chi^2 values were determined. For a better correlation between the model and the point distribution the higher analyte concentrations were not considered in the analysis. Results can be observed in Fig. 43 and Table 16.

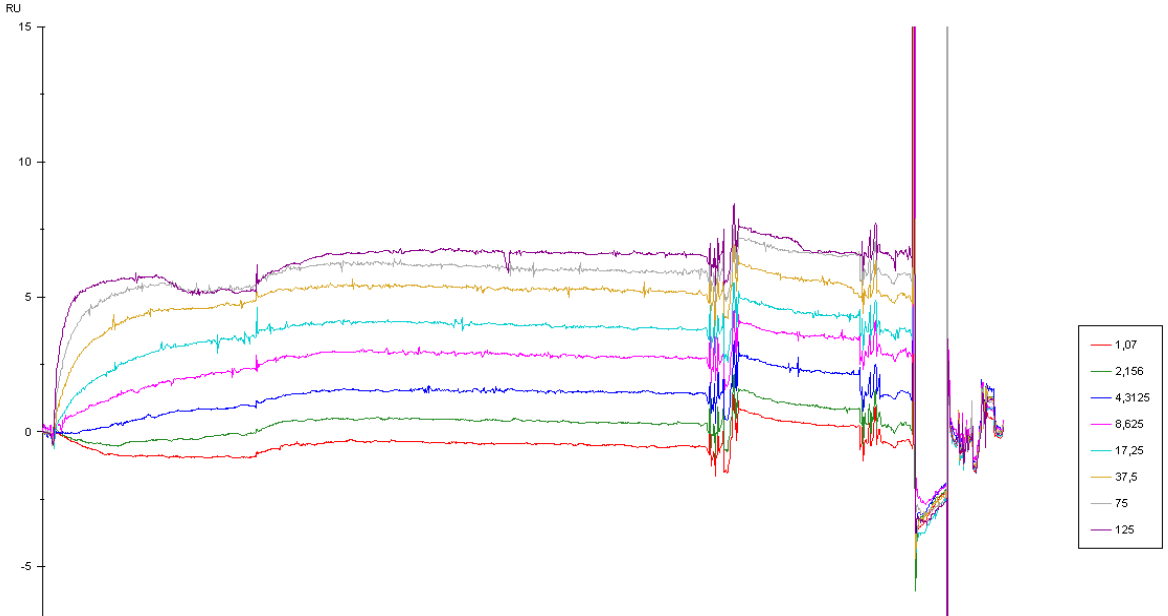

Figure 42: Response (RU) of different IgG concentrations per time (s) on Second flow channel of the modified CM5 sensor chip surface in 20 mM MOPS + 150 mM NaCl pH7,4. Glycine-HCl pH 1.5 used as regeneration solution.

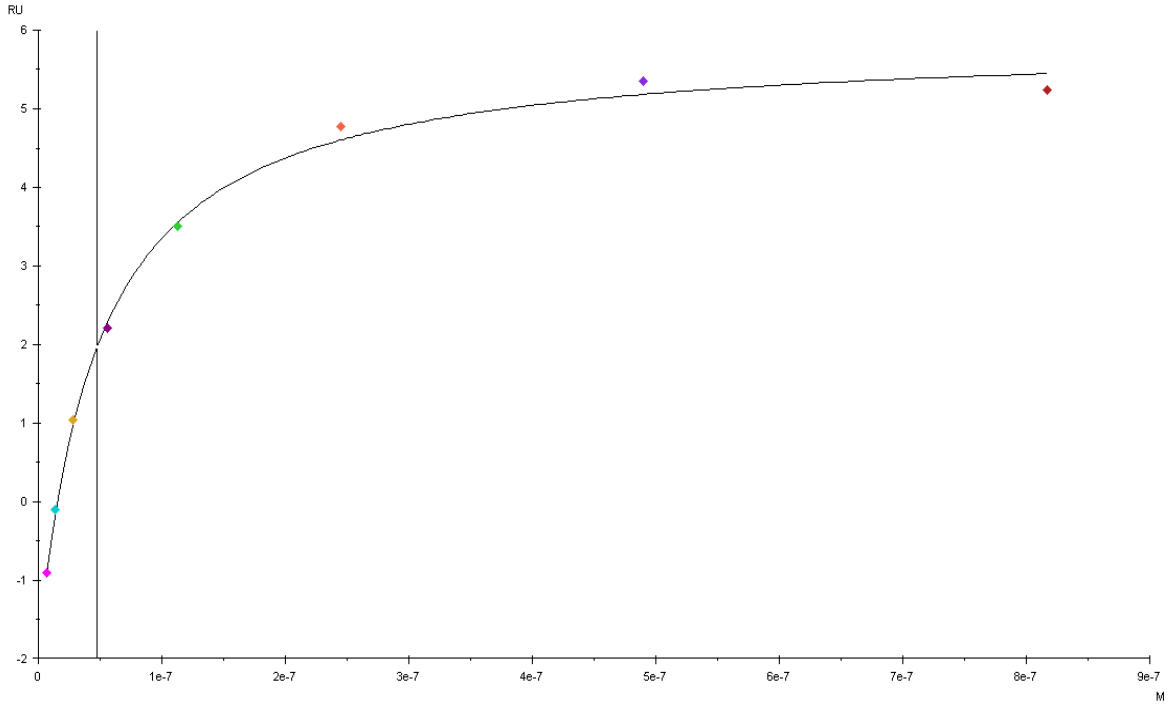

Figure 43: Affinity results obtained by SPR for IgG adsorption onto a modified CM5 sensor chip in presence of 20 mM MOPS + 150 mM NaCl pH 7,4. IgG concentrations ranging from1.07 μg/L to 1000 μg/L. Glycine-HCl pH 1.5 used as regeneration solution. Results from sensor chip flow channel 2.

As it can be seen, the model adjusted very well to the different points, although, the isotherm starts in negative values, and these points should be excluded from the affinity calculations. Recalculation of the affinity parameters discharging these values leaves to very similar results (Table 16), however some caution as to be taken since the response is too near to the sensor detection limit and the determined parameters are overestimated.

Table 16: Dissociation constant, maximum response and error (Chi square) obtained from the modified CM5 chip

	K_D (M)	R (maximum)	Chi^2	Excluded points
FC2	$4.81x10^{-8}$	7.775	0.0241	250, 500 and 1000 μg/mL
FC2	$4.90x10^{-8}$	7.729	0.0299	1.07, 250, 500 and 1000 μg/mL

when using for ligand immobilization a ligand solution of 50 μg/mL.

Accordingly, to the instruction's manual (Thermoscientific 22324) primary amine buffers should not be used on this type of immobilization, once the presence of primary amines, during immobilization may block the binding sites necessary for the maleimide groups capture, reducing the ligand immobilization success. Although, MOPS is not a primary amine buffer, is N-substituted amino sulfonic acid with a morpholinic ring. Consequently, in other to make sure that there is no interference from the buffer on this new trial a 20mM phosphate + 150 mM NaCl pH 7.4 buffer was used instead of MOPS. Again, the ligand concentration for the immobilization was 50 μg/mL, and we did the procedure on FC4.

Using this buffer, the immobilization profile changed mainly in the sulfo-GMBS step and the ligand step remained almost without isotherm. Differently from the last immobilization, the sulfo-GMBS presented a low isothermal profile, instead of the supposed massive rectangular peak. It was also noticed a huge difference in the immobilization final response, this time 1238.4 RU, 4 times higher than the immobilization performed in FC2. Again, the analyte (IgG) was injected through the surface, in phosphate buffer but with the same analyte concentration range. The sensorgram was presented in figure 44 and the response was negative, suggesting that the running buffer is not the problem; in the fact that there was no ligand immobilized on the surface to interact with the analyte. In this case, it was unable to fit the isotherm model. Therefore, the dissociation constant and the other parameters are not determined.

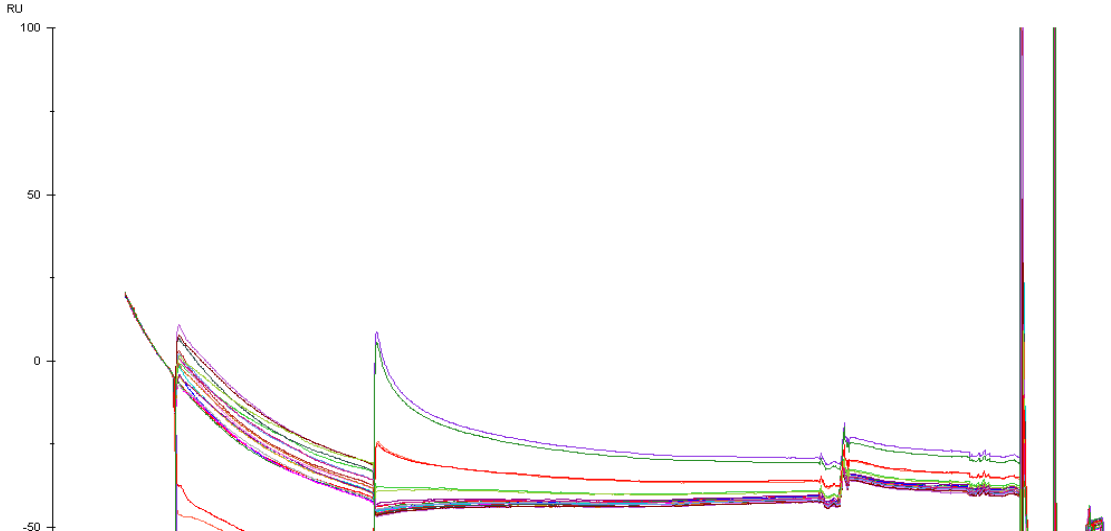

Figure 44: Response (RU) of different IgG concentrations per time (s) on the 4th flow channel of the modified CM5 sensor chip surface in 20 mM phosphate + 150 mM NaCl pH 7.4. *Glycine-HCl pH 1.5* used as regeneration solution.

A possible explanation for the reduced ligand immobilization by maleimide coupling could be related with the presence of aggregates at the ligand solution received from Munich, a tendency observed with similar engineered Protein A ligands [125]. To assess whether these aggregates would be present and possibly explain what was happening in this sensor chip, a PAGE electrophoresis was performed, as described before (Fig. 45).

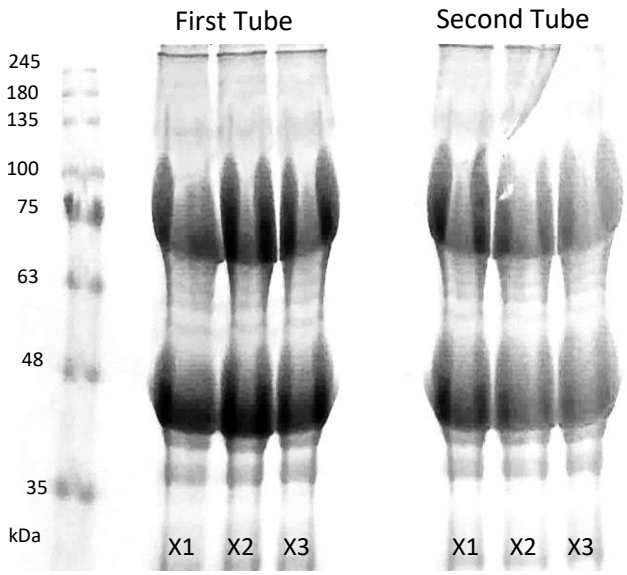

Figure 45: Page electrophoresis result, samples received from Munich were tested in triplicate.

The PAGE presented in figure 45 shows two pronounced bands around 46 and 74 kDa, corresponding to the protein and aggregate, respectively. This allowed to conclude that aggregates are presented on the ligand samples, explaining the results obtained in CM5 chip.

4.2.3. Comparison of the novel ligand with the commercial already existent engineered Z form

Summarizing, the results obtained with protein A sensor chip, the optimized range of concentrations was 0.25 μg/mL to 250 μg/mL. In terms of running buffer, the dissociation constant and maximum response achieved were similar in the different buffers used. However, the minor error is reached when the analyte is injected in 20 mM MOPS + 150 mM NaCl at pH 7.4.

For modified NTA sensor chip, the optimized regeneration solution was 100 mM glycine-HCl pH 3, using two regeneration pulses between each cycle and 300 s of stabilization between each pulse. The analyte concentration values used range from 1.172 μg/mL to 1 mg/mL. Even with some drawbacks in regenerate the highest concentrations of analyte, this protocol led to the lowest chi square, but some caution has to be taken when considering the reached K_D, as the plateau characteristic of a 1:1 binding isotherm has not been attained. All the experiments in this sensor chip were performed in 20 mM MOPS + 150 mM NaCl at pH 7.4.

In presence of the modified CM5 sensor chip, the optimized result achieved was using 50 μg/mL of ligand in 20 mM MOPS + 150 mM NaCl at pH 7.4, with analyte concentrations range from 1 mg/mL to 1.07 μg/mL and regenerating with Glycine-HCl pH 1.5 between each injection. Although, the 1:1 binding model adjusted very well to the dose-response curve, response was too near to the sensor detection limit and ligand immobilization results were distant from what was expected.

Affinity to IgG parameters obtained in presence of the different ligands studied: commercial Protein A (Protein A sensor chip), prototype variant marked with a poly-histidine tag (B_8-$(RH)_4$) (immobilized on the NTA sensor chip) and prototype variant tagged with cysteine-lysine-cysteine-lysine tail (B8-cys-lys-cys-lys) can be find in Table 17.

Table 17: IgG affinity to Protein A and prototype engineered 8 B domains Protein A

	KD (M)	R (maximum)	Chi^2
Protein A	$2.39x10^{-7}$	1638.42	38.78
B_8-$(RH)_4$ (NTA)	$2.51x10^{-6}$	47.4	0.336
B8-cys-lys-cys-lys (CM5)	$4.81x10^{-8}$	7.775	0.024

Taking in account all the discussion previously made, at this point the data presented in table 17 cannot be compared, since for the NTA sensor chip during analysis the plateau in the dose-response curve was not reached which may lead to an erroneous K_D and for the CM5 sensor chip, even presenting a very low error, responses are too close to the sensor chip limit of detection. A prove that additional work needs to be performed to optimize ligands immobilization and conditions for IgG – ligand interactions is the different K_D values obtained for the prototype engineered Protein A ligand, $2{,}51x10^{-6}$ and $4{,}81x10^{-8}$ M when immobilized respectively onto the NTA and CM5 sensor chips. As the ligand is the same, similar values would be expected.

Nevertheless, results from the CM5 sensor chip are in accordance to what was expected, since the dissociation constant presents a lower value when compared to the value obtained in presence of the Protein A sensor chip. Previous studies were two multimeric Protein A ligands were compared, presented the same trend. When the ligand hexamer structure was compared to its tetramer structure (same commercial Protein A ligand used in the present study) a lower affinity was observed by the ligand with the lower number of binding sites [134]. It will be also expectable a higher capacity in antibody capture for the engineered eight binding domains protein A ligand compared to. the four existing in the Commercial Z form. Last year Hober and co-workers [125] demonstrated a trend among the multimeric variants toward improved binding performance with the increasing number of binding domains.

Chapter 5. – Conclusions and Future perspectives

In this study, for the first time, it was possible to analyze in the flow mode the thermodynamics of a convective media, more precisely, the complexity of BSA adsorption onto a 2,5% QA monolithic matrix was investigated with the use of flow microcalorimetry. Thermograms were analyzed considering the mechanism proposed by Yamamoto and co-workers [131]. Endothermic heat major contribution was suggested to be from water molecules and ions release (desolvation process), while major exothermic heats contributions were related to the electrostatic attraction between BSA and QA-monolith and also to the secondary adsorption of already adsorbed molecules.

Differences between thermograms resulting from injections with the 30, 100 and 230 μL loop, presenting one endothermic signal overlapped with an exothermic signal, were noticed when comparing to results from the injection with the 500 μL loop. This one, presented in addition to the endothermic peak, two exothermic overlapping peaks. Profile expected, as in the presence of this higher loop, the adsorption happens under volume overloading conditions.

Additionally, in order to evaluate response under overloading conditions, four injections were performed consecutively using the 230 μL loop. Under these circumstances, endothermic and exothermic peaks, both decrease in magnitude as the protein loading increases, a trend which is not observed when a washing step is introduced between each injection.

In terms of net heat of adsorption, similarly to what happened in the last non-consecutive monolith injections when using loops below 500 μL, the values of net heat tend to be positive. Due to desolvation, the endothermic heat is compensated by water and ions releasing entropy gain, ensuring the adsorption of the biomolecule to the monolith. Yet, already in the second consecutive injection the value change to negative and with loading protein increasing the value turns even more negative (two exothermic signals can be seen). So, at this point, the process turns from endothermic and entropically driven to exothermic and enthalpically driven, meaning that as surface concentration increases, the contribution from desolvation becomes less important, being the adsorption process controlled by electrostatic interactions and reorganizations of already adsorbed molecules. Behavior also observed when injection is made under volume overloading conditions (use of the 500 μL).

Regarding the SPR biosensor results, where it was intended the evaluation of an engineered ligand for antibody capture. Protein A chip only presented an acceptable Chi^2 value after disregarding initial points. Results from the NTA sensor chip did not reach isotherm saturation leading to an unreliable K_D value. And in CM5 chip, the analyte response was low and close to the sensor chip limit of detection. In this last situation, the ligand immobilization step was compromised as it was identified by PAGE the presence of aggregates in the ligand solution.

Expected response for the new ligand (Protein A exhibiting eight binding domains) would be getting a lower K_D value when compared to the Protein A tetrameric Z form, independently from the tag used for immobilization on the sensor surface. Only the K_D value obtained with the CM5 sensor chip correspond to a higher association constant when compared to the value obtained with the Protein A sensor chip, indicating the expected higher ability in antibody capture for the novel Protein A ligand.

Future perspectives should be the optimization of the two remaining sensor chip protocols (NTA and CM5). In the protein A sensor chip since it is sold as a ready-to-use chip. The ligand is already immobilized onto the surface, so all that could be changed is the analyte concentration range, starting from the lowest value included in the fourth approach of NTA chip (1.172 ug/mL) and with more points between it and the maximum value (1000 ug/mL). Also, the regeneration solution must be changed to the 100 mM glycine-HCl pH 3, as optimized for the NTA sensor chip instead of 10 mM glycine-HCl pH= 1.5. For NTA sensor chip, the concentration range should be adjusted for convenient flatten out from the dose-response curve. For CM5 sensor chip, a treatment with TCEP (tris (2-carboxyethyl) phosphine) must be

performed in order to cleave the protein dimers. This approach was already tried before when this problem emerged in a previous study, and it solved properly the aggregates formation. After this treatment, the ligand must be immobilized, and analyte should be injected through it. The ligand concentration will depend on the capture response and the analyte concentration range used should be similar to the other two chips in order to lead to a reliable comparison between them. Also, it would be interesting to immobilize the ligand at 50 μg/mL and to use the 20 mM MOPS + 150 mM NaCl at pH 7.4 running buffer.

Finally, is intended to develop and optimize for IgG purification a monolithic matrix modified with the studied engineered Protein A (exhibiting eight binding domains) giving preference to the immobilization procedure that revealed to be more efficient.

Chapter 6. - Bibliography

[1] B. Leader, Q.J. Baca, D.E. Golan, Protein therapeutics: a summary and pharmacological classification, Nature reviews Drug discovery 7(1) (2008) 21-39.
[2] H. Keen, J. Pickup, R. Bilous, A. Glynne, G. Viberti, R. Jarrett, R. Marsden, Human insulin produced by recombinant DNA technology: safety and hypoglycaemic potency in healthy men, The Lancet 316(8191) (1980) 398-401.
[3] A. Jungbauer, G. Carta, Protein Chromatography: Process Development and Scale-Up, Wiley-VCH2010.
[4] D.E. Golan, Principles of pharmacology : the pathophysiologic basis of drug therapy, Wolters Kluwer/Lippincott Williams & Wilkins, Philadelphia, Pa.; London, 2008.
[5] J.M. Reichert, Trends in development and approval times for new therapeutics in the United States, Nature Reviews Drug Discovery 2(9) (2003) 695-702.
[6] D.M. Ecker, S.D. Jones, H.L. Levine, The therapeutic monoclonal antibody market, MAbs, Taylor & Francis, 2015, pp. 9-14.
[7] A. Komar, The Art of Gene Redesign and Recombinant Protein Production: Approaches and Perspectives, 2016.
[8] L. Yu, L. Zhang, Y. Sun, Protein behavior at surfaces: Orientation, conformational transitions and transport, Journal of Chromatography A 1382 (2015) 118-134.
[9] J.A. Alberts B, Lewis J, et al., Molecular Biology of the Cell, 2014.
[10] M.K.F. Campbell, S. O., Biochemistry, 2013.
[11] M. Kastner, Protein Liquid Chromatography, 2000.
[12] M. Graille, E.A. Stura, A.L. Corper, B.J. Sutton, M.J. Taussig, J.-B. Charbonnier, G.J. Silverman, Crystal structure of a Staphylococcus aureus protein A domain complexed with the Fab fragment of a human IgM antibody: structural basis for recognition of B-cell receptors and superantigen activity, Proceedings of the National Academy of Sciences 97(10) (2000) 5399-5404.
[13] S. Hober, K. Nord, M. Linhult, Protein A chromatography for antibody purification, Journal of Chromatography B 848(1) (2007) 40-47.
[14] D. Richman, P. Cleveland, M. Oxman, K. Johnson, The binding of staphylococcal protein A by the sera of different animal species, The Journal of Immunology 128(5) (1982) 2300-2305.
[15] K. Swinnen, A. Krul, I. Van Goidsenhoven, N. Van Tichelt, A. Roosen, K. Van Houdt, Performance comparison of protein A affinity resins for the purification of monoclonal antibodies, Journal of Chromatography B 848(1) (2007) 97-107.
[16] U. Gottschalk, Process scale purification of antibodies, Wiley Online Library2009.
[17] T.M. Pabst, J. Thai, A.K. Hunter, Evaluation of recent Protein A stationary phase innovations for capture of biotherapeutics, Journal of Chromatography A 1554 (2018) 45-60.
[18] B. Nilsson, T. Moks, B. Jansson, L. Abrahmsen, A. Elmblad, E. Holmgren, C. Henrichson, T.A. Jones, M. Uhlen, A synthetic IgG-binding domain based on staphylococcal protein A, Protein Engineering, Design and Selection 1(2) (1987) 107-113.
[19] A.A. Kosky, U.O. Razzaq, M.J. Treuheit, D.N. Brems, The effects of alpha-helix on the stability of Asn residues: deamidation rates in peptides of varying helicity, Protein Science 8(11) (1999) 2519-2523.
[20] N. Kruljec, T. Bratkovič, Alternative affinity ligands for immunoglobulins, Bioconjugate chemistry 28(8) (2017) 2009-2030.
[21] J. González-Valdez, A. Yoshikawa, J. Weinberg, J. Benavides, M. Rito-Palomares, T.M. Przybycien, Toward improving selectivity in affinity chromatography with PEG ylated affinity ligands: The performance of PEG ylated protein A, Biotechnology progress 30(6) (2014) 1364-1379.

[22] Z. Liu, S.S. Mostafa, A.A. Shukla, A comparison of Protein A chromatographic stationary phases: Performance characteristics for monoclonal antibody purification, Biotechnology and applied biochemistry 62(1) (2015) 37-47.
[23] N.A. Buss, S.J. Henderson, M. McFarlane, J.M. Shenton, L. De Haan, Monoclonal antibody therapeutics: history and future, Current opinion in pharmacology 12(5) (2012) 615-622.
[24] T.J. Berg JM, Stryer L, Antibodies Possess Distinct Antigen-Binding and Effector Units, in: N.Y.W.H. Freeman (Ed.), Biochemistry, 2002.
[25] M. Salvalaglio, L. Zamolo, V. Busini, D. Moscatelli, C. Cavallotti, Molecular modeling of protein A affinity chromatography, Journal of chromatography A 1216(50) (2009) 8678-8686.
[26] S.J. Kim, Y. Park, H.J. Hong, Antibody engineering for the development of therapeutic antibodies, Molecules & Cells (Springer Science & Business Media BV) 20(1) (2005).
[27] G. Vidarsson, G. Dekkers, T. Rispens, IgG subclasses and allotypes: from structure to effector functions, Frontiers in immunology 5 (2014) 520.
[28] L.E. Rayner, G.K. Hui, J. Gor, R.K. Heenan, P.A. Dalby, S.J. Perkins, The solution structures of two human IgG1 antibodies show conformational stability and accommodate their C1q and FcγR ligands, Journal of Biological Chemistry 290(13) (2015) 8420-8438.
[29] E.O. Saphire, P.W. Parren, R. Pantophlet, M.B. Zwick, G.M. Morris, P.M. Rudd, R.A. Dwek, R.L. Stanfield, D.R. Burton, I.A. Wilson, Crystal structure of a neutralizing human IGG against HIV-1: a template for vaccine design, Science 293(5532) (2001) 1155-9.
[30] M.A. Van Dijk, J.G. Van De Winkel, Human antibodies as next generation therapeutics, Current opinion in chemical biology 5(4) (2001) 368-374.
[31] P.A. Todd, R.N. Brogden, Muromonab CD3, Drugs 37(6) (1989) 871-899.
[32] D.S. Pisal, M.P. Kosloski, S.V. Balu-Iyer, Delivery of Therapeutic Proteins, Journal of Pharmaceutical Sciences 99(6) (2010) 2557-2575.
[33] A. ElBakri, P.N. Nelson, R.O. Abu Odeh, The state of antibody therapy, Human Immunology 71(12) (2010) 1243-1250.
[34] P. Marichal-Gallardo, M.M. Alvarez, State-of-the-art in downstream processing of monoclonal antibodies: process trends in design and validation, Biotechnology progress 28(4) (2012) 899-916.
[35] G. Köhler, C. Milstein, Continuous cultures of fused cells secreting antibody of predefined specificity, nature 256(5517) (1975) 495.
[36] A. Karpas, A. Dremucheva, B.H. Czepulkowski, A human myeloma cell line suitable for the generation of human monoclonal antibodies, Proceedings of the National Academy of Sciences 98(4) (2001) 1799-1804.
[37] M.A. Roguska, J.T. Pedersen, C.A. Keddy, A.H. Henry, S.J. Searle, J.M. Lambert, V.S. Goldmacher, W. Blättler, A.R. Rees, B.C. Guild, Humanization of murine monoclonal antibodies through variable domain resurfacing, Proceedings of the National Academy of Sciences 91(3) (1994) 969-973.
[38] C. Ezzell, Magic bullets fly again, Scientific American 285(4) (2001) 34-41.
[39] J.G. Elvin, R.G. Couston, C.F. van der Walle, Therapeutic antibodies: market considerations, disease targets and bioprocessing, International journal of pharmaceutics 440(1) (2013) 83-98.
[40] S. Aldington, J. Bonnerjea, Scale-up of monoclonal antibody purification processes, Journal of Chromatography B 848(1) (2007) 64-78.
[41] F. Li, A. Shen, A. Amanullah, Cell culture processes in monoclonal antibody production, Pharmaceutical Sciences Encyclopedia: Drug Discovery, Development, and Manufacturing (2010) 1-38.
[42] J. Dumont, D. Euwart, B. Mei, S. Estes, R. Kshirsagar, Human cell lines for biopharmaceutical manufacturing: history, status, and future perspectives, Critical Reviews in Biotechnology 36(6) (2016) 1110-1122.
[43] B.K. Kelley, G. Blank, A. Lee, Downstream processing of monoclonal antibodies: current practices and future opportunities, (2008) pp. 1-23.

[44] R. Kunert, D. Reinhart, Advances in recombinant antibody manufacturing, Applied microbiology and biotechnology 100(8) (2016) 3451-3461.
[45] W.G. Whitford, Fed-batch mammalian cell culture in bioproduction, BioProcess International 4(4) (2006) 30-40.
[46] R.J. Kaufman, P.A. Sharp, Amplification and expression of sequences cotransfected with a modular dihydrofolate reductase complementary DNA gene, Journal of molecular biology 159(4) (1982) 601-621.
[47] B.I. Schweitzer, A.P. Dicker, J.R. Bertino, Dihydrofolate reductase as a therapeutic target, The FASEB Journal 4(8) (1990) 2441-2452.
[48] T. Lai, Y. Yang, S.K. Ng, Advances in mammalian cell line development technologies for recombinant protein production, Pharmaceuticals 6(5) (2013) 579-603.
[49] A.A. Shukla, J.R. Kandula, Harvest and recovery of monoclonal antibodies from large-scale mammalian cell culture, BioPharm International 21 (2008) 34-45.
[50] J.H. Chon, G. Zarbis-Papastoitsis, Advances in the production and downstream processing of antibodies, New biotechnology 28(5) (2011) 458-463.
[51] E.-M.S. Palomares L.A., Ramírez O.T. , Production of Recombinant Proteins, in: L.A. Balbás P. (Ed.), Recombinant Gene Expression, Humana Press, Methods in Molecular Biology, 2004.
[52] Y. Sun, Q.H. Shi, L. Zhang, G.F. Zhao, F.F. Liu, 2.47 - Adsorption and Chromatography, in: M. Moo-Young (Ed.), Comprehensive Biotechnology (Second Edition), Academic Press, Burlington, 2011, pp. 665-679.
[53] K. Hostettmann, Hostettmann, M., & Marston, A. Preparative chromatography techniques: Applications in natural product isolation, 1986.
[54] J. Huang, F. Wang, M. Ye, H. Zou, Enrichment and separation techniques for large-scale proteomics analysis of the protein post-translational modifications, Journal of Chromatography A 1372 (2014) 1-17.
[55] R. Matsuda, J. Anguizola, K.S. Joseph, D.S. Hage, Analysis of drug interactions with modified proteins by high-performance affinity chromatography: Binding of glibenclamide to normal and glycated human serum albumin, Journal of Chromatography A 1265 (2012) 114-122.
[56] G. Healthcare, Hydrophobic Interaction and Reversed Phase Chromatography: Principles and Methods, GE Healthcare Handbooks, 2012.
[57] J. Li, Han, W. & Yu, Y. , Chromatography method, Protein Engineering- Technology and Application, InTech, 2013, pp. 33-60.
[58] E. Müller, Properties and Characterization of High Capacity Resins for Biochromatography, Chemical Engineering & Technology 28(11) (2005) 1295-1305.
[59] A.M. Lenhoff, Protein adsorption and transport in polymer-functionalized ion-exchangers, J Chromatogr A 1218(49) (2011) 8748-8759.
[60] A. Biosciences, Ion exchange chromatography & chromatofocusing, Principles and Methods, edition AA (2004).
[61] L. REACH Devices, Protein Purification by Ion-Exchange Chromatography, 2017.
[62] H. Walton, Ion-exchange chromatography, Anal. Chem.2015, p. 187.
[63] G. Healthcare, Ion Exchange Chromatography principles and methods, GE Healthcare handbooks, 2016.
[64] A.C.A. Roque, C.S.O. Silva, M.Â. Taipa, Affinity-based methodologies and ligands for antibody purification: Advances and perspectives, Journal of Chromatography A 1160(1) (2007) 44-55.
[65] S. Magdeldin, A. Moser, Affinity Chromatography: Principles and Applications, 2012.
[66] S. Ghose, M. Allen, B. Hubbard, C. Brooks, S.M. Cramer, Antibody variable region interactions with Protein A: implications for the development of generic purification processes, Biotechnology and bioengineering 92(6) (2005) 665-673.

[67] P. Gagnon, R. Nian, D. Leong, A. Hoi, Transient conformational modification of immunoglobulin G during purification by protein A affinity chromatography, Journal of Chromatography A 1395 (2015) 136-142.
[68] A.A. Shukla, B. Hubbard, T. Tressel, S. Guhan, D. Low, Downstream processing of monoclonal antibodies—application of platform approaches, Journal of Chromatography B 848 (2007) 28-39.
[69] J. Deisenhofer, Crystallographic refinement and atomic models of a human Fc fragment and its complex with fragment B of protein A from Staphylococcus aureus at 2.9- and 2.8-.ANG. resolution, Biochemistry 20(9) (1981) 2361-2370..
[70] F. Sousa, L. Passarinha, J. Queiroz, Biomedical application of plasmid DNA in gene therapy: A new challenge for chromatography, Biotechnology & genetic engineering reviews 26 (2010) 83-116.
[71] X. Shi, L. Qiao, G. Xu, Recent development of ionic liquid stationary phases for liquid chromatography, Journal of Chromatography A 1420 (2015) 1-15.
[72] A. Podgornik, S. Yamamoto, M. Peterka, N.L. Krajnc, Fast separation of large biomolecules using short monolithic columns, Journal of Chromatography B 927 (2013) 80-89.
[73] A. Jungbauer, R. Hahn, Polymethacrylate monoliths for preparative and industrial separation of biomolecular assemblies, Journal of Chromatography A 1184(1) (2008) 62-79.
[74] A. Podgornik, A. Savnik, J. Jančar, N.L. Krajnc, Design of monoliths through their mechanical properties, Journal of Chromatography A 1333 (2014) 9-17.
[75] G. Sharma, A. Tara, V.D. Sharma, Advances in monolithic silica columns for high-performance liquid chromatography, Journal of Analytical Science and Technology 8 (2017) 16.
[76] V. Rajamanickam, C. Herwig, O. Spadiut, Monoliths in Bioprocess Technology, Chromatography 2(2) (2015).
[77] M. Merhar, A. Podgornik, M. Barut, M. Žigon, A. Štrancar, Methacrylate monoliths prepared from various hydrophobic and hydrophilic monomers – Structural and chromatographic characteristics, Journal of Separation Science 26(3-4) (2003) 322-330.
[78] P. Gerster, E.-M. Kopecky, N. Hammerschmidt, M. Klausberger, F. Krammer, R. Grabherr, C. Mersich, L. Urbas, P. Kramberger, T. Paril, M. Schreiner, K. Nöbauer, E. Razzazi-Fazeli, A. Jungbauer, Purification of infective baculoviruses by monoliths, Journal of Chromatography A 1290 (2013) 36-45.
[79] M. Szumski, B. Buszewski, Preparation of Monolithic Capillary Chromatographic Columns Using Supercritical Fluid as a Porogen Solvent, Chromatographia 77(15-16) (2014) 1009-1017.
[80] J. Ou, Z. Liu, H. Wang, H. Lin, J. Dong, H. Zou, Recent development of hybrid organic-silica monolithic columns in CEC and capillary LC, Electrophoresis 36(1) (2015) 62-75.
[81] J.A. Wolff, R.W. Malone, P. Williams, W. Chong, G. Acsadi, A. Jani, P.L. Felgner, Direct gene transfer into mouse muscle in vivo, Science 247(4949) (1990) 1465-1468.
[82] F.W. Krainer, R. Pletzenauer, L. Rossetti, C. Herwig, A. Glieder, O. Spadiut, Purification and basic biochemical characterization of 19 recombinant plant peroxidase isoenzymes produced in Pichia pastoris, Protein expression and purification 95 (2014) 104-112.
[83] M.-L. Chen, L.-M. Li, B.-F. Yuan, Q. Ma, Y.-Q. Feng, Preparation and characterization of methacrylate-based monolith for capillary hydrophilic interaction chromatography, Journal of Chromatography A 1230 (2012) 54-60.
[84] I. Nikolayenko, O.Y. Galkin, N. Grabchenko, M.Y. Spivak, Preparation of highly purified human IgG, IgM, and IgA for immunization and immunoanalysis, Ukrainica Bioorganica Acta 2(2) (2005) 3-11.
[85] G.N. Ferreira, J.M. Cabral, D.M. Prazeres, Studies on the batch adsorption of plasmid DNA onto anion-exchange chromatographic supports, Biotechnology progress 16(3) (2000) 416-424.
[86] P. Aguilar, A. Twarda, F. Sousa, A. Dias-Cabral, Thermodynamic study of the interaction between linear plasmid deoxyribonucleic acid and an anion exchange support under linear and overloaded conditions, Journal of Chromatography A 1372 (2014) 166-173.

[87] J. Bellot, J. Condoret, Modelling of liquid chromatography equilibria, Process Biochemistry 28(6) (1993) 365-376.
[88] G. Silva, F. Marques, M. Thrash Jr, A. Dias-Cabral, Enthalpy contributions to adsorption of highly charged lysozyme onto a cation-exchanger under linear and overloaded conditions, Journal of Chromatography A 1352 (2014) 46-54.
[89] D.S. Gill, D.J. Roush, K.A. Shick, R.C. Willson, Microcalorimetric characterization of the anion-exchange adsorption of recombinant cytochrome b5 and its surface-charge mutants, Journal of Chromatography A 715(1) (1995) 81-93.
[90] F.Y. Lin, W.Y. Chen, M.T. Hearn, Thermodynamic analysis of the interaction between proteins and solid surfaces: application to liquid chromatography, Journal of Molecular Recognition 15(2) (2002) 55-93.
[91] M.E. Thrash Jr, N.G. Pinto, Characterization of enthalpic events in overloaded ion-exchange chromatography, Journal of Chromatography A 944(1-2) (2002) 61-68.
[92] M.E. Thrash Jr, N.G. Pinto, Flow microcalorimetric measurements for bovine serum albumin on reversed-phase and anion-exchange supports under overloaded conditions, Journal of Chromatography A 908(1-2) (2001) 293-299.
[93] J.M. Phillips, N.G. Pinto, Calorimetric investigation of the adsorption of nitrogen bases and nucleosides on a hydrophobic interaction sorbent, Journal of Chromatography A 1036(1) (2004) 79-86.
[94] L. Blum, Biosensors for Protein Detection: A Review, Analytical Letters - 38 (2005) 1491-1517.
[95] J. Homola, Electromagnetic Theory of Surface Plasmons, in: J. Homola (Ed.), Surface Plasmon Resonance Based Sensors, Springer Berlin Heidelberg, Berlin, Heidelberg, 2006, pp. 3-44.
[96] C. Nylander, B. Liedberg, T. Lind, Gas detection by means of surface plasmon resonance, Sensors and Actuators 3 (1982) 79-88.
[97] B. Liedberg, C. Nylander, I. Lunström, Surface plasmon resonance for gas detection and biosensing, Sensors and Actuators 4 (1983) 299-304.
[98] D.R. Shankaran, K.V. Gobi, N. Miura, Recent advancements in surface plasmon resonance immunosensors for detection of small molecules of biomedical, food and environmental interest, Sensors and Actuators B: Chemical 121(1) (2007) 158-177.
[99] H. Šípová, J. Homola, Surface plasmon resonance sensing of nucleic acids: A review, Analytica Chimica Acta 773 (2013) 9-23.
[100] J. Homola, Surface Plasmon Resonance Sensors for Detection of Chemical and Biological Species, Chemical Reviews 108(2) (2008) 462-493.
[101] J. Homola, Present and future of surface plasmon resonance biosensors, Analytical and Bioanalytical Chemistry 377(3) (2003) 528-539.
[102] W.M. Mullett, E.P.C. Lai, J.M. Yeung, Surface Plasmon Resonance-Based Immunoassays, Methods 22(1) (2000) 77-91.
[103] Y. Jung, J.Y. Jeong, B.H. Chung, Recent advances in immobilization methods of antibodies on solid supports, Analyst 133(6) (2008) 697-701.
[104] S. Ferretti, S. Paynter, D.A. Russell, K.E. Sapsford, D.J. Richardson, Self-assembled monolayers: a versatile tool for the formulation of bio-surfaces, TrAC Trends in Analytical Chemistry 19(9) (2000) 530-540.
[105] J.M. Lee, H.K. Park, Y. Jung, J.K. Kim, S.O. Jung, B.H. Chung, Direct Immobilization of Protein G Variants with Various Numbers of Cysteine Residues on a Gold Surface, Analytical Chemistry 79(7) (2007) 2680-2687.
[106] I.-H. Cho, E.-H. Paek, H. Lee, J.Y. Kang, T.S. Kim, S.-H. Paek, Site-directed biotinylation of antibodies for controlled immobilization on solid surfaces, Analytical Biochemistry 365(1) (2007) 14-23.

[107] L. Torrance, A. Ziegler, H. Pittman, M. Paterson, R. Toth, I. Eggleston, Oriented immobilisation of engineered single-chain antibodies to develop biosensors for virus detection, Journal of Virological Methods 134(1) (2006) 164-170.
[108] A. Biacore, Biacore sensor surface handbook, GE Healthcare Bio-Sciences AB: Uppsala, Sweden (2003).
[109] E. Briand, M. Salmain, C. Compère, C.-M. Pradier, Immobilization of Protein A on SAMs for the elaboration of immunosensors, Colloids Surf B Biointerfaces 53(2) (2006) 215-224.
[110] A. Hirlekar Schmid, S.E. Stanca, M.S. Thakur, K.R. Thampi, C. Raman Suri, Site-directed antibody immobilization on gold substrate for surface plasmon resonance sensors, Sensors and Actuators B: Chemical 113(1) (2006) 297-303.
[111] M. Sarikaya, C. Tamerler, D. Schwartz, F. Baneyx, Materials assembly and formation using engineered polypeptides, Annu. Rev. Mater. Res 34 (2004) 373-408.
[112] T. Ibii, M. Kaieda, S. Hatakeyama, H. Shiotsuka, H. Watanabe, M. Umetsu, I. Kumagai, T. Imamura, Direct Immobilization of Gold-Binding Antibody Fragments for Immunosensor Applications, Analytical Chemistry 82(10) (2010) 4229-4235.
[113] N. Soh, T. Tokuda, T. Watanabe, K. Mishima, T. Imato, T. Masadome, Y. Asano, S. Okutani, O. Niwa, S. Brown, A surface plasmon resonance immunosensor for detecting a dioxin precursor using a gold binding polypeptide, Talanta 60(4) (2003) 733-745.
[114] C.R. So, J.L. Kulp, E.E. Oren, H. Zareie, C. Tamerler, J.S. Evans, M. Sarikaya, Molecular Recognition and Supramolecular Self-Assembly of a Genetically Engineered Gold Binding Peptide on Au{111}, ACS Nano 3(6) (2009) 1525-1531.
[115] N. Granqvist, H. Liang, T. Laurila, J. Sadowski, M. Yliperttula, T. Viitala, Characterizing ultrathin and thick organic layers by surface plasmon resonance three-wavelength and waveguide mode analysis, Langmuir 29(27) (2013) 8561-8571.
[116] C.M. Miyazaki, T.P. Pereira, D.B.T. Mascagni, M.L. de Moraes, M. Ferreira, Monoamine oxidase B layer-by-layer film fabrication and characterization toward dopamine detection, Materials Science and Engineering: C 58 (2016) 310-315.
[117] H. Liang, H. Miranto, N. Granqvist, J.W. Sadowski, T. Viitala, B. Wang, M. Yliperttula, Surface plasmon resonance instrument as a refractometer for liquids and ultrathin films, Sensors and Actuators B: Chemical 149(1) (2010) 212-220.
[118] A. Olaru, C. Bala, N. Jaffrezic-Renault, H.Y. Aboul-Enein, Surface plasmon resonance (SPR) biosensors in pharmaceutical analysis, Critical reviews in analytical chemistry 45(2) (2015) 97-105.
[119] H. Kamimori, K. Hall, D.J. Craik, M.-I. Aguilar, Studies on the membrane interactions of the cyclotides kalata B1 and kalata B6 on model membrane systems by surface plasmon resonance, Analytical biochemistry 337(1) (2005) 149-153.
[120] R.F. Dutra, L.T. Kubota, An SPR immunosensor for human cardiac troponin T using specific binding avidin to biotin at carboxymethyldextran-modified gold chip, Clinica Chimica Acta 376(1-2) (2007) 114-120.
[121] J.B. Fasoli, R.M. Corn, Surface enzyme chemistries for ultrasensitive microarray biosensing with SPR imaging, Langmuir 31(35) (2015) 9527-9536.
[122] C. Situ, M.H. Mooney, C.T. Elliott, J. Buijs, Advances in surface plasmon resonance biosensor technology towards high-throughput, food-safety analysis, TrAC Trends in Analytical Chemistry 29(11) (2010) 1305-1315.
[123] B.-K. Oh, W. Lee, Y.-K. Kim, W.H. Lee, J.-W. Choi, Surface plasmon resonance immunosensor using self-assembled protein G for the detection of Salmonella paratyphi, Journal of biotechnology 111(1) (2004) 1-8.
[124] J. Homola, J. Dostalek, S. Chen, A. Rasooly, S. Jiang, S.S. Yee, Spectral surface plasmon resonance biosensor for detection of staphylococcal enterotoxin B in milk, International journal of food microbiology 75(1-2) (2002) 61-69.
[125] J. Scheffel, S. Kanje, J. Borin, S. Hober, Optimization of a calcium-dependent Protein A-derived domain for mild antibody purification, mAbs 11(8) (2019) 1492-1501.

[126] A.K. Hunter, G. Carta, Effects of bovine serum albumin heterogeneity on frontal analysis with anion-exchange media, Journal of Chromatography A 937(1-2) (2001) 13-19.
[127] H. Amartely, D. Some, A. Tsadok, M. Lebendiker, Ion Exchange Chromatography (IEX) Coupled to Multi-angle Light Scattering (MALS) for Protein Separation and Characterization, JoVE (Journal of Visualized Experiments) (146) (2019) e59408.
[128] F.-Y. Lin, C.-S. Chen, W.-Y. Chen, S. Yamamoto, Microcalorimetric studies of the interaction mechanisms between proteins and Q-Sepharose at pH near the isoelectric point (pI): effects of NaCl concentration, pH value, and temperature, Journal of Chromatography A 912(2) (2001) 281-289.
[129] M.E. Thrash, J.M. Phillips, N.G. Pinto, An analysis of the interactions of BSA with an anion-exchange surface under linear and non-linear conditions, Adsorption 10(4) (2005) 299-307.
[130] W.-Y. Chen, M.-S. Lin, P.-H. Lin, P.-S. Tasi, Y. Chang, S. Yamamoto, Studies of the interaction mechanism between single strand and double-strand DNA with hydroxyapatite by microcalorimetry and isotherm measurements, Colloids and Surfaces A: Physicochemical and Engineering Aspects 295(1-3) (2007) 274-283.
[131] J. Korfhagen, A.C. Dias-Cabral, M.E. Thrash, Nonspecific effects of ion exchange and hydrophobic interaction adsorption processes, Separation Science and Technology 45(14) (2010) 2039-2050.
[132] G. Healthcare, Biacore T200 Software Handbook, Uppsala, Sweden: General electric company (2010).
[133] G. L. Silva, J. Plewka, H. Lichtenegger, A.C. Dias-Cabral, A. Jungbauer, R. Tscheließnig, The pearl necklace model in protein A chromatography: Molecular mechanisms at the resin interface, Biotechnology and bioengineering 116(1) (2019) 76-86.
[134] G.F. da Silva, J. Plewka, R. Tscheließnig, H. Lichtenegger, A. Jungbauer, A.C. Dias-Cabral, Antibody Binding Heterogeneity of Protein A Resins, Biotechnology journal 14(8) (2019) 1800632.
[135] C.F. Poole, Fundamentals of preparative and nonlinear chromatography: G. Guiochon, S. Golshan-Shirazi and AM Katti Academic Press, Boston, MA. 1994, xv+ 701 pp. Elsevier, 1995.

Chapter 7. – Publications

Oral communications within this dissertation:

- Rodrigo A. Rouqueiro, Yasmin K. Baghbaderani, Carla Cruz, Sonja Berensmeier, Cristina Dias- Cabral, “Screening of novel protein A ligands by surface plasmon resonance for antibody capture” XV Annual CICS-UBI symposium, October 2020, Covilhã, Portugal.

Scientific papers:

- Stefan Rauwolf, Saientan Bag, Rodrigo Rouqueiro, Sebastian Schwaminger, Wolfgang Wenzel, Cristina Diaz Cabral, Sonja Berensmeier, “Silica for protein purification: from amino acid interaction to rational development of a peptide tag”, under preparation.